Alma Mater Studiorum – Università di Bologna

DOTTORATO DI RICERCA IN

ONCOLOGIA, EMATOLOGIA E PATOLOGIA

Ciclo 35

Settore Concorsuale: 05/F1 - BIOLOGIA APPLICATA

Settore Scientifico Disciplinare: BIO13 - BIOLOGIA APPLICATA

GENOTYPE-PHENOTYPE CORRELATION IN TRISOMY 21

Presentata da: Francesca Antonaros

Coordinatore Dottorato — Prof.ssa Manuela Ferracin

Supervisore — Prof.ssa Maria Chiara Pelleri

Esame finale anno 2023

INDEX

ABSTRACT

Down syndrome (DS) or trisomy 21 (T21) is the most common genetic cause of intellectual disability (ID). Subjects with DS are characterized by complex and variable clinical features including intellectual disability (ID) and craniofacial dysmorphisms.

The aim of the thesis is to uncover genotype-phenotype relationships in DS possibly useful to devise therapies based on molecular and cellular mechanisms.

In this work, we have investigated different aspects of DS:

- we have collected clinical data of children with DS and we have evaluated the cognitive impairment through specific cognitive tests
- we have analysed genomics of DS through the study of partial trisomy (PT21) cases. We have described new PT21 cases confirming the hypothesis of the highly restricted DS critical region (HR-DSCR) recently identified as the minimal region whose duplication is shared by all PT21 subjects diagnosed with DS, while it is absent in all PT21 non-DS subjects. Moreover, we have characterized new transcripts included in the HR-DSCR;
- we have studied gene expression through RNAseq in blood cells of children with DS;
-metabolic alterations in plasma of children with DS were identified through different methods: Nuclear Magnetic resonance, routine blood exams performed during the follow up of the subjects and enzyme-linked immunosorbent assay (ELISA);
- to test possible correlations between specific Hsa21 regions and alterations in transcriptomics and metabolomics, we have used trisomic iPSCs and differentiated them into neuronal derivatives.

Significant alterations in gene expression and metabolic profiles have been identified, as well as significant correlations with clinical and cognitive aspects. Specific genes and the HR-DSCR may play a role in these alterations: cell models need to be developed to investigate this role. Neural derivatives from trisomic iPSCs are a promising model to better understand genotype-phenotype correlations in DS.

1. INTRODUCTION

1.1 Down syndrome: main clinical features

Down syndrome (DS) or trisomy 21 (T21) (Lejeune et al., 1959a) is defined by the presence of an extra full or partial copy of chromosome 21 (Hsa21) (Pelleri et al., 2019). It is the most common human chromosomal disorder and, with an incidence of 1 in ~800 live births (Bull, 2020), is the first genetic cause of intellectual disability (ID) (Antonarakis et al., 2020). Trisomy 21 is due to an error during the process of cell division in oocytes or spermatozoa, in 95% of cases, the error occurs in meiosis and have maternal origin, while only 5% occur during spermatogenesis (Antonarakis et al., 1993). It was observed that recombination is reduced among non-disjoined chromosomes 21 in meiosis I; this decrease seems to be related to the maternal age (Warren et al., 1987).

Subjects with DS are characterized by a complex and variable phenotype associated with several clinical features of which the most constant are ID and craniofacial dysmorphisms (Strippoli et al., 2019a). More in details, they present a specific neurocognitive and neurobehavioral phenotype characterised by a slower developmental trajectory, delay in the acquisition of the main psychomotor developmental milestones and subnormal neuropsychological testing (Locatelli et al., 2021). ID results associated with typical brain imaging and neural structural correlates, like reduction in brain size and weight, delayed myelination and reduction of neuronal interconnections (Lukowski et al., 2019;Strippoli et al., 2019a). Typical areas of weakness are verbal processing, abstract thinking, expressive language, and problem solving. Despite these difficulties, relative strengths are found in receptive language, visual processing, and non-verbal abilities (Fidler, 2008;Grieco et al., 2015). Regarding adaptive functioning, socialisation is the strongest domain, followed by communication and finally daily living skills (Marchal et al., 2016). Craniofacial dysmorphisms includes slightly flat nose and almond shaped eyes with the greater frequency, small mouth with protruding tongue, single crease across the palms, clinodactyly of hand fifth finger and a larger than normal space between the first and second toes (Pelleri et al., 2016).

Even if subjects with DS are affected by other symptoms and diseases with a great variability, physicians can suspect DS diagnosis based on some physiognomic features. In 1972, after observation of 150 individuals suspected to be affected by DS, Lee and Jackson drafted the so-called Jackson's checklist, a list of 25 signs of DS (Lee and Jackson, 1972). The presence of 6 or more of these signs leads to the presumably correct clinical diagnosis of DS (Hall, 1966). The probability of being affected is then different according to the number of signs found, those with 5 or 6 signs have 23% probability of having DS, 7 to 9 signs 60% probability, 10 to 12 signs 84% probability (Lee and Jackson, 1972). Despite the utility of the Jackson checklist the real diagnosis remains linked to the demonstration of the excess of Hsa21 material. Some pathological conditions

result to be present with a higher frequency in DS compare with the general population. 40% of subjects with DS present cardiovascular defects, particularly atrioventricular septal defect (AVSD) (Gardiner et al., 2010) and endocrine disorders including hypothyroidism in the 15% of subjects. They could show an increased risk for immune disorders, such as increased susceptibility to infections and to autoimmune diseases, like alopecia, celiac disease and diabetes. They are likely to present duodenal stenosis or atresia, Hirschprung disease, imperforate anus, hearing loss, and leukaemia from 10 to 20 times with respect to normal population, particularly acute megakaryocytic leukaemia (Pelleri et al., 2014). Amyloid precursor protein gene (*APP*) is located on chromosome 21 and it is reported as overexpressed (Chen et al., 2021), this condition might cause an excess of APP protein and promote the formation of characteristic senile plaques and neurofibrillary tangles and the early outcome of Alzheimer disease around the age of forty (Chen et al., 2021).

1.2 Genomics of Down syndrome: trisomy of full or partial chromosome 21

DS features are the consequence of having three copies of chromosome 21 in the karyotype (Lejeune et al., 1959b). The presence of this supernumerary copy of the chromosome can be the outcome of different events, occurring at different stages of gametogenesis or development. The most common origin of trisomy 21 is meiotic chromosomal non-disjunction (Figure 1) during maternal gametogenesis, which occurs with a frequency of around 90%, taking place in the first maternal meiotic division (MI) or during the second maternal meiotic division (MII) (Yoon et al., 1996). In 2% of cases of trisomy 21 non-disjunction happens during mitosis (Papavassiliou et al., 2009), leading to mosaic conditions: DS phenotype heavily depends on the moment of development in which the mutation takes place and, on the tissues, involved in the event.

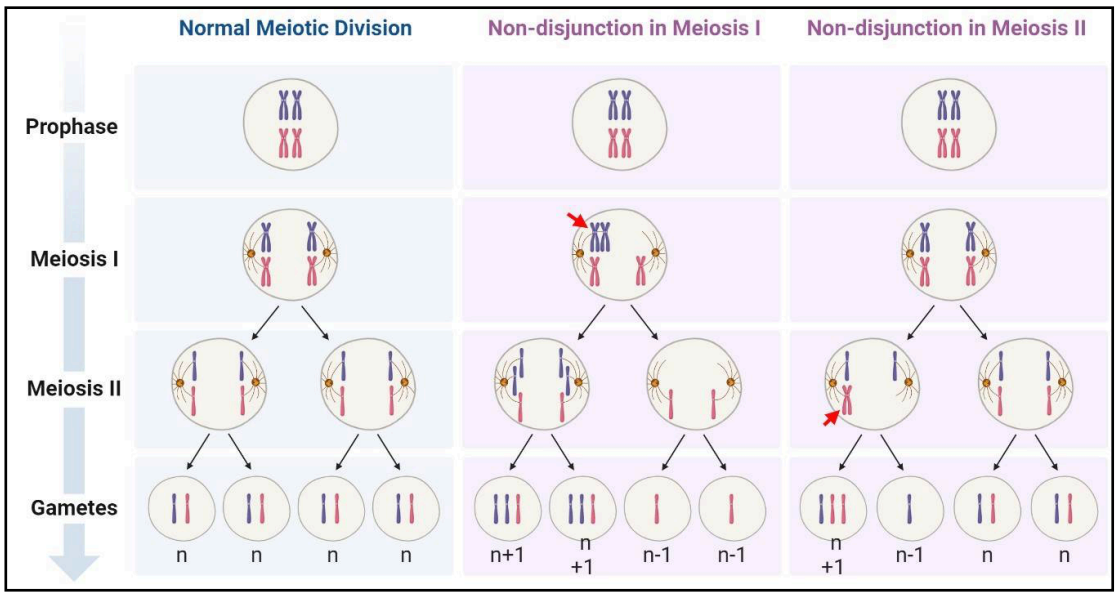

Figure 1. Comparison of disjunction and non-disjunction in meiosis. The diagram represents normal meiosis (on the left), non-disjunction in meiosis I (middle), non-disjunction in meiosis II (right). Gametes resulting from each process are shown (https://www.microbiologiaitalia.it/).

Another process that can lead to DS is Robertsonian translocation (Figure 2), which is the explanation of 2-4% of the cases.

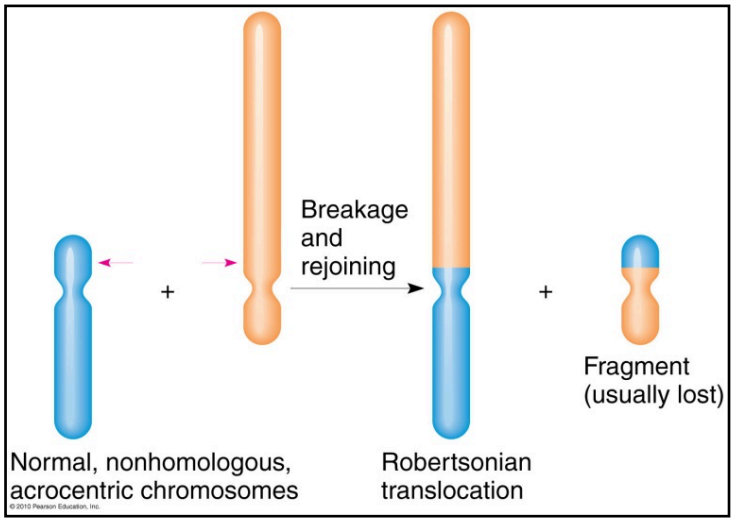

Figure 2. Robertsonian translocation. (2010 PJ Russell, iGenetics 3rd ed.; all text material).

There are cases in which trisomy 21 is not complete but just some portions of the chromosome 21 are present in three copies. This extremely rare condition (only 200 reported cases in literature from '70s to today) is known as partial trisomy 21 (PT21) or segmental trisomy 21 (Pelleri et al., 2016). PT21 is mainly the outcome of discordant segregation of deleted chromosomes 21 or translocations involving segments of the long arm of Hsa21, called 21q (Pelleri et al., 2016). The study of the extremely rare cases of PT21 is a key model for linking genotype and phenotype in

subjects with DS (Korbel et al., 2009;Lyle et al., 2009;Pelleri et al., 2016;Pelleri et al., 2017). PT21 is characterized by the duplication of only a segment of Hsa21 that may or may not be associated with DS diagnosis (Shapiro, 1999).

Since the early 1970s, thanks to the introduction of the banding method, it has been possible to carry out more accurate cytogenetic analyses and demonstrate that persons without full trisomy 21 but with a phenotype indistinguishable from DS may have a portion of Hsa21. In 1974 Niebuhr and coll. were the first to advance the hypothesis that the duplication of a delimited segment of Hsa21 was sufficient for the manifestation of the DS (Niebuhr, 1974). In their work, they reviewed 14 previously described cases of PT21 and reported a new one, excluding 65% of Hsa21 and identifying a region of 17.4 Mb in the 21q22 locus needed to manifest DS (Niebuhr, 1974).

In the early 2000, the availability of the nucleotide sequence of Hsa21 (Hattori et al., 2000) together with the continuous reporting of new cases of PT21 and the introduction of higher resolution methods (such FISH and CGH array) allowed to further restrict the Has21 region involved in the DS manifestation (Hamerton, 1971;Daniel, 1979;Rahmani et al., 1989). The limits of 17.4 Mb region were further restricted thanks to the analysis of other PT21 cases (McCormick et al., 1989;Rahmani et al., 1989;Delabar et al., 1993) that allowed the identification of the Down syndrome critical region (DSCR) (Rahmani et al., 1989) converged in a small region within 21q22 and narrowed to 0.6 Mb. The concept of DSCR was postulated for the first time by Rahmani and coll. and indicate a region that causes the most critical and shared signs of DS (Rahmani et al., 1989).

Recently, a systematic reanalysis of all described cases of PT21 from 1973 to 2019 was performed (Pelleri et al., 2016;Pelleri et al., 2019) to identify subregions responsible for most common clinical findings: a recognizable form of ID and typical DS facies. It was demonstrated that the presence of a highly restricted Down syndrome critical region (HR-DSCR) of only 34 kb located on distal 21q22.13 from 37,929,229 to 37,963,130 shared by all subjects with PT21 and with diagnosis of DS (see Figure 3) (Pelleri et al., 2019). The HR-DSCR sequence was conserved during evolution in the *Hominidae* family, suggesting a role in the development of higher brain functions (Saber et al., 2016). It is described as an intergenic region but the strict association between HR-DSCR and diagnosis of DS deriving from clinical data suggests that it could contain active loci. In order to characterize the organization of the HR-DSCR locus it is necessary to conduct an intensive study of this region to identify unknown transcripts included in it.

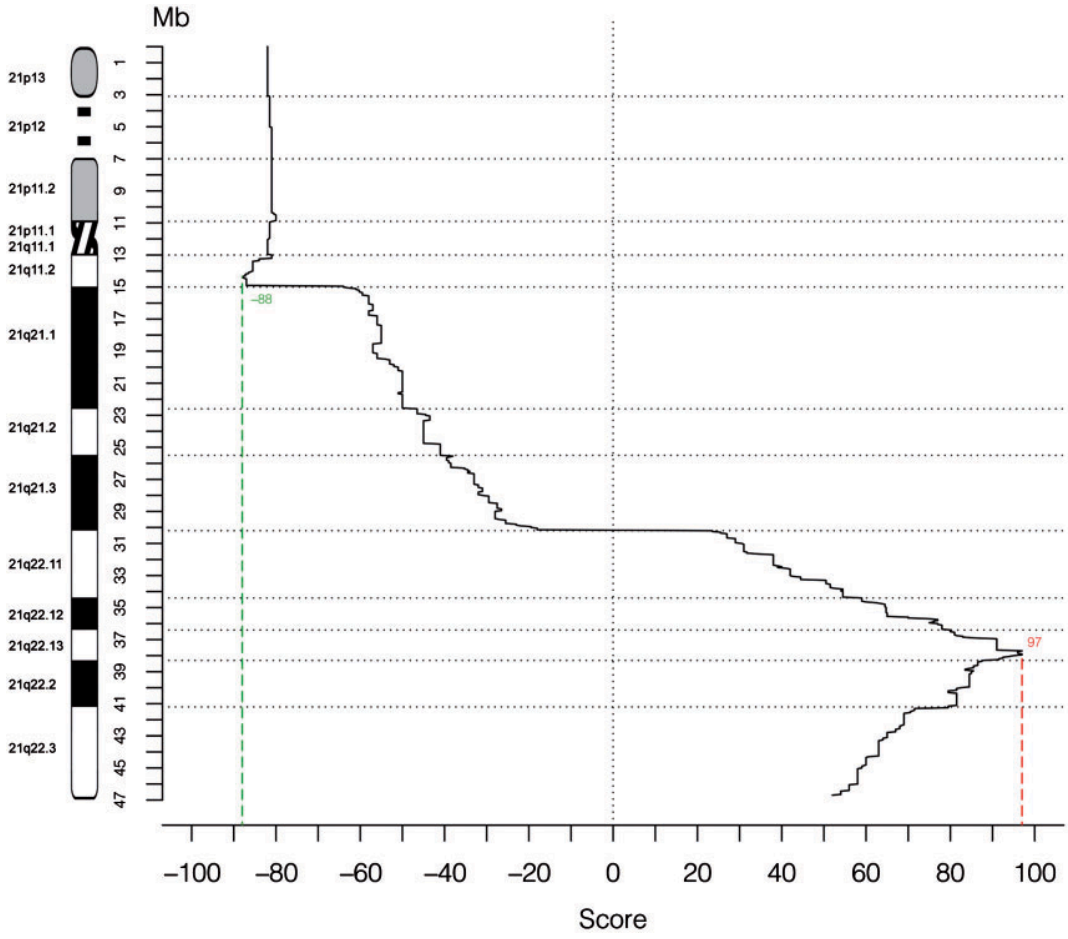

Figure 3. Genotype–phenotype correlation in 125 cases of partial trisomy 21. The X-axis displays the score for association with DS for each sequence interval of 50 kb, shown as median of the values assigned to each map row that is comprised in each interval. The Y-axis represents the position along Hsa21 (scale in Mb) (Published in Pelleri et al. 2016)

1.3 Transcriptome analysis

Studying a complex and not monogenic condition such as DS, a clear correlation between genetic cause and phenotypic effect might be difficult to find. Subjects with full trisomy 21 have three copies of the genes on Hsa21 and they present large individual phenotypic differences (Roizen and Patterson, 2003;Strippoli et al., 2019b;Bull, 2020). Theoretically, the supernumerary copy of Hsa21 is expected to result in a 50% increase in the level of transcripts of all genes mapping on Hsa21 and subsequentially, but there is evidence of under-expressed Hsa21 genes and dysregulation of genes located on other chromosomes than Hsa21 (Letourneau et al., 2014;Pelleri et al., 2018). The previous literature has showed that the genetic deregulation affects not only Hsa21 but also genes located on other chromosomes(Letourneau et al., 2014;Olmos-Serrano et al., 2016;Pelleri et al., 2018), indeed there is not always a direct correlation between genomic imbalance (deletion or duplication) and transcript level of genes (Lyle et al., 2004;Prandini et al., 2007). The expression levels of Hsa21 genes and the global gene expression of the whole genome have been profiling on

DS cells to assess their expression and their involvement in the pathogenesis of DS (Vilardell et al., 2011;Letourneau et al., 2014;Guedj et al., 2016).

Different studies conducted on trisomic cells deriving from different tissue or at different developing stage, suggest that the DS phenotype may be caused by both, the over expression of specific genes on Hsa21 and a generalized dysregulation of the genome as an indirect effect of the extrachromosomal copy, two mechanisms likely not mutually exclusive (Mao et al., 2003;Patterson, 2009;Weick et al., 2013;Olmos-Serrano et al., 2016;Sullivan et al., 2016;Antonarakis, 2017). In 2011, Vilardell and coll. (Vilardell et al., 2011), performed a meta-analysis of gene expression studies, integrating data from 45 different experiments on the transcriptome and proteome level conducted on trisomic human and mouse cells. The authors identified 324 genes with significant genome-wide dosage effects of which 77 are located on Hsa21 and 247 genes on other chromosomes. Proportionally, Hsa21 contributed mostly to the detected dosage effects; on the other hand, it is remarkable that only a third of all Hsa21 genes (77 out of 255) showed consistent effects across the different experiments (Vilardell et al., 2011), confirming the complexity of the gene expression regulation in trisomy 21.

In 2018, Pelleri and coll. (Pelleri et al., 2018) performed a systematic selection of all the available trisomic vs. normal microarray experiments from different human tissues. Thanks to TRAM (Transcriptome Mapper) software (Lenzi et al., 2011), transcript expression levels between trisomic and euploid condition was compared in brain, lymphoblastoid cell lines (LCL), blood cells, fibroblasts, thymus and induced pluripotent stem cells (iPSCs) (Pelleri et al., 2018). TRAM is a software able to combine, normalize, and integrate datasets from different sources and across different experimental platforms, and to generate a quantitative expression value for each gene and segmental trend of gene expression along each chromosome (Lenzi et al., 2011;Vitale et al., 2017). Regarding whole chromosomes, the DS/normal expression ratio showed that the most over-expressed chromosome is Hsa21, specifically the 21q22 band (Pelleri et al., 2018). A functional enrichment study of over- and under-expressed genes in all the genome reported as altered genes involved in embryogenesis, cell growth and neurogenesis consistent with previous studies (Lockstone et al., 2007;Weick et al., 2013). Moreover, the functional enrichment analysis of Hsa21 genes with expression ratio ≥1.30 showed that the most enriched Hsa21 molecular functions, might be related to the one carbon cycle including the folic acid cycle and the homocysteine pathway, involving the *CBS*, *GART* and *FTCD* gene products (Pelleri et al., 2018).

In 2019 Araya and coll. analysed transcriptome data from White Blood Cells (WBCs) from 19 individuals, 10 of them with T21, underlining in subjects with DS a general state of autoimmunity with interferon hyperactivity (Araya et al., 2019). Four of the 6 interferon (IFN)

receptor subunits (IFNRs), involved in immune control, are encoded by Hsa21 (Sullivan et al., 2016), suggesting a role of the extra chromosome in the immune dysregulation. Analysis of differentially expressed genes (DEGs) revealed that T21 causes a distinct gene expression signature consisting of 497 down-regulated messengers RNAs (mRNAs), and 406 up-regulated mRNAs 96 of which encoded on Hsa21. The transcriptome analysis showed a consistent activation of the IFN transcriptional response including elevated levels of proinflammatory cytokines, such as IL-6, TNF-α, MCP-1, and IL-22 and a higher number of CD8+ T cells, in T21 (Araya et al., 2019). These results are coherent with the T cell dysregulation associated with IFN hyperactivity as a contributor to autoimmunity in DS.

In 2019, Sobol and coll. performed a transcriptome profile of neural derivates from induced pluripotent stem cells (iPSCs) with T21, in order to study the molecular perturbation in DS cells during the neurogenesis (Sobol et al., 2019). Two DS and three healthy iPSCs lines were induced to a self-renewing neural progenitor cell (NPC) stage and to a more differentiated neural stage (DiffNPC) by non-directed differentiation for 30 days (Falk et al., 2008) 2012. In trisomic NPCs the transcriptome analysis identified 922 differentially expressed genes (DEGs), 734 of which upregulated; while in DiffNPC the corresponding number of DEGs was 879, 634 of which upregulated. In trisomic NPCs, 10.6% of Hsa21 genes were found upregulated compared to an average of 3.4% for non Hsa21 genes. The number of upregulated Hsa21 genes in DiffNPC increased to 17.8% compared to an average of 2.8% on all the other autosomes. Trisomic cells at the early NPC stage showed a general but non-significant down regulation of the mitochondrial (MT) genes, while they were significantly down regulated in trisomic DiffNPCs. These observations indicate a pronounced down regulation of MT transcription with differentiation in T21 neural lines. This founding is in line with previous studies on cardiac tissue and fibroblast from DS cases supporting a ubiquitous down regulation of mitochondrial activity (Conti et al., 2007). Transcriptome analysis reported an elevated expression of *GFAP*, *VIM* and *S100*B in trisomic lines, mainly at the NPC stage, consistent with increased formation of glia cells and astrocytes in DS (Colombo et al., 2005), a slight reduction in expression of genes for neuronal marker such as *LMX1B*, and a general deregulation of myelination process (6–7-fold down-regulation of transcription factors *OLIG1* and *OLIG2* in trisomic NPCs). The strongest dysregulations in DiffNPCs were observed for *CYYR1*, encoding a Shisa-protein implicated in growth factor receptor activity (Justice et al., 2017), and for *C2CD2*, encoding a transmembrane protein with yet unclear functions. The strongest and most consistent upregulation at both NPC and the DiffNPC stages was identified for *RUNX1* encoding the transcription factor *AML1*, supporting its recently reported role in DS neurogenesis (Halevy et al., 2016). The analysis, based on both transcriptome and proteome

data, showed dysregulation of DNA-replication, collagen, cell-adhesion, ECM-receptor interactions, integrin complex, TGF-ß signalling, oxidative phosphorylation and glycolysis at both stages, and dysregulation of pluripotency, synaptic maturation, neuroactive signalling and collagen binding clusters only at NPCs stage (Sobol et al., 2019). These observations suggest that regulation of cell growth and transition from a progenitor stage are predominant defects at an early stage in trisomic neural cells. These data correlate with Vilardell and coll. with a 23% of homology for the genes in NPCs and 38% in DiffNPCs, including *SOD1*, *APP* and *RUNX1* (Vilardell et al., 2011).

In 2021, De Toma and coll. performed a meta-analysis integrating the differential expression (DE) analyses of all publicly transcriptomic data (67 studies, 56 from published articles by 24/01/2020) of trisomic and euploid samples of human and mouse models (most frequent was the Ts1Cje model, followed by the Ts65Dn) (De Toma et al., 2021). Their analyses included microarray and high-throughput RNA sequencing (RNA-Seq) experiments derive from different tissues and organs, in particular "Blood/bone marrow", "Brain", "Endothelial", "Fibroblasts", "Heart", "Liver", "Muscle", "Placenta/amnios", and "Undifferentiated". They detected 51902 genes across all comparisons and reported 147 up-regulated genes and 35 down-regulated genes, 67/147 of the consistently up-regulated genes were on Hsa21 (66% of DE genes), and 80/147 mapped on other chromosomes. As expected, most of the comparisons showed an upregulation of around 1.5-fold for Hsa21 genes and when zooming in to the band level, the band with the highest number of consistently DE genes was the 21q21.3 and the complete 21q22 confirming by Pelleri and coll. as over-expressed (Pelleri et al., 2018). However, some Hsa21 genes were also down-regulated, as previously described (Vilardell et al., 2011) and none of mapped on Hsa21, even though some Hsa21 genes were down-regulated in specific comparisons. They hypothesized that the consistently down-regulated genes could be targets of micro-RNA (miRNA) mapping on Hsa21 (Jonas and Izaurralde, 2015) since miRNAs are known to play a role in DS phenotype (Brás et al., 2018). Other genes could be downregulated because of specific deletions in mouse models. They built a network in which each node is a gene found consistently DE, and each edge connects two genes that are co-differentially expressed. They detected 4 principal clusters: the first included genes involved in acute megakaryoblast leukaemia (AMKL) and acute myeloid leukaemia (AML), both reported with an increase frequency in DS subjects (Laurent et al., 2020); the second included genes involved in hydroxymethyl and formyl pathways, the third cluster is involved in neuronal differentiation, aging and extracellular matrix regulation; and the fourth included genes related to inflammation and ubiquitin systems, reinforcing the concept that DS is an inflammatory disease. Two clusters out of four including the Hsa21 *SOD1* gene. *SOD1* was found preferentially DE in the brain, blood, fibroblasts and placenta/amnios, and was the gene with the highest number of gene-disease

associations (GDAs) including nerve degeneration, hyperthyroidism, hypertensive disease, diabetes mellitus and depressive disorders, which are known comorbidities in DS (De Toma et al., 2021). A highly significant overlap with the "DS genes" is found with Vilardell and coll. (Vilardell et al., 2011) but their analysis included 9 times more comparisons and 8 times more transcriptomic studies revealing 421 DS genes not previously identified.

In conclusion, these studies confirm that the genome wide deregulation produced because of T21 is not arbitrary but involves deregulation of whole molecular cascades in which both Hsa21 genes and Hsa21 interactors are more consistently deregulated compared to other genes. In addition, the gene expression alteration seems to be linked with the marked alterations in various Krebs cycle and one-carbon intermediates, pathophysiological depletion of high energy phosphates and with a general state of inflammation and aging process reported in DS.

1.4 Down syndrome and metabolic alterations

1.4.1 Down syndrome as a progeroid syndrome

Down syndrome has been proposed by George Martin as a segmental progeroid syndrome since 1978 involving some but not all organs and tissues (Martin, 1978). The idea of the accelerated aging disorder in trisomic subjects is supported by three different evidences: clinicopathological features; high levels of age-associated biomarkers; acceleration of molecular mechanisms of aging (Franceschi et al., 2019).

Concerning clinicopathological features, subjects with DS are characterized by accelerated cognitive decline with a high incidence of early-onset Alzheimer-like dementia (Perluigi et al., 2020), chronic oxidative stress (Valenti et al., 2011;Garlet et al., 2013), aging of central nervous system (Lott, 2012) and of the immune system (Gensous et al., 2020). From the immunological point of view, NK cell activity is diminished, the number of T and B lymphocytes is decreased, T lymphocytes's telomeres are interested by erosion, and the risk of autoimmune disorders is increased compared with euploid subjects. Trisomic subjects present other age-associated diseases including hypothyroidism (Amr, 2018;Whooten et al., 2018), osteoporosis and osteopenia (García-Hoyos et al., 2017), overweight (Xanthopoulos et al., 2017), visual and hearing impairment (Evenhuis et al., 2001).

A biological parameter able to predict the lifespan better than chronological age is the so-called biomarker of age (Baker and Sprott, 1988;Butler et al., 2004;Johnson, 2006). So far, four different biomarkers of age namely: telomere shortening, GlycoAgeTest, Horvath's epigenetic clock, and brain predicted age, have been analysed in DS persons (Franceschi et al., 2019).

Telomere attrition is a well-established marker of age, and their shortening has been associated with age decline (Vaiserman and Krasnienkov, 2020). It has been demonstrated that DS persons have shorter telomeres than age-matched controls (Vaziri et al., 1993). The GlycoAgeTest derives from the relative amounts of N-glycans of plasma which increases with age after 40 years (Vanhooren et al., 2007;Vanhooren et al., 2009;Dall'Olio et al., 2013). Recently, Borelli et al. investigated N-glycomic profiles in 76 DS persons, as compared with their mothers and siblings, and demonstrated that GlycoAgeTest values resulted increased in DS persons as compared to their siblings (Borelli et al., 2015). Epigenetic aging biomarkers, which rely on the widespread DNA methylation changes occurring with age (Field et al., 2018;Horvath and Raj, 2018), and one of the widely used epigenetic biomarkers of age is Horvath's epigenetic clock (Horvath et al., 2015). Epigenetic clocks, which measure changes in a few hundred specific CpG sites, can accurately predict chronological age in a variety of species, including humans. A small fraction (~2%) of the CpG sites show age-related changes, either hypermethylation or hypomethylation with aging.

In 2015 Horvath and coll. studied DNA methylation in series of human tissues across a range of chronological ages, analysing the DNA methylation levels of 353 specific CpGs (Horvath et al., 2015). DNA methylation levels were assessed in peripheral blood leukocytes, various brain regions, whole blood and buccal epithelium. As expected, DNA methylation age has a strong positive correlation with chronological age in the control samples. They detected CpGs that are hypermethylated in DS subjects and have a positive correlation with age acceleration; and two CpGs that are both hypomethylated in DS subjects and have a negative correlation with age acceleration. According to this study, DS persons resulted as significantly older than their calendar age, with an age acceleration ranging from 2.8 years in buccal cells to 11.5 years in brain (Horvath et al., 2015). More recently, they investigated whether accelerated aging in DS is already detectable in blood at birth (Xu et al., 2022), demonstrating that accelerated epigenetic aging in the blood of DS patients begins prenatally, with implications for the pathophysiology of immune-senescence and other aging-related traits in DS.

In 2015 Bacalini and coll. used the Infinium HumanMethylation450 BeadChip to investigate DNA methylation patterns in whole blood from 29 DS persons, using their relatives (mothers and unaffected siblings) as controls (Bacalini et al., 2015). Although differentially methylated regions (DMRs) displayed a genome-wide distribution, they were enriched on chromosome 21. DMRs mapped in genes involved in developmental functions, including embryonic development (*HOXA* family) and haematological (*RUNX1* and *EBF4*) and neuronal (*NCAM1)* development. Moreover, genes involved in the regulation of chromatin structure (*PRMD8, KDM2B, TET1*) showed altered methylation. Their analysis supports the perspective of DS as a developmental disease (Briggs et

al., 2013), as many of the identified DMRs are involved in morphogenetic and developmental processes that are established early during development (Kusters et al., 2009).

Cole et al., 2017, reported a trend of accelerated aging in DS brains by using a magnetic resonance imaging (MRI) (Cole et al., 2017). The analysis of MRI data observed a brain predicted age difference of 7.69 years between adult DS persons and age-matched controls (Cole et al., 2017).

Recently, three independent studies started to dissect the epigenetic characteristics of DS, describing the DNA methylation patterns of different tissues at the genome wide level (Kerkel et al., 2010;Eckmann-Scholz et al., 2012;Jin et al., 2013). The studies were concordant in showing marked DNA methylation alterations in DS cells that were not enriched in Hsa21 but were spread across the entire genome. Those studies underline that the main molecular mechanisms involved in the aging process are markedly altered in DS, including DNA methylation processes that are involved in the development of nervous and immune systems.

1.4.2 Down syndrome and oxidative metabolism alterations

Mitochondrial abnormal activity has been documented in DS, in particular, an accumulation of damaged mitochondria and a fragmentation of the mitochondrial network was observed in trisomic cells suggesting a decline of biogenesis and turnover of the mitochondria (Piccoli et al., 2013;Izzo et al., 2017;Mollo et al., 2020). It has been also demonstrated a significant decrease in respiratory capacity, mitochondrial membrane potential and ATP production, as well as an increase of oxidative stress, in trisomic cells (Helguera et al., 2013;Caracausi et al., 2018;Rueda Revilla and Martínez-Cué, 2020).

Mitochondria are organelles that mainly control energy conversion in the cell, and participate in many relevant activities, such as the regulation of apoptosis and calcium levels, and other metabolic tasks, all closely linked to cell viability. Mitochondrial homeostasis is based on the interplay between mitochondrial biogenesis and mitophagy, two processes that regulate intracellular mitochondrial content and organization. The multiple functions of mitochondria are mechanistically linked to their morphology, which is defined by ongoing events of fission and fusion of the outer and inner membranes (Cogliati et al., 2016), mutations or loss of the fission proteins block mitochondrial division, shifting the balance towards fusion ((Smirnova et al., 2001).

Many genes and mitochondrial RNA mapping on Hsa21 are dysregulated in trisomic tissues. Several of the up-regulated genes in DS are indirectly involved in mitochondrial function and morphology (Izzo et al., 2018), while genes involved in oxidative phosphorylation are mostly down-regulate, indeed it is documented that trisomy of Hsa21 negatively affects mitochondrial function (Valenti et al., 2017;Pecze et al., 2020). DS individuals have a lower resting metabolic rate

compared with control subjects, impaired exercise tolerance (Allison et al., 1995); marked alterations in various Krebs cycle intermediates, pathophysiological depletion of high energy phosphates and a suppression of the cellular energy charge, pointing to the existence of a cellular 'pseudohypoxic' state (Pecze et al., 2020).

In 2021 Pecze and coll. have conducted a meta-analysis of transcriptomic alterations in DS, with special attention on the genes encoding enzymes involved in mitochondrial processes, bioenergetic mechanisms and cellular metabolism (Pecze and Szabo, 2021). They identified 17,805 genes: the number of downregulated genes was 1003 and the number of upregulated genes was 912. As regards Hsa21 genes, 109 were found to be upregulated and none were found to be downregulated. This means that more than 60% of genes mapped on Hsa21 are significantly upregulated. Interestingly, genes related to oxidative phosphorylation are mostly downregulated in DS: the activity of Complex IV was found to be significantly inhibited in DS cells due to the inhibitory effect of the upregulation of the endogenous gaseous transmitter hydrogen sulfide (H2S) (Panagaki et al., 2019;Panagaki et al., 2022). *CBS* encoding the cystathionine ß-synthase (*CBS*) mapped on Hsa21, shows a significant upregulation in DS ("gene dosage effect"), and it is involved in the production of H2S, a gaseous signalling molecule (Szabo, 2020;Panagaki et al., 2022).

Genes related to oxidative phosphorylation are mostly downregulated in DS one of those is *PFKL* encoded the liver (L) subunit of phosphofructokinase (Magnani et al., 1987;Panagaki et al., 2019). This enzyme catalyses the conversion of D-fructose 6-phosphate to D-fructose 1,6-bisphosphate. Five genes related to oxidative phosphorylation were detected to be upregulated *(NDUFV3, COX15, ATP5PF, ATP6V1H, ATP5PO*), and out of these five genes, three of them are mapped to chromosome 21 (*ATP5PF, NDUFV3* and *ATP5PO*). Nine genes related to oxidative phosphorylation were identified to be downregulated (*NDUFS2*, *NDUFS1, NDUFA10, COA1, ATP5MC1, ATP5F1E, ATP12A*), their products are essential constituents of Complex I (NADH dehydrogenase), Complex II (Succinate dehydrogenase), Complex III (Ubiquinol cytochrome C oxidoreductase), Complex IV (Cytochrome C oxidase) and ATP synthase (which is not an electron transporter, and its former, somewhat misleading designation is mitochondrial Complex V) (Pecze and Szabo, 2021). The coordinated function of the four electron transport complexes and the subsequent function of ATP synthase are essential for aerobic ATP generation in the mitochondria of all mammalian cells. Dysregulation of these genes would predict significant disturbances in aerobic ATP generation.

Prior studies showed the flux in oxidative phosphorylation is reduced in DS while, fluxes in glycolysis, citric acid cycle, lactate levels, lipid metabolism pentose and phosphate pathway are upregulated in DS cells compared to control (Tanner et al., 2018;Ascenção et al., 2021). All these

findings point to an increased glycolytic flux in DS, perhaps as a compensatory reaction to the suppression of mitochondrial (aerobic) ATP generation.

The mitochondrial network of DS human fibroblasts appeared highly fragmented with an increased number of shorter mitochondria and a smaller average mitochondrial volume (Izzo et al., 2018). The disruption of mitochondrial network has been also reported in trisomic mouse embryonic fibroblasts (MEFs) (Zamponi et al., 2018), in astrocytes and neurons (Helguera et al., 2013). Electron microscopy data of trisomic fibroblasts and neurons revealed a significant number of damaged mitochondria, with broken, shorter, concentric or highly swollen cristae (Piccoli et al., 2013;Izzo et al., 2018).

The PGC-1α and mTOR pathways regulate mitochondrial dynamics playing a central role in the control of fission/fusion and biogenesis/mitophagy processes. They are closely interconnected, and both involved in the organization of the mitochondrial network architecture (Mollo et al., 2020). What emerges clearly from the scientific literature is that both these pathways are altered in DS (Valenti et al., 2010;Valenti et al., 2011) PGC-1α pathway is inhibited, while mTOR signalling is hyperactive (Iyer et al., 2014). This leads to fragmentation of mitochondrial network and accumulation of damaged mitochondria.

1.4.3 Down syndrome and one carbon cycle alterations

Several authors reported one carbon cycle as imbalanced in subjects with DS (Lejeune, 1979;Rosenblatt et al., 1982;Peeters et al., 1995;Song et al., 2015;Funk et al., 2020). One-carbon metabolism is a universal metabolic process in which mono-carbon units at different oxidation state were transfer for the biosynthesis of several metabolites. It is involved in DNA synthesis (purine and pyrimidine synthesis) (Zöllner, 1982); amino acid homeostasis with the production of several amino acid included glutamate, glycine and cysteine necessary to produce glutathione involved in the antioxidant generation (Lu, 2013); and in the epigenetic regulation by methionine-homocysteine cycle where there is the generation of S-adenosyl-methionine (SAM) the major methyl donor for DNA methylation (Gao et al., 2018). This biochemical pathway is driven by folate and methionine-homocysteine cycle.

Figure 4 is a simplify scheme of folate and methionine-homocysteine cycles and it shows how those cycles and their metabolites are interconnected. Folate or vitamin B9 is the form of folate that we normally intake by diet, it is sequentially reduced to first dihydrofolate (DHF) and then in its biologically active forms tetrahydrofolate (THF) which can enter in the folate cycle. THF after the addiction of a formate group and multiple reaction could be convert into 5-methyl-THF or 5-formyl-THF. 5-formyl-THF, does not play a direct biosynthetic role, but it is a reserve of one

carbon unit in cells; 5-methyl-THF is the most representative folate form in plasma and the only form able to cross the blood-brain barrier (Grapp et al., 2013). 5-methyl-THF is the major donor of the methyl group for the conversion of homocysteine (Hcy) to methionine (Met) which can be subsequentially transformed into S-adenosyl-methionine (SAM) require for more than 100 methylation reactions including DNA methylation (Bottiglieri and Reynolds, 2010;Bottiglieri, 2013). The ratio between SAM and SAH is a well know indicator of cellular methylation capacity (Obeid et al., 2012).

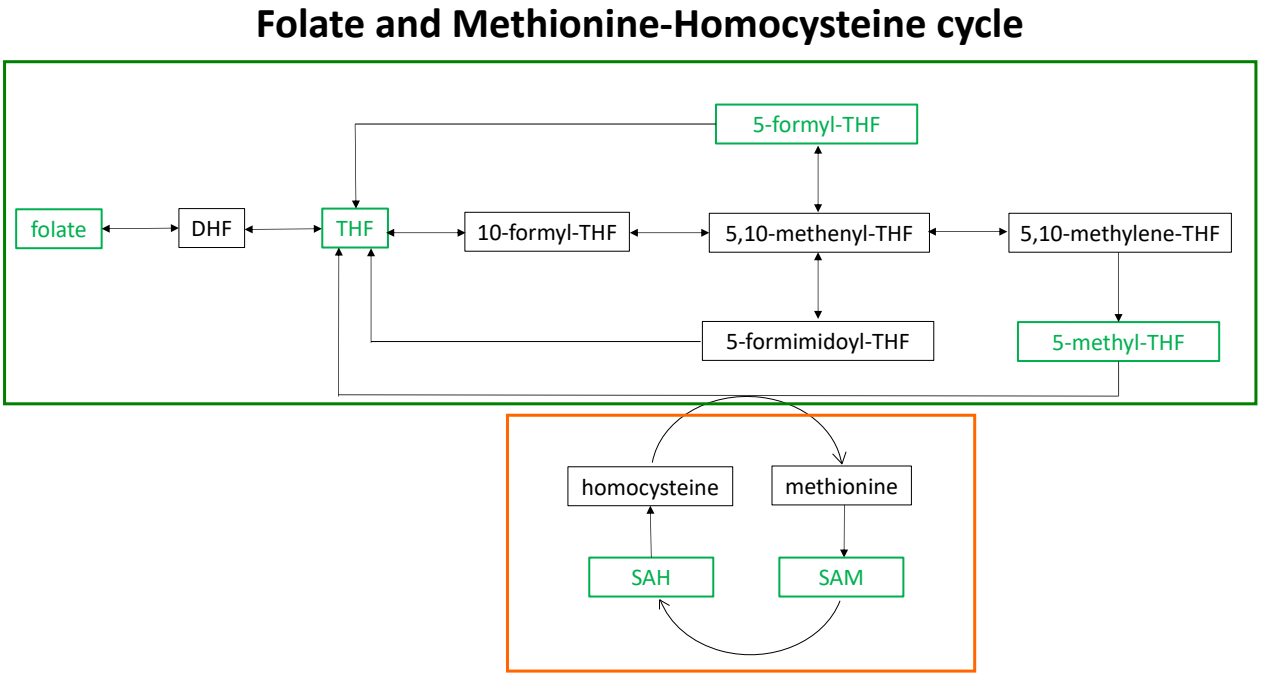

Figure 4. Simplify scheme of folate and methionine-homocysteine cycles. The scheme represents folate cycle (in green) and methionine-homocysteine cycle (in orange), and it shows how those cycles, and their metabolites are interconnected.

Looking at the complete scheme of folate cycle obtained by KEGG pathway database (see Figure 5) it is possible to note that THF is the product of ten different enzymatic reaction, most of which reversible. This redundant scheme suggests a rescue mechanism to ensure the THF production, indeed, it is well known that folate cycle alterations were involved in early neurodevelopment defects such as neural tube defects and could cause neurological and neuropsychiatric disorders (Pope et al., 2019).

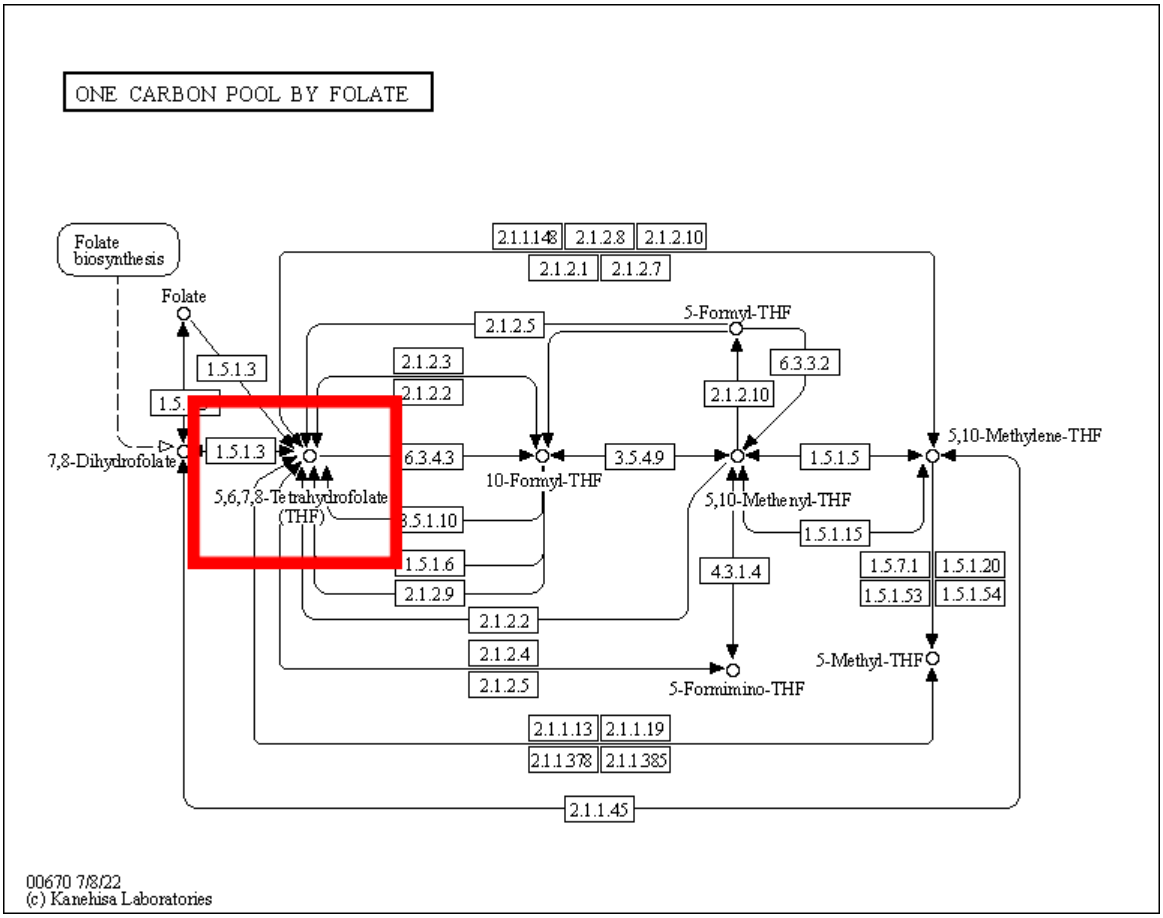

Figure 5. One-carbon cycle obtained by KEGG pathway database. THF, highlight in the figure in red, is the final product of ten different enzymatic reaction.

Cerebral folate deficiency (CFD) are conditions associated with developmental delay and/or regression, progressive ataxia and movement disorders (Pope et al., 2019). These conditions are characterized by a low level of 5-methyl THF which represent the major folate specie in the cerebrospinal fluid even in the presence of normal peripheral levels of 5-methyl-THF. They could be due to inborn errors of folate metabolism such as deficiency of receptors or enzymes involve in folate pathway (Banka et al., 2011;Cario et al., 2011;Rodan et al., 2018); or they could have secondary causes such as drug effects, immune response and oxidative stress (Ramaekers et al., 2005;Garcia-Cazorla et al., 2008;Vezmar et al., 2009). Lejeune was the first to hypothesize that DS could be a metabolic disease and to observe a folate deficiency in trisomic cells, showing that methotrexate (MTX) was twice as toxic in trisomic lymphocytes compared to euploid ones (Lejeune et al., 1986). MTX is a cytotoxic drug used as chemotherapeutic agent and it is a folic acid analogue able to inhibit cellular proliferation. The increase sensitivity in Down syndrome cells to the toxic effect of MTX suggest a folate cycle alteration. In a recent survey, erythrocyte folate concentrations in children with DS were compared with a cohort of subjects with juvenile arthritis as euploid control, in order to understand if the MTX treatment toxicity in children with DS is

related to altered erythrocyte folate concentrations. They reported a lower concentration level of total folate, 5-methyl-THF and 5,10-methenyl-THF in the erythrocytes of subjects with DS. These reductions in erythrocyte folates were also associated with a decrease in short-chain folate polyglutamation 5-methyl-THFGlu3-6 and a corresponding increase in longer chain 5-methyl-THFGlu7-10 (Funk et al., 2020). These data suggest that in trisomic cells there is a biological adaptation to folate deficiency by an increased level of long-chain folate polyglutamation; indeed, increased expression of folylpolyglutamate synthetase (*FPGS*) gene was already reported in vitro and in animal models (Ifergan et al., 2004;Pelleri et al., 2018;Funk et al., 2020). Focusing on one carbon cycle alteration observed in Down syndrome, one of the key enzymes involved in this pathway is CBS, encoded by Hsa21 and reported as over-expressed in trisomy 21 cells (Szabo, 2020). CBS permanently removes Hcy and serine to obtain cystathionine and, subsequently, cysteine. Its overexpression in trisomic cells could be link with the increase levels of cysteine and cystathionine, and to a reduce availability of Hcy and Met reported in Down syndrome (Pogribna et al., 2001;Pereira et al., 2004;Obeid et al., 2012;Watkins and Rosenblatt, 2012). SAM and SAH levels were found to be higher in young individuals with DS with a SAM/SAH ratio decrease compare with healthy subjects (Obeid et al., 2012;Gao et al., 2018). A low SAM/SAH ratio indicate a general state of hypomethylation which is connected to aging acceleration, supporting the notion that DS is a progeroid trait (Obeid et al., 2012). Folate metabolism plays a role in the catabolism of choline, histidine, serine and glycine (Brosnan et al., 2015); and support critical cellular functions such as cell proliferation, mitochondrial respiration and epigenetic regulation (Mattson and Shea, 2003). The purine metabolism, in particular adenosine and uric acid, is increase in subjects with DS and the overexpression of *GART* gene, located on Hsa21, seems to have a role in this alteration being involve in the novo purine synthesis (Knox et al., 2009;Mazzarino et al., 2021;Pareek et al., 2021). Down syndrome is also associate to an increase of creatine and creatinine synthesis, both involved in the process of energy-dependent muscle activity, this alteration together with an increase of formate levels suggest a one carbon alteration in mitochondria (Caracausi et al., 2018). Finally, a lower level of folate and vitamin B12 were found in DS subjects compared with healthy ones (Song et al., 2015;Gao et al., 2018). Figure 6 shows the metabolites and genes reported as altered in subjects with DS by previous literature.

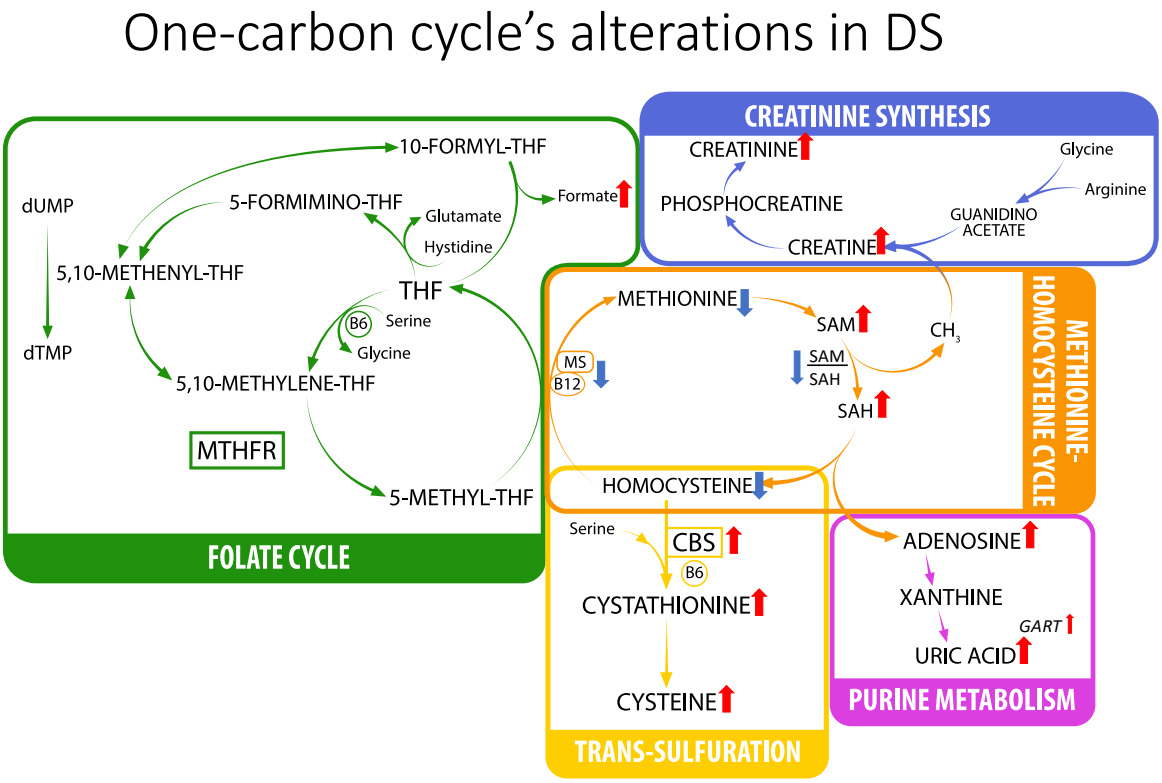

Figure 6. One-carbon cycle's alterations in subjects with DS. The figure shows the one-carbon pathway including: folate cycle (in green), homocysteine-methionine cycle (in orange), trans-sulphuration pathway (in yellow), and purine metabolism (in purple). Red arrows pointing up indicate metabolites or genes reported as increase in DS. Blue arrows pointing down indicate metabolites or genes reported as decrease in DS.

1.5 Models of trisomy 21

1.5.1 Human cellular models of trisomy 21

Primary cells obtained by subjects with DS have been extensively used over decades to model cellular and molecular features of T21, such as cell proliferation, enzyme activity, gene expression, and DNA repair (Vitale et al., 2019). The most used model were fibroblast and lymphocyte cell lines, because of the facility of the obtainment. These in vitro models are useful to study general characteristics of T21 cells, but lack the proximity to neural cell types likely to be involved in the mechanisms leading to ID. More recently, an induced pluripotent stem cell (iPSC) model has emerged, that may be induced to differentiate toward various cell types and tissues (Antonarakis, 2017), thus elucidating the role of Hsa21 genes by comparing effects of their trisomic or disomic (control) state in a certain cell type. Human T21 iPSC lines have been obtained by fibroblasts of

subjects with DS or by amniocytes, along with relative control euploid cells. The first report about T21 iPSCs was published in 2008 (Park et al., 2008) and has been followed by reports studying T21 iPSCs differentiated in neurons (Bhattacharyya et al., 2018), hematopoietic progenitors (Maclean et al., 2012), and recently astrocytes (Araujo et al., 2018). iPSCs have been shown to be useful for the study, among others, of genetic and neural developmental features of DS etiology (Briggs et al., 2013). Possible pitfalls of the iPSC model include the possibility that they suffer deep genotype rearrangements (Sobol et al., 2015) or spontaneous chromosome loss (Li et al., 2012). Due to variability of iPSC lines produced even from a single sample, it has been suggested that more than one such iPSC line per sample should be produced (Antonarakis, 2017). Finally, the obtainment in vitro of T21 cells with a copy of *XIST* transferred through zinc finger nucleases (ZNFs) in one Hsa21 resulting in an inactivation of one extra copy of the chromosome (Jiang et al., 2013) paves the way for the study of the differences between T21 and functionally euploid cells of the same line. This possibility was first foreseen in a therapeutic perspective by Lejeune when in 1977 he proposed "turning off the extra chromosome by some kind of induced inactivation (like the lyonization of supernumerary X chromosomes)" (Lejeune, 1977), when the basic mechanism of this inactivation was still unknown. The discovery of *XIST* as the gene able to switch off one of the two X chromosomes in female cells through production of a large noncoding RNA responsible for X heterochromatinization (lyonization) (Clemson et al., 1996) made this option available in an iPSC model by the same group (Jiang et al., 2013). While there are also some limits in this model (5% of the Hsa21 genes remain active and they could maintain a possibly significant part of the phenotype or the two homologous chromosomes remaining active might be the ones from the same parent thus leading to uniparental disomy), it has recently been used to demonstrate normalization of hemopoietic defects in vitro following Hsa21 inactivation through *XIST* (Chiang et al., 2018).

1.5.2 Animal models of human trisomy 21

The most useful animal model would in theory be a trisomic chimpanzee, being that *Pan troglodytes* is the animal with the genome, anatomy, and physiology most like humans. In addition, chimpanzees appear to date to be the only animal with a naturally occurring aneuploidy equivalent to human T21, with a case being described in 1969 (McClure et al., 1969) and a new case recently in 2017 (Hirata et al., 2017). However, due to difficulty and costs of chimpanzee maintenance, they are of very limited use in DS research as well as in research in general. The basis for the proposal of mice as a model organism for DS was the fact that both mice and humans belong to the mammal class and there is the conservation of many protein coding genes between Hsa21 and murine (Mmu) chromosomes 10, 16, and 17 (Edgin et al., 2012). The first, and still most used, mouse model for

T21 was obtained by Davisson in 1990 establishing Ts65Dn, a murine strain with a segmental trisomy of Mmu16, limited to the part of the chromosome homolog to Hsa21 (Davisson et al., 1990). Since then, many other murine models have been proposed and they are reviewed in several articles (Liu et al., 2011;Edgin et al., 2012;Kleschevnikov et al., 2012;Rueda et al., 2012). One of the recent strains has rearranged Mmu16, Mmu17, and Mmu10 in order to possibly include trisomy of the full spectrum of Hsa21 genes with orthologs on mice (Yu et al., 2010). Nevertheless, mice mimicking DS remain difficult to grow and breed, and great differences still exist between the two species, hampering a direct translation of evidence derived from the murine DS model to humans (Bhattacharyya et al., 2018). For instance, memantine was reported to be effective in DS model mice but it was shown to be ineffective in adults with DS (Hanney et al., 2012) and to ameliorate some abilities in young adults with DS (Boada et al., 2012). Therefore, while mouse models for DS appear to be a very common approach to the study of T21, attention should be brought to the known multiple limits of these models (Nelson and Gibbs, 2004), when comparing the impairment of superior functions exclusive of human intelligence (Lejeune, 1966) such as abstraction and language, specifically damaged in DS, to alterations of mouse behaviour (Nuffield Council on Bioethics, 2002). Finally, although murine *Kcnj6* and *Kcnj15* are syntenic with the human orthologs, no relevant homology may be found in the mouse genome with the HR-DSCR sequence itself that is located between *KCNJ6* and *KCNJ15* in humans (Pelleri et al., 2016).

2. AIM OF THE THESIS

The aim of the thesis is to uncover genotype-phenotype relationships in DS possibly useful to devise therapies based on the molecular and cellular mechanisms. The project is based on the hypothesis that an extra copy of all or part of Hsa21 triggers developmental mechanisms leading to alterations in gene expression and metabolic profile and eventually cognitive decline in DS.
In this work, we have investigated different aspects of Down syndrome:

- in collaboration with Prof. Silvia Lanfranchi, University of Padua, we have evaluated the cognitive impairment in children with DS analysing possible correlations to clinical or molecular data.

- We have analysed genomics of DS through the study of PT21 cases, very rare cases of segmental trisomy in which only a delimited part of Hsa21 is duplicated. New PT21 cases, reported in our study, confirm the hypothesis of HR-DSCR, the only region of Hsa21 present in three copies on PT21 case with DS diagnosis and never duplicated in PT21 cases without diagnosis of DS. Moreover, we have characterized new transcripts included in the HR-DSCR.

- We have studied gene expression level alteration through RNA-Seq on blood cells of children with DS.

- Metabolic alterations in plasma of children with DS were identified through different methods: NMR, routine blood exams performed during the follow up of the subjects and enzyme-linked immunosorbent assay (ELISA).

- To test possible correlation between specific Hsa21 regions and alterations in transcriptomics and metabolomics, we have used trisomic iPSCs and differentiated them into neuronal derivatives, in collaboration with Prof. Niklas Dahl, Uppsala University, Sweden.

Significant alterations in gene expression and metabolic profiles have been identified, as well as significant correlations with clinical and cognitive aspects. Nevertheless, the genetic cause of these alterations is unknown. Specific genes and the HR-DSCR may play a role in these alterations. Cell models need to be developed to investigate correlations between genotype (complete or partial trisomy 21) and phenotypes (gene expression and metabolic alterations). Neural derivatives from trisomic iPSCS are a promising model to better understand genotype-phenotype correlations in DS.

3. MATERIAL AND METHODS

All methods were performed in accordance with the Ethical Principles for Medical Research Involving Human Subjects of the Helsinki Declaration. The present study was approved by the independent Ethics Committee of the University Hospital St. Orsola-Malpighi Polyclinic, Bologna, Italy (approval no. 39/2013/U/Tess). Inclusion criteria for subjects with DS were diagnosis of DS with homogeneous or mosaic T21 and minimum age of 3 years. Clinical information and biological sample were collected in the context of the annual follow-up at the Unit of Neonatology of St. Orsola-Malpighi Polyclinic in Bologna, Italy**.** Cognitive assessment was carried out thanks to the collaboration with the Department of Developmental Psychology and Socialisation, University of Padua, Padua, Italy.

3.1 Down syndrome: main clinical features

3.1.1 Cognitive profile of DS

The DS cognitive phenotype is usually characterized by relative strengths in non-verbal skills and deficits in verbal processing, but high interindividual variability has been registered in the syndrome (Silverman, 2007;Grieco et al., 2015). The following studies have the aim to clarify which factors have a major role in shaping the cognitive variability involved in the syndrome and give information on the cognitive heterogeneity of children and adolescent with DS. In particular, in Locatelli et al. 2021 (Locatelli et al., 2021) we described the acquisition of developmental milestones and their relationship with subsequent development of child with DS; in Onnivello 2022 et al. (Onnivello et al., 2022a) we explored the executive functions (EFs) and adaptive behaviour in DS, finally in another study by Onnivello et al. 2022 (Onnivello et al., 2022b) we analysed the cognitive profile, considering verbal and non-verbal intelligence, of children/adolescents with DS, also taking into account interindividual variability.

In Locatelli and coll. 2021, in order to expand the knowledge of developmental milestone acquisition in DS, a total of 105 children/adolescents with DS recruited from February 2014 to July 2019 were considered. (Locatelli et al., 2021). The final sample was composed of 65 males and 40 females, they were divided in two groups by age and school attendance: 39 were in the preschooler group (aged between 3 and 6.11 years), 66 in the school-age group (between 7 and 16 years old). Personal, genetic, diagnostic, clinical, and developmental information from both the neonatal period and the time of the visit were collected. Moreover, parents were interviewed regarding the age at which the child started babbling (“Babbling”), sitting without support (“Sitting”), walking without assistance (“Walking”), and controlling sphincter and urination (“Sphincter control”). For children

between 3 and 6.11 years of age the cognitive functioning of participants was assess by Griffiths-III scales (Green et al., 2016). To assess the cognitive functioning of participants older than 7 years the Wechsler Preschool and Primary Scale of Intelligence (WPPSI-III) (Wechsler, 2002) was used, following a procedure already used in previous work (Antonaros et al., 2020;Antonaros et al., 2021a). In tables 1 and 2 the Griffiths-III and WPPSI-III subtests which measure child's development across different areas were listed. Following an increasingly widespread procedure in the field of intellectual disability (Fidler et al., 2019), the cognitive level was assessed through tests appropriate for expected mental age rather than for chronological age. Since age equivalent (AE) scores increase with chronological age, in every statistical analysis involving AE values for the effect of chronological age has been partialled. Moreover, an IQ score was calculated as the ratio of the subject's AE to his/her chronological age, multiplied by 100.

Griffiths-III Test					
A AE	**B AE**	**C AE**	**D AE**	**E AE**	**IQ (A AE/CA)**
Foundations of Learning	Language and Communication	Eye and Hand Coordination	Personal-social-emotional Abilities	Gross motor	Intelligence Quotient

Table 1. Griffiths-III subtests. List of different areas measured to assess child's development and IQ in children between 3 and 6.11 years of age. CA= Chronological age.

WPPSI -III Test			
Total AE	**Verbal AE**	**Non-verbal AE**	**IQ=** Intelligence Quotient (**Total AE/CA)**

Table 2. WPPSI-III subtests. List of different areas measured to assess child's development and IQ in children older than 7 years. CA= Chronological age.

The clinical and cognitive data were entered into an Excel spreadsheet and analysed using R. To explore the onset of developmental milestones (Sitting, Babbling, Walking, and Sphincter Control), descriptive statistics were calculated both separately for the two groups and for the whole sample. In addition, correlations between developmental milestones were calculated. To describe the relationship between milestones and later development separately in the two groups, correlations between developmental milestones and variables describing later motor, cognitive, communication, and adaptive development were calculated.

In another recent study (Onnivello et al., 2022a) we characterized the EFs and adaptive behaviour profiles of children/adolescents with DS, exploring any differences by age, and analysing the relationship between EFs and adaptive behaviour in this population. In the previous literature generalised executive functions (EF) and adaptive behaviour difficulties were seen in individuals with DS (Dykens et al.;Lee et al., 2011;Loveall et al., 2017).

Briefly, EFs describes a set of higher order cognitive processes that are important for completing goals (Stuss, 1986;Welsh, 1991;Zelazo, 1997). Abilities which have been classified as EFs including working memory, shifting, planning and organisation, cognitive flexibility, monitoring and emotional control (Pennington and Ozonoff, 1996;Miyake et al., 2000;Friedman et al., 2006). A measure widely used in this context is the Behaviour Rating Inventory of Executive Function BRIEF (Gioia, 2000) or its version for preschoolers, BRIEF-P (Gioia, 2003). These rating scales are completed by parents and/or teachers to assess EF-related behaviour at school and at home.

Adaptive behaviour refers to the conceptual, practical and social skills that individuals use in their everyday lives (Schalock et al., 2010). Vineland Adaptive Behaviour Scales, Second Edition (VABS-II) (Sparrow, 2005) is a semi-structured interview for parents/caregivers of DS individuals subminister to investigate adaptive behaviour of DS.

Parents/caregivers of 100 individuals with DS from 3 to 16 years old participated in the study. The sample was divided into parents of preschoolers (3–6.11 years old) or school-age children (7–16 years old). Parents/caregivers completed either the BRIEF-P (for children 2–6.11 years old) or BRIEF (for individuals 7 + years old) for asses EFs of their children, while DS adaptive behaviour was assessed with the VABS-II.

Finally, in Onnivello and coll. 2022 (Onnivello et al., 2022b) we analysed the cognitive profile, focusing on verbal and non-verbal indices, as assessed with the WPPSI-III, to provide further evidence on interindividual variability in DS. The correlation between cognitive profile and medical condition, parents' education levels and developmental milestones was explored in 72 children/adolescent with DS aged 7-16 years. Caregivers provided family background and information on their children development, including any medical conditions, when they reached the main milestones on their children's development, and whether they attend any intervention programs. The issue of cognitive interindividual variability focusing on verbal and non-verbal indices in DS was addressed by Tsao and Kindelnerg (Tsao and Kindelberger, 2009).

3.1.2 Phenotypic signs in subjects with DS

A reassessment of the characteristic phenotypic signs in subjects with DS was performed following the more comprehensive feature list proposed by Jackson for the DS clinical diagnosis (Lee and Jackson, 1972;Jackson et al., 1976) and published in Locatelli et al. 2022. Regarding the 25 phenotypic signs of DS described in Jackson's checklist, the brushfield spots feature was not considered because it was not possible to make the correct evaluation with near-infrared light (Postolache and Parsa, 2018). A total of 233 children/young adults with diagnosis of DS, with

homogeneous or mosaic (2 subjects) trisomy 21 and age >2 years were considered for this analysis. To evaluate the effectiveness of the Jackson's checklist for the clinical diagnosis of DS, we considered only those children with genetic diagnosis of DS for whom at least 18 signs were collected (207 subjects): 132 (63.77%) have at least (≥) 13 signs and thus a certain clinical diagnosis, 75 (36.23%) have 5 to 12 signs present and none have less than (<) 5 features present.

A cognitive assessment was also available for 114 children from ages 3 to 16 years in the context of our main project. The cognitive development of 43 DS subjects between 3 years and 6 years and 11 months of age was assessed using the Griffiths-III scale (Green et al., 2016). Seventy-one DS subjects from 7 to 16 years old were assessed using the WPPSI-III scale (Wechsler, 2002). In order to identify associations between each possible pair of Jackson's signs, we used 2x2 contingency tables with Fisher's exact test and we calculated a two-tailed p-value. The whole set of association p-values was checked by FDR correction. For the study of IQ scores and their association with each Jackson's sign, we divided the children into two subgroups according to whether their IQ score was higher than/equal to (H group) or lower than (L group) the mean value calculated in all subjects. We used contingency analysis and Fisher's exact test to define the statistical significance of the associations. All associations were checked by FDR correction. Unpaired t-test was used to test if IQ means were significantly different between subjects with and without each Jackson's feature considering the whole sample or either subject based on cognitive test (Griffiths-III and WPSSI-III separately). Finally, for the correlation between the number of Jackson's signs that are present and IQ scores, we considered only subjects for whom at least 18 signs were collected. The percentage of signs present for each child was calculated in order to better reflect the number of present signs out of the total number of signs collected for each child. For this analysis, we used bivariate analysis calculating the Pearson correlation coefficient. Then, in the same subgroup of subjects for whom at least 18 signs were collected, the label "Yes" was used if the number of Jackson's signs present is at least 13 (and "No" otherwise) and the association of this characteristic and IQ score, divided as described above, was tested with contingency analysis and Fisher's exact test. Unpaired t-test was used to test if IQ means were significantly different between subjects with at least 13 Jackson's signs or less than 13 considering the whole sample or either subject based on cognitive test (Griffiths-III and WPSSI-III separately). All statistical analyses were performed with JMP software (SAS Institute, version 14).

3.2 Genomics of Down syndrome: trisomy of full or partial chromosome 21

3.2.1 Partial Trisomy 21 (PT21)

PT21 cases are a very useful model for the identification of critical regions associated to DS phenotype. To better understand phenotype-genotype correlation in DS we focused on DS diagnosis itself as the phenotype to be mapped. Through the study of selected literature cases and the description of two new PT21 clinical cases, we were able to update the PT21 map previously published (Pelleri et al., 2019): in total, 137 PT21 cases, 96 of which with DS and 41 without DS. Case 1 was an Italian 2-year-old girl with PT21 and clinical diagnosis of DS. Patient enrollment was performed in the context of the routine follow up provided for DS. Case 2 was an Italian 9-year-old girl with PT21, without diagnosis of DS. Patient enrollment was performed in the context of a follow up for a psychomotor development delay. Clinical data were obtained during the routine follow up visits, including personal, genetic, diagnostic, clinical and auxological information from both the neonatal period and the time of the visit (Pelleri 2022 accepted *BMC Medical Genomics*).

Concerning Case 1, fluorescence in situ hybridization (FISH) analysis was carried out on samples of the proband and their parents on peripheral blood lymphocytes, according to standard techniques. FISH analysis was performed using Vysis Totelvysion DNA probes: D21Z1 (21p11.1-q11.1), wcp, AML, VIJyRM2029. Array-based comparative genomic hybridization (array-CGH) analysis was performed using an Agilent SurePrint G3 ISCA v2 CGH 8x60K microarray, with an average resolution of 120 kb (higher in ISCA regions), following the manufacturer's protocol (Agilent Technologies, Santa Clara, CA). Chromosomal imbalances were called through the ADM1 algorithm considering at least three consecutive oligonucleotides with similar log2ratio. A graphical visualization of the results was provided by the Genomic Workbench software v.7.0. In the present study genomic coordinates were converted to the matching current Genome Reference Consortium (GRC) human genome assembly GRCh38, or hg38, December 2013, using the online tool LiftOver (https://genome.ucsc.edu/cgi-bin/hgLiftOver).

Concerning Case 2, array-CGH analysis was performed using an Agilent 180 K oligonucleotide array according to the manufacturer's protocol (Agilent Technologies, Santa Clara, CA). Data analysis was performed using Cytogenomics V.2.5.8.1. To verify the presence and the parental origin of the unbalanced translocation der(20)t(20;21) suggested by microarray analysis, FISH analysis with subtelomeric probes D20S1157 (20p13) and D21S1146 (21q22.3) (Tel Vysion, Vysis Abbott Molecular, Des Plaines, Illinois, USA) was performed on metaphases from the proband and her parents. All the genomic coordinates related to previous versions of the

human genome sequence were converted in the matching current coordinates on hg38 using the online tool LiftOver (https://genome.ucsc.edu/cgi-bin/hgLiftOver).

Following systematic bibliographic searches, 125 PT21 reports were identified from the literature and selected for the study of a critical region for DS (Pelleri et al., 2016). Subsequently, the bibliographic search has been repeated and an updated analysis has been performed, building a map of a total of 132 PT21 cases with or without DS (Pelleri et al., 2019). Here, we have repeated the bibliographic search to retrieve any new reports of PT21 and to integrate the new data in the previously published PT21 map (Pelleri et al., 2019). In addition, weekly automated updates from NCBI reporting articles found with the “My NCBI” saved search: "Down Syndrome"[Mesh] OR "Down Syndrome" OR "Trisomy 21" were considered, to identify articles escaping the above search strategy. We applied inclusion and exclusion criteria as previously described (Pelleri et al., 2016) in order to only include cases with sufficient and unambiguous description at cytogenetic, molecular and clinical levels.

3.2.2 Highly restricted Down syndrome critical region (HR-DSCR)

HR-DSCR is a region of Hsa21 present in three copies in all individuals with PT21 and a diagnosis of DS (Pelleri et al., 2016). This region, located on distal 21q22.13, is 34 kbp long and is annotated as an intergenic region between *KCNJ6-201* transcript encoding for potassium inwardly rectifying channel subfamily J member 6 and *DSCR4-201* transcript encoding Down syndrome critical region 4. Two transcripts recently identified by massive RNA-Seq and automatically annotated on Ensembl database reveal that the HR-DSCR seems to be partially crossed by *KCNJ6-202* and *DSCR4-202* isoforms. In this study, published in Antonaros et al. 2021b, we performed *in silico* and *in vitro* analyses in order to characterize *KCNJ6-202* and *DSCR4-202* isoforms. Ensembl Genome Browser (https://www.ensembl.org/index.html) was used to annotate the exon limits of the investigated isoforms and to observe their location in comparison to the HR-DSCR limits. BLASTN software was used to align exon junction sequences (used as query sequence) with RNA-Seq experiments, in order to evaluate tissue isoform expression. We considered only alignments with at least 95% of query cover and 97% of identity as significative. RNA-Seq experiments were selected on *KCNJ6* (https://www.ncbi.nlm.nih.gov/gene/3763) and *DSCR4* (https://www.ncbi.nlm.nih.gov/gene/10281) NCBI Gene schedule under the "Expression" heading. The three bio-projects selected were: "HPA RNA-Seq normal tissues (PRJEB4337)"; "RNA-Seq of total RNA from 20 human tissues (PRJNA280600)"; "Illumina bodyMap2 transcriptome (PRJEB2445)". We included the bio-project (PRJNA635385), in which RNA-Seq was performed

on RNA samples extracted following the same procedures and conditions of RNA used in this work for *in vitro* analyses (Antonaros et al., 2021c).

The euploid tissues selected from the four bio-projects were: adrenal gland, brain, cerebellum, cerebral cortex, heart, liver, placenta, skeletal muscle, skin, testis, thymus, thyroid, white blood cells and blood cells. The T21 tissue selected was T21 blood cells. For the molecular biology experiments, we used commercially available RNA samples (Clontech, Mountain View, CA, USA), derived from the following human euploid tissues: adrenal gland, brain, cerebellum, cerebral cortex, heart, liver, placenta, skeletal muscle, testis, thymus, thyroid. The results reported by the *in vitro* analyses were compared with those reported by the RNA-Seq experiments carried out on the same tissues and listed above.

It was possible to detect the expression of *KCNJ6* and *DSCR4* both in euploid and trisomic tissues only for RNA derived from fibroblast and blood cells obtained as follows. Normal and T21 blood samples were collected at the Neonatology Unit of S. Orsola-Malpighi Hospital of Bologna, in the context of the "Genotype-phenotype correlation in trisomy 21 (Down syndrome)" project. Blood samples were collected and treated as previously described (Chomczynski and Sacchi, 1987) The results reported by the *in vitro* analyses were compared with those reported by the RNA-Seq experiments (PRJNA635385) performed on normal and T21 blood samples. Normal and T21 primary fibroblast cell lines were provided by Galliera Genetic Bank (GGB), member of the "Network Telethon of Genetic Biobanks". All the cell lines were tested for mycoplasma to exclude possible contamination. Furthermore, a karyotype analysis was carried out on T21 cell lines by GGB to confirm the cytogenetic diagnosis. Five mL of denaturing solution was added to the cell flasks, and they were stored at -20°C until RNA extraction. The results reported by the *in vitro* analyses performed on euploid fibroblast cell lines were compared with those reported by the RNA-Seq experiments (PRJEB4337) performed on normal skin tissues. RNA extraction from blood samples and fibroblast cell lines was performed with the method of Chomczynski and Sacchi (Chomczynski and Sacchi, 1987), and RNA quantity and quality were verified as previously described (Antonaros et al., 2021c). Pools of RNA samples were created from RNA derived from T21 and normal control blood cells: one with three T21 blood cell RNA samples (330 ng of each) and the second with three normal control blood cell RNA samples (330 ng of each).

Reverse transcription (RT) was conducted on 1 μg of RNA using "SuperScript III First-strand Synthesis Supermix" kit (Invitrogen by Life technologies, Grand Island, NY, USA) according to manufacturer instructions. Amplification products were analysed by electrophoresis on agarose gel and by Sanger sequencing with Applied Biosystems ABI 3730 DNA. Finally, we

compared the results obtained by RT-PCR, SRA-BLAST alignments and data available on Ensembl to determine the structure of *KCNJ6* and *DSCR4* transcripts.

3.3 Transcriptome analysis

The aim of this section was to analyze T21, and normal control blood cell gene expression profiles obtained by total RNA-Seq (Antonaros et al. 2021c). The results were elaborated by TRAM (Transcriptome Mapper) software which generated a differential transcriptome map between human T21 and normal control blood cells providing the gene expression ratios for 17,867 loci (Antonaros et al., 2021c). The obtained gene expression profiles were validated through Real-Time RT-PCR (reverse transcription-polymerase chain reaction) assay and compared with previously published data.

For RNA-Seq analyses were used 4 subjects with DS and 4 normal control samples while for the Real-Time RT-PCR was used RNA samples from 6 children with DS and 6 normal controls, analyzing five genes over-expressed in the RNA-Seq experiments. The two groups analyzed by Real-Time RT-PCR are comparable with the mean age of the two groups analyzed by RNA-Seq. All the subjects were recruited in the context of our main project.

Blood samples (3 mL) from DS and normal control donors, were collected and treated as previously described (Chomczynski and Sacchi, 1987) and stored at -20°C until RNA extraction. Total RNA extraction was performed with the method of Chomczynski and Sacchi (Chomczynski and Sacchi, 1987) and the RNA quantity and quality have been verified through electrophoresis on agarose gel (GelDoc 2000 and Quantity One software, Bio-Rad Laboratories, Hercules, CA, Bio-Rad Laboratories, Hercules, CA, USA) and through Nanodrop spectrophotometer (ND-1000 spectrophotometer, ThermoFisher Scientific, Waltham, MA, USA).

Four T21 and 4 normal control blood samples were used to perform RNA-Seq analyses. Briefly, library preparation, sequencing, read mapping and counting was carried out by "Sequentia Biotech SL" (Barcelona, Spain), TruSeq Stranded Total RNA with Ribo-Zero Gold (Illumina, San Diego, CA) was used for library preparation following the manufacturer's instructions, starting with 200 ng of RNA as input. The CASAVA 1.8.2 version of the Illumina pipeline was used to process raw data for both format conversion and de-multiplexing. Raw sequencing data were processed with BBDuk (https://jgi.doe.gov/data-and-tools/bbtools/) in order to perform trimming and clipping. The quality of the reads, before and after trimming, was checked with the software FASTQC (https://www.bioinformatics.babraham.ac.uk/projects/fastqc/). High-quality reads were mapped against the GRCh38 human reference genome, downloaded from Ensembl (Cunningham et al., 2019), with the software STAR (version 2.5.2b, https://github.com/alexdobin/STAR). Only reads

with a mapping quality higher than 30 were used for this scope. Raw and processed files have been deposited in NCBI's Gene Expression Omnibus (Barrett and Edgar, 2006) and are accessible through GEO Series accession number GSE151282 (https://www.ncbi.nlm.nih.gov/geo/query/acc.cgi?acc=GSE151282) (Antonaros et al., 2021c).

To elaborate the RNA-Seq data we used the last empty version available of TRAM (TRAM 1.3, http:/apollo11.isto.unibo.it/software/) that was manually configured following the software guide with human chromosome and human gene data downloaded from the National Center for Biotechnology Information (NCBI) Genome and Genes (NCBI Resource Coordinators, 2018). TRAM software (Lenzi et al., 2011) can perform intra- and inter-sample normalizations of gene expression values. The value for each locus, in each biological condition (T21 (pool A) and normal control (pool B) conditions), is represented by the mean value of all the values available for that locus. The mean value of the gene expression of the whole genome is used to determine the percentile of expression for each gene (Lenzi et al., 2011). TRAM generates a differential transcriptome map, where the gene expression ratios (A/B) for each locus were shown in addition to the gene expression values of the single pools (Lenzi et al., 2011).

For the validation of the RNA-Seq results, we performed Real-Time RT-PCR on nineteen genes with low inter-sample variability using two pools of RNA samples obtained from the same RNA samples used for RNA-Seq analysis in this work. The first pool was created by mix of three T21 blood cell RNA samples (one T21 sample was no more available for Real-Time PCR analysis) and the second was created by mix of four normal control blood cell RNA samples (Antonaros et al., 2021c). In addition, we performed Real-Time RT-PCR experiments on a different and larger cohort of samples (12 RNA samples, 6 from children with DS and 6 from normal controls) on 6 genes reported by RNA-Seq experiments as statistically significant over-expressed in T21 vs normal control subjects (Antonaros et al., 2021c). Four genes mapping on Hsa21 (T*SPEAR, MX1, SLC19A1* and *GART*) and one gene mapping on chromosome 10 (*IFIT1*). The relative gene expression value of each gene vs a gene chosen as reference (*GAPDH*) was obtained through the 2-ΔCt method in both DS and N groups. The results obtained by Real-Time RT-PCR were compared with the gene expression ratios from RNA-Seq analysis through bivariate statistical analyses using JMP 14.2 Pro software.

Finally, T21 and normal control single transcriptome maps and T21 vs normal control differential transcriptome map were compared with those obtained in the meta-analysis performed by Pelleri and coll. on WBC samples (Pelleri et al., 2018) and with RNA-Seq experiment performed by Powers and coll. on WBC samples (Powers et al., 2019). Gene expression values were compared

performing nonparametric correlation test (Spearman correlation by rank) using JMP 14.2 Pro software.

3.4. Down syndrome and metabolic alterations

3.4.1 Metabolomic profile through Nuclear Magnetic Resonance (NMR)

In order to confirm the alteration of mitochondrial metabolism in DS and investigate if metabolite levels are related to cognitive aspects of DS, we analysed the metabolomic profiles of plasma samples from 129 subjects with DS and 46 healthy control (CTRL) subjects by Nuclear Magnetic Resonance (NMR) and we collected cognitive data for a total of 61 DS children/adolescents (Antonaros et al., 2020). Because of the paediatric age of most of the subjects, it was not always possible to collect samples at a fasting state. Thus, to avoid that non-fasting conditions could alter the results, we performed multivariate and univariate analyses for two groups of subjects: the "all" group including fasting and non-fasting subjects, and the "fasting" group (Antonaros et al., 2020).

Blood samples were collected from all subjects enrolled in the study, and plasma was isolated according with the previous standard procedure reported in (Caracausi et al., 2018). NMR sample preparation, spectra processing and spectral analysis were prepared according with the previous procedures (Caracausi et al., 2018).

Cognitive data were collected and processed for a total of 61 DS children/adolescents from 3 to 16 years old. Children from 3 to 6 years and 11 months were assessed using the Griffiths-III scale (Green et al., 2016), and children/adolescents from 7 to 16 years old were assessed using the WPPSI-III scale (Wechsler, 2002).

The multivariate statistical analysis was performed using both Carr-Purcell-Meiboom-Gill (CPMG) and Nuclear Overhauser Effect Spectroscopy (NOESY) spectra. Unsupervised Principal Component Analysis (PCA) was used to obtain a preliminary outlook of the data (visualization in reduced space, cluster detection, screening for outliers). Partial Least Squares (PLS) analysis was employed to perform supervised data reduction and classification between samples from healthy and diseased volunteers. Canonical analysis (CA) was used in combination with PLS to increase supervised data reduction and classification. The accuracy for classification was assessed by means of a Monte Carlo validation scheme. The resulting confusion matrix was reported, and its discrimination accuracy, specificity and sensitivity were estimated according to standard definitions. Each classification model was also validated using permutation test (n = 500) and the resulting p-value was reported. Univariate analysis of the NMR data was performed on Fourier transformed and calibrated CPMG spectra.

The relative concentrations of the various metabolites were calculated by integrating the corresponding signals in the spectra 50, using the AssureNMR Software (Bruker BioSpin) and a home-made tool for R Software. The nonparametric Wilcoxon-Mann-Whitney test was used for the determination of the meaningful metabolites. Here, a p-value < 0.05 was considered statistically significant. Considering FDR, the p-value was corrected using the Benjamini-Hochberg formula and reported as pFDR (Benjamini and Hochberg, 2000). SPSS Statistics (IBM, Version 25 for Mac OS X) was used to perform partial correlation between the level of each metabolite and the levels of all the other metabolites checking for the effect of chronological age (at the moment of blood-collection). We considered r-value between 0.4 and 0.7 as moderate correlation and $r > 0.7$ as strong correlation (Schober et al., 2018). To analyse the correlations between metabolite levels and AE scores obtained from Griffiths-III and WPPSI-III tests, we performed a partial correlation checking for the effect of chronological age (at the moment of the cognitive test) using SPSS Statistics software. To investigate the influence of the different IQ scores on the metabolomic profiles, we divided the metabolome results into two groups: those deriving from subjects with DS having taken the Griffiths-III test and those deriving from subjects with DS having taken the WPPSI-III test. We distinguished the subjects according to the IQ scores obtained from the two kinds of cognitive tests for both groups. It is known that the IQ scores have a mean of 100 and an SD of 15 and that a subject with an IQ < -2SD has an intellectual disability. All subjects with DS included in this study have an IQ < -2SD. To perform the multivariate statistical analysis between a significant number of metabolomic profiles for each kind of cognitive test, we decided to create two main groups of data: a group of metabolomic profiles from subjects with an $IQ > 40$ (between 2 and 4 SD below average) and a second group from subjects with an $IQ \leq 40$ (more than 4 SD below average).

3.4.2 One-carbon cycle characterization through blood routine analyses

We have investigated the role of Hcy, folate, vitamin B12, uric acid (UA), and creatinine levels in the intellectual impairment of subjects with DS (Antonaros et al., 2021a). Hcy, folate, vitamin B12, UA, creatinine levels and *MTHFR* C677T genotype were analysed in 147 subjects with DS. For 77 subjects, metabolite levels were correlated with cognitive tests. Griffiths-III test was administered to 28 subjects (3.08-6.16 years) and WPPSI-III test was administered to 49 subjects (7.08-16.08 years). Information on drugs and vitamin supplements assumed by subjects with DS were collected at blood draw and subjects whose samples might have been altered by these medications were excluded from the study.

Two aliquots of blood samples were collected at the Neonatology Unit of S. Orsola-Malpighi Hospital of Bologna and metabolite dosage was detected by "Laboratorio unico Metropolitano" (LUM) of Maggiore Hospital, Bologna, Italy. The first aliquot, used for *MTHFR* C677T genotyping and plasma Hcy dosage, was collected in ethylenediaminetetraacetic acid (EDTA)-coated blood collection tubes and plasma fraction was isolated within two hours from blood collection as previously described (Salvi et al., 2019). Plasma fraction was stored at -80°C until it was sent to LUM for Hcy plasma level detection. The second aliquot was collected in EDTA free tubes and directly sent to LUM for routine blood analyses, which included folate, vitamin B12, UA and creatinine dosage.

The physiological range established by LUM were 0.5-1.2 mg/dL for creatinine, 2.6-7.2 mg/dL for UA, 3.1-19.3 ng/mL for folate, 145-914 pg/mL for vitamin B12 and 5-15 μmol/L for Hcy plasma level. *MTHFR* C677T polymorphism was analysed according to our previously published protocol (Antonaros et al., 2019) based on an improved polymerase chain reaction-restriction fragment length polymorphism (PCR-RFLP) reaction.

Among the subjects enrolled who decided to participate in a cognitive evaluation, only the cognitive tests administrated within two months from blood sample collection were considered in order to correlate these data with metabolite levels. Thus, cognitive test results were available for 77 DS children out of the 147 subjects enrolled in the context of our clinical experimental study. Depending on the age of the participant, the Griffiths-III test (Green et al., 2016) was administered to 28 subjects aged from 3.08 to 6.16 years, while the WPPSI-III test (Wechsler, 2002) was administered to 49 subjects from 7.08 to 16.08 years. For this study, scale A and scale B of Griffiths-III test were considered (See Material and Methods).

Statistical analyses were carried out with SPSS Statistics (IBM, Version 25 for MacOSX). The p-value after FDR were generated using JMP Pro software, Version 14 of the SAS System for MacOSX. For all results, a $p<0.05$ was considered statistically significant; $r<0.4$ was considered as weakly correlated, $0.4<r<0.7$ as moderately correlated and $r>0.7$ as strongly correlated. The total of 147 subjects was divided into three groups depending on the *MTHFR* C677T genotype (CC, CT or TT).

Contingency tests were used to assess differences in sex among CC, CT and TT genotype groups, performed with SPSS Statistics software. The Kruskal-Wallis test was used to assess differences in age distribution in Genotype groups (CC, CT, TT), performed with SPSS Statistics software. One-way ANOVA was used to assess differences in Hcy concentrations among the three genotypes. Analysis with the Tukey-Kramer method was performed as a post-hoc test for mean comparisons when ANOVA showed statistically significant results (p-value<0.05). A linear

correlation was performed with SPSS Statistics software to determine if the correlation between age and metabolite levels existed. Correlations between sex and metabolite levels and between fasting/non-fasting state and metabolite levels were investigated with an unpaired t-test. Partial correlation corrected by age at blood draw was used to correlate each metabolite level with all other metabolite concentrations. Only fasting subjects were included. FDR correction was applied to p-values obtained from these statistical analyses.

Statistical analyses on cognitive tests were performed by dividing the subjects into two different groups according to the test used for collecting their cognitive data (Griffiths<7 years; WPPSI>7 years). Taking the study of Guéant and coll. (Gueant et al., 2005) as a model, the threshold concentration of Hcy, folate, vitamin B12, UA and creatinine levels were calculated by SPSS software using quartiles. The concentration value of the 25th, 50th or 75th percentiles was used as a reference for dividing the subjects into two groups, one with a metabolite concentration value lower than the reference (Low or L group) and the other with a concentration value higher than or equal to the reference (High or H group). Partial correlation corrected by age at the time of cognitive test was performed to test correlations between percentile groups of Hcy, folate, vitamin B12, UA and creatinine levels and Griffiths-III/WPPSI-III subtests' scores.

3.4.3 One-carbon cycle characterization through ELISA assay

In subjects with DS, one-carbon metabolism was considered to be imbalanced by several authors (Lejeune, 1979;Rosenblatt et al., 1982;Peeters et al., 1995;Song et al., 2015;Funk et al., 2020), and interesting data in the same direction have been obtained by the analyses previously described and detailed below in the "Results" section (Antonaros et al. 2020; Antonaros et al. 2021a; Antonaros et al. 2021c): for this reason we decided to investigate plasma level alteration of 5 intermediates of one-carbon metabolism in a group of subjects with DS compared to a group of euploid subjects as control (Vione, 2022). We performed enzyme-linked immunosorbent assays (ELISAs) in plasma samples obtained from a total of 164 subjects with DS compared to 54 euploid subjects to measure the concentration of: tetrahydrofolate (THF; DS n=108, control n=41), 5-methyltetrahydrofolate (5-methyl-THF; DS n=140, control n=34), 5-formyltetrahydrofolate (5-formyl-THF; DS n=80, control n=21), S-adenosyl-homocysteine (SAH; DS n=94, control n=20) and S-adenosyl-methionine (SAM; DS n=24, control n=15). Moreover, we investigated the association between metabolite concentrations in the DS group and control group and the correlation with folic acid, vitamin B12 and Hcy in the DS group.

For this work, we considered in the DS group subjects with diagnosis of DS with homogeneous or mosaic T21, availability of an adequate amount of plasma to perform at least one

ELISA assay and a similar mean age as close as possible to control group. Concerning control group, we considered subjects with an adequate amount of plasma to perform at least one ELISA assay and a similar mean age as close as possible to DS group.

Two blood sample aliquots were collected. The first aliquot was sent to LUM of Maggiore Hospital (Bologna, Italy) for routine blood analyses of the DS group including folic acid and vitamin B12 (Antonaros et al., 2021a). The second aliquot was kept at room temperature and treated within two hours from blood draw as previously described (Antonaros et al., 2021a) and used for ELISA assays.

We evaluated the quantitative measurement of THF, 5-methyl-THF, 5-formyl-THF and SAH plasma concentrations using specific ELISA kits manufactured by MyBioSource (San Diego, California, USA) and SAM plasma concentration using a specific ELISA kit manufactured by Biovision (Milpitas, California, USA). Ninety-six well plates were used for all the assays and all standard and plasma samples were tested in duplicate. Due to preliminary studies, plasma samples used for the measurement of 5-methyl-THF were diluted 1:10 and plasma samples used for the measurement of SAH were diluted 1:5 in Plates 1, 2, 3 and 4, and 1:3 in Plates 4 and 5 to avoid excessive dilution of the metabolite. The standard samples were provided by the kits and were reconstituted and serially diluted as suggested.

In order to perform the assays, the manufacturer instructions of each kit were followed, and the final spectrophotometric reading was carried out by microplate reader (Perkin Elmer Wallac 1420 Victor 2 Multi-Label) set at a wavelength of 450 nm. To create the standard curve for each ELISA assay, standard O.D. mean values were plotted on the x-axis and the known standard concentration values were plotted on the y-axis using Microsoft Excel and following manufacturer instructions. The transformation of standard concentration values in their logarithm (Log_{10}) is required to build the standard curves in THF and 5-formyl-THF ELISA assays. The subtraction of the background O.D. mean value ("standard 8") from the O.D. mean values of the other standards and plasma samples is required in SAH ELISA assay. The transformation of standard O.D. mean values in their inverse (1/O.D. mean) is required to build the standard curves in the case of the SAM assay. The polynomial trend lines of each plot were created using Excel, and the resulting polynomial equations ($y = a + bx + cx^2$) were used to determine metabolite concentrations of plasma samples using interpolation.

Statistical analyses were carried out with SPSS Statistics (IBM, Version 25 for Mac OS X) and for all results, a $p<0.05$ was considered statistically significant; $r<0.4$ was considered as weakly correlated, $0.4<r<0.7$ as moderately correlated and $r>0.7$ as strongly correlated. For each metabolite (THF, 5-methyl-THF, SAH and SAM) we performed an unpaired student t-test between DS and

control group using the "Graph Pad" t-test calculator online (https://www.graphpad.com/quickcalcs/ttest1.cfm), while for 5-formyl-THF level we performed Mann Whitney test online (https://www.socscistatistics.com/tests/mannwhitney/). A linear correlation was used to determine if the correlation between age and molecule levels existed. Unpaired t-test was used to test whether sex and fasting/non-fasting state might affect the main results. SPSS Statistics software was used to perform a linear correlation between the level of each molecule and the levels of all the other molecules. Partial correlation analyses checked for the effect of chronological age were used to investigate associations between the level of the involved molecules and other molecules.

3.5 Trisomic induced pluripotent stem cells (iPSCs)

During the period abroad of the PhD course at Prof. Niklas Dahl Laboratoly, Upssala University, Sweden, I had the opportunity to learn methods to apply to a very useful DS model: iPSCs and their neuronal derivatives.

Recently, the research group of Prof. Dahl generated iPSCs from trisomic and euploid fibroblasts (Schuster et al., 2020;Vasylovska et al., 2020), that were differentiated into neuronal derivatives (Hackland et al., 2017). In particular, directed induction of human iPSC into Neural crest cells (NCC) was performed using top-down inhibition of BMP signalling, following a previously established protocol (Hackland et al., 2017); neuroepithelial stem cell (NES) were generated following the previously protocol (Falk et al., 2012) and organoids were generated following the protocol described by Pellegrini et al. (Pellegrini et al., 2020). Preliminary single cells RNA sequencing (scRNAseq) analysis performed on these neuronal derivatives revealed four major cells clusters from the expression of specific markers:

- Neural progenitors (NPC; *SOX2*)
- Mesenchymal cells of the choroid plexus (mChP; *COL1A1*)
- Intermediate neuronal progenitors (nIPC, *SOX2* and *HES6*)
- neurons (*STMN2*)

Notably, as shown in Figure 7, the neuronal cells with T21 revealed a marked increase in the proportion of mesenchymal cells of the choroid plexus when compared to the corresponding euploid cells. Conversely, the proportion of neural cells was decreased in T21 cells.

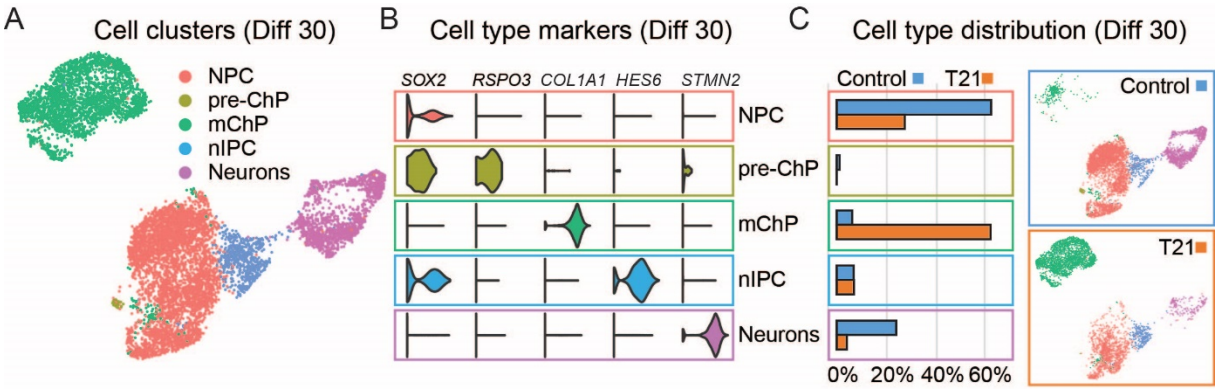

Figure 7. Neural differentiation of human T21 NES cells results in overrepresentation of cells with mesenchymal choroid plexus characteristics. A) NES cells from control and T21 differentiated for 30 days (Diff 30) result in five separate cell clusters. B) Cluster analysis show that neural progenitor cells (NPC) cells can be identified by the expression of *SOX2*, immature choroid plexus (pre-ChP) cells by *SOX2* and *RSPO3*, mesenchymal choroid plexus (mChP) cells by *COL1A1*, neuronal intermediate precursor cells (nIPC) by *SOX2* and *HES6* and Neurons by *STMN2*. C) Cell clusters separated by sample (control and T21) show a higher proportion of cells with mChP characteristics (mChP: WT 6% and T21 62%) and a reduced proportion of neuronal cells (Neurons: WT 24% and T21 4%) in the T21 sample. Independent cell lines: Control n=1, T21 n=1.

The same differences in distribution of neural cell populations were observed when comparing T21 and euploid organoids. The mesenchymal cells of the choroid plexus were observed in T21 organoids: in these cells was highlighted the expression of *SOX10*, a specific marker of NCC. These preliminary data suggest that mesenchymal cells of the choroid plexus may derive from NCC (Jan Hoeber et al. In the drafting phase); for this reason, we decided to differentiate trisomic and euploid iPSCs in NCC and analyze their transcriptome.

The scRNAseq data showed an under-expression of DNA methyltransferase 3-ß (*DNMT3B*) in NCCs with T21 (Jan Hoeber et al. In the drafting phase). This study aimed to observe whether modulation of *DNMT3B* expression was associated with a phenotypic variation in euploid and trisomic NCCs. Different concentration of Nanaomycin A inhibitor (Kuck et al., 2010) were used to inactivate DNMT3B in euploid NCCs, to observe if the reduced activity of DNMT3B in euploid NCCs could mimic the T21 phenotype. NCCs treated with Nanaomycin A were compared with unmanipulated trisomic and euploid NCC lines. An expression vector for *DNMT3B* was inserted in

the trisomic NCCs to bring the gene expression back to a level comparable with the controls and observe a possible recovery of phenotype. Over and under-expression of *DNMT3B* in cellular models may allow us to clarify how *DNMT3B* itself, or the mechanisms related to the reduction of its expression, are correlated with the alteration in the neurodevelopment in the DS.

In the present study two iPSC lines from healthy donors CTL10 (Uhlin et al., 2017) and JLBI (Vasylovska et al., 2020); and three iPSC lines from individuals with full trisomy 21 DS1.1, DS2B, DS3.1 (Schuster et al., 2020) were differentiated in NCC to observe whether modulation of *DNMT3B* expression was associated with a phenotypic variation in euploid and T21 NCCs.

3.5.1 iPSC maintenance

Human iPSC lines were maintained in E8 media (Essential 8TM Basal media (Gibco) supplemented with 1x Penicillin and Streptomycin (Gibco)) on Laminin-521 coated plastic (LN-521, Biolamina). For coating of plastic, LN-521 was diluted in PBS containing Ca2+ and Mg2+ to a final concentration of 5 µg/mL and plates were incubated over night at 4°C. iPSC cultures were passaged at 60-80% confluence using incubation with TrypLE (Gibco) for 3min at 37°C, collection and addition of one volume of DTI (Defined Trypsin Inhibitor, Gibco), centrifugation for 5min at 300g, followed by seeding at a 1:5 ratio onto LN-521 coated plastic. All cell lines have been subjected to Short Tandem Repeats (STRs) genotyping with "Qubit® dsDNA BR Assay Kits**"** and measured by "Qubit 3.0" and tested for expression of pluripotency markers by flowcytometry (Natunen et al., 2011). Concerning flowcytometry, iPSC cultures were incubated with TrypLE (Gibco) for 3min at 37°C and transferred to flow cytometry tubes and three volumes of FlowBuffer (containing 1% BSA and 0.05 mM EDTA in PBS) were added. The suspension was centrifuged for 5min at 300g, the supernatant discarded and primary antibody (α-SSEA-4 (mouse IgG) and α-TRA-1-60 (mouse IgM): 1:100 in Flow buffer) was added and incubated for 30min at room temperature (rt). After addition of three more volumes of FlowBuffer, cells were collected using centrifugation, the supernatant decanted and resuspended in secondary antibody (α-mouse IgG Alexa488 and α-mouse IgM Alexa555; 1:1000 diluted in FlowBuffer). After 20min of light protected incubation at rt, cells were pelleted using centrifugation, supernatant decanted, the pellet resuspended in 600 µl FlowBuffer and placed on ice. α-SSEA-4 and α-TRA-1-60 immune labelled and unlabelled samples were analysed using a Flowcytometer (LSR Fortessa) with DIVA software. Unlabelled samples were used to set a cut off using their auto-fluorescence in the 585±15 nm range, cells above the threshold were considered positive. Representative density plots were made using FlowJo V10.7.1.

3.5.2 Neural crest induction

Directed induction of human iPSC into NCC was performed following a previously established protocol with slight deviations (Hackland et al., 2017). Ten thousand cells/cm^2 of the two controls (CTL10 and JLBI) and three T21 (DS1.1, DS2B DS3.1) iPSC lines were seeded onto Laminin-521 coated plastic in E8 media supplemented with 10 µM ROCK1 and ROCK2 inhibitor Y-27632 (Stemcell Technologies). The next day, E8 media was exchanged to TDi medium (DMEM/F12 (Gibco), 1x N2 (Gibco), supplemented with 15 ng/mL rhBMP4 (R&D Systems), 1 µM CHIR99021 (R&D Systems), 2 µM SB431542 (Millipore) and 1 µM DMH1 (Tocris)). TDi medium was changed completely every day for 7 days. By day 7 NCC had reached complete confluence and exhibited a NCC typical cobblestone morphology. For differentiation of NCC under "brain-like" conditions, TDi medium was exchanged for CDA media with medium changes every other day. 7 days after induction of differentiation, CDA supplemented with 14ng/ml rhBDNF (Gibco) was used for medium changes every other day.

3.5.3. Nanaomycin treatment of euploid cells

Different concentration of Nanaomycin A inhibitor (Kuck et al., 2010) were used to inactivate DNMT3B in euploid NCCs. For selective inhibition of DNMT3B activity, NCC were treated with either DMSO, 0.5 µM or 0.75 µM of Nanaomycin A. Treatment started at the day of NCC induction and ceased at day 7, after which NCC were differentiated using "brain-like" conditions, time-line study is shown in figure 8.

Figure 8. Time-line study. The figure shows 0.75µM of Nanaomycin A inhibitor treatment to euploid cells started at the day of NCC induction and ceased at day 7. RNA was collected at days 0;3;5;7;14;21 for qPCR experiments.

3.5.4 RNA and DNA isolation

Total RNA was extracted from cell lysates with RNeasy® Mini Kit (Qiagen) following the manufacturer's instructions quantity and quality have been verified through Nanodrop spectrophotometer (ND-1000 spectrophotometer, ThermoFisher Scientific, Waltham, MA, USA) and Agilent RNA 6000 Nano Kit (Agilent Tachnologies, Santa Clara, CA, USA). Total DNA was extracted from cell lysates with NucleoSpin Tissue (Macherey-Nagel, Duren, Germany) following

the manufacturer's instructions quantity and quality have been verified through Nanodrop spectrophotometer.

3.5.5 PCR Amplification of Target Fragment (DNMT3B and GFP)

Amplification of *DNMT3B* sequence with overhangs to *Eco*RI site (5′) and overhangs to GFP site (3′) called here **EcoRI-DNMT3B-GFP (2500 bp);** and amplification of *GFP* sequence with overhangs to *DNMT3B* site (5′) and overhangs to BamHI site (3′) called here **DNMT3B-GFP-BamHI (700 bp)** were performed using CloneAmp HiFI PCR premix (Cat.NO. 639298 ThermoFisher, Waltham, Massachusetts, USA) in a final volume of 25 µL.

EcoRI-DNMT3B-GFP amplicon (2500 bp) was generated using as template 57 ng/µL of pcDNA3/Myc-DNMT3B1**;** 10 µM of forward primer **(EcoRI-**DNMT3Bfw**):** CCCTCGTAAA**GAATTC**atgaagggagacaccaggcatctcaatg; and 10 µM of reverse primer (DNMT3B-GFPRv): CTTGCTCACCATGGTGGCGACttcacatgcaaagtagtccttcag.

DNMT3B-GFP-BamHI amplicon (700) was generated using as template 1 ng/µL of pEGFP-N1**;** 10 µM of forward primer **(**DNMT3B-GFPfw) ctgaaggactactttgcatgtgaaGTCGCCACC ATGGTGAGCAAG; and 10 µM of reverse primer (**BamHI-**GFPrv) GAGGTGGTCT **GGATCC** *TTA* CTT GTA CAG CTC GTC CAT GCC GAG; see Figure 9.

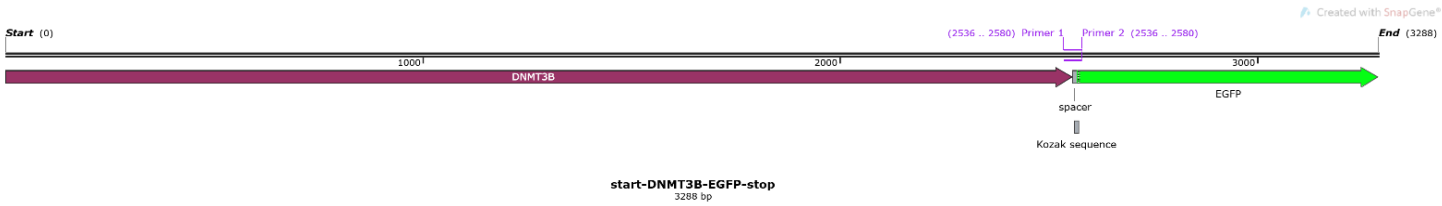

Figure 9. Amplification of *DNMT3B* sequence with overhangs to GFP site 3'.

Agarose Gel at 2% was used to check correct amplification of EcoRI-DNMT3B-GFP (2500 bp) and DNMT3B-GFP-BamHi (700 bp) fragments**.** Band isolation and gel purification were performed using the NucleoSpin Gel kit (Machery-Nagel). Measure fragment concentration was assessed with Nanodrop.

3.5.6 Preparation of a Linearized Vector by restriction enzyme digestion

pLVX-TetOne-Puro.dna vector (950 ng) was incubated with 1 µL of *Bam*HI and 1 µL of *Eco*RI at 37°C for 2h 80°C for 5' following the manufactory's instruction (Fast digest, ThermoFisher, Waltham, MA, USA). Linearized vector was added on 1.5% agarose gel, the band was purified using the PCR Clean-Up kit (Bioanalysis, Macherey-Nagel, Duren, Germany) and measure at

Nanodrop. The linearized and purified vector was transfected into competent cells following the manufactory's instruction.

3.5.7 Insertion of target segments in the linearized vector

Molar ratio recommendations, when is cloning more than two fragments at once, is 2:1 (two moles of each insert for each mole of linearized vector), final molar ratio of two inserts with one vector should be 2:2:1. Ligation Calculator **http://www.insilico.uni-duesseldorf.de/Lig_Input.html** was used to assess Linearized Vector and Target Fragments concentrations necessary for the ligation reaction with In-Fusion HD Cloning (Takara Bio, CA 94043, USA). We store the cloning reactions at –20°C before the transformation procedure using Lenti-X Packaging Single Shots (Takara Bio, CA 94043, USA). To determine the presence of the insert, plasmid DNA was isolated using miniprep and it was analyzed by restriction digestion and sequencing. The insert was transfected in Human embryonic kidney (HEK) cells throw lipofectamine and the GFP fluoresce was check with microscope the day after transfection. Briefly, the transfected cells, in presence of doxycycline (DOX), will express the Gene Of Interest (GOI). In particular, the Tet-on 3G protein when bound by Dox undergoes a conformation change that allows it to bind to Tet operator sequences located in the PTRE3GS promoter. The inducible promoter PTRE3GS is located upstream of a minimal CMV promoter and activates transcription of the downstream GOI. The Tet-On 3G transactivator is expressed in the forward direction from the human phosphoglycerate kinase 1 promoter, and the cloned GOI is expressed from the PTRE3GS promoter in the reverse orientation. Lenti-X Packaging Single Shots (VSV-G) can generate lentivial packaging systems. Figure 10 below show the Lentivirus technology used in this work.

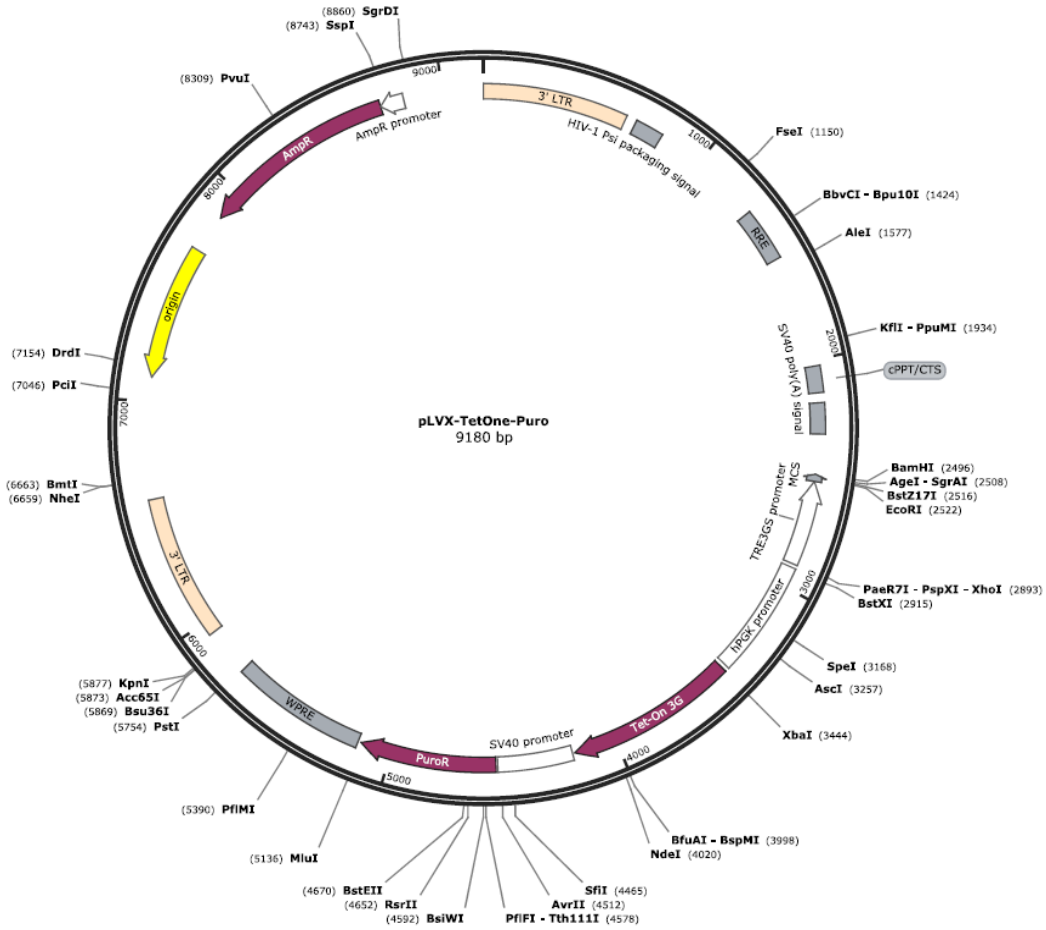

Figure 10. pLVX-TetOne-Pure Lentivirus. Figure shows Lentivirus technology used in this work obtained by SnapGene, representing the gene and the restriction site present in the plasmid.

4. RESULTS

4.1 Down syndrome: main clinical features

4.1.1 Cognitive profile of DS

The first aim of Locatelli 2021 (Locatelli et al., 2021) study is to contribute knowledge on the acquisition of developmental milestones in DS. Considering motor development in the study sample, children acquired sitting at approximately 9 months of age and walking at approximately 24 months. These ages are in line or slightly in advance with respect to previous studies. Indeed, in previous studies the reported age of sitting was 10 months (Winders et al., 2019) or 11 months (Tudella et al., 2011;Kim et al., 2017) and 26 (Kim et al., 2017) or 28 months (Winders et al., 2019) for walking. Considering language development, the mean age of acquisition of babbling is approximately 15 months, confirming that in children with DS the onset of babbling is delayed and continues into the second year of life (Roberts, J.E; 2007). Furthermore, in this case the interindividual variability is quite high (approximately 10 months). Finally, the mean age of sphincter control acquisition is approximately 44 months. For this variable the interindividual variability is very high (22 months) and that 23 children in the younger group had not yet acquired sphincter control.

All these results on developmental milestone acquisition are consistent with the fact that children with DS develop at a slower rate compared with typically developing (TD) children and for this reason milestones are acquired later with respect to their TD peers. Moreover, our results are in line with recent research on DS underlying high heterogeneity in development (Karmiloff-Smith et al., 2016).

The second aim of this study (Locatelli et al. 2021) is to determine the relationship between developmental milestones and the subsequent development of the child. For the preschoolers, sitting resulted to be a significant predictor of later gross motor development, both assessed directly or indirectly through parent reports of everyday life behaviours. Therefore, the earlier a child with DS started to sit, the earlier he/she started to walk, run, and have stronger leg muscles that allow him/her to jump and have better general coordination or balance, all skills assessed in Griffiths-III Gross-Motor scale. However, in the School-age group, sitting becomes less important in predicting everyday life motor development as assessed through parents' reports. In this group walking showed a moderate correlation with later development, although when considered in a model with other variables, it was not a significant predictor. Moreover, motor milestones resulted to also be related to other developmental domains. In fact, in preschoolers the age of onset of sitting showed a

moderate correlation and an anecdotal predictive power of later communication skills as described by parents

(VABS-II Communication). In the School-age group, motor milestones showed a moderate relation with later cognitive and adaptive development, although when considered in a more complex model these variables did not show a predictive role. Considering language milestones, in preschoolers babbling showed a moderate correlation to later everyday life communication, while in school-age participants it resulted moderately correlated with later communication and cognition. Considered together with other developmental milestones it emerged to be one of the significant predictors of later verbal cognitive development. Finally, our data suggest that the onset of sphincter control has an important role in development. Preschoolers that have already acquired sphincter control have better motor, adaptive, and socio-emotional developmental levels. However, the influence of sphincter control on development is bigger in older children. In fact, in school age children sphincter control resulted as significant predictor of later motor, cognitive, communication, adaptive behaviour, and motor development. The correlations between developmental milestones and later development in Preschoolers are reported in Table 3.

The table reports Pearson coefficients for the correlations between Sitting, Walking, Babbling, Sphincter Control, and variables describing later development. Biserial correlations were run for sphincter control since it has been considered as a dichotomous variable, since a high number of children in this group did not yet show sphincter control.

	Sitting	Babbling	Walking	Sphincter Control
Griffiths-III Foundations of Learning	-0.080	0.158	-0.011	0.209
Griffiths-III Language and Communication	-0.238	-0.002	0.135	0.307
Griffiths-III Eye and Hand Coordination (n=25)	-0.137	-0.040	-0.148	0.280
Griffiths-III Personal-Social-Emotional (n=251)	-0.167	0.099	0.105	0.321
Griffiths-III Gross Motor Skills (n=251)	-0.445*	0.033	0.022	0.266
DP-3 Motor	-0.233	-0.062	0.131	0.331
DP-3 Socio-Emotional	0.167	0.074	0.253	0.400*
DP-3 Adaptive Skills	0.093	-0.053	0.222	0.430*
DP-3 Cognitive	-0.114	0.063	0.238	0.246
DP-3 Communication	-0.220	-0.300	0.203	0.291
VABS-II Communication	**-0.360***	-0.161	0.067	0.230
VABS-II Daily Living Skills	-0.239	0.136	-0.07	0.120
VABS-II Socialization	-0.152	0.024	0.097	0.213
VABS-II Motor Skills	**-0.397***	0.127	-0.098	0.102

Table 3. Correlations between developmental milestones and cognitive, language, adaptive and motor skills in the Preschooler group. N=30. * =p<.05; **=p<.01; ***=p<.001. [1] For these variables the numerosity is reduced because 5 participants did not complete the Griffiths-III assessment.

In a second work (Onnivello et al., 2022a), our aim was to clarify the EF and adaptive behaviour profiles in children/adolescents with DS, explore differences by age, and analyse the relationship between EF and adaptive behaviour in this population. Two groups of individuals with DS, one aged from 3 to 6.11 years, and the other aged from 7 to 16 years, were assessed on their EFs (with the BRIEF/BRIEF-P) and adaptive behaviour (with the VABS-II). Generalised EF difficulties were seen in individuals with DS, consistently with the previous literature (Lee et al., 2011;Loveall et al., 2017) and no difference between the two age groups in terms of the severity of EF difficulties were described by parents. The preschooler group showed a relative strength in Emotional Control, while they were more impaired in Shift, Plan/Organise and Inhibit, and most impaired in Working Memory. The school-age group showed a relative strength in Emotional Control and Organisation of Materials; intermediate ability levels for Inhibit and Self-Monitor; and a relative weakness in Shift, Initiate, Working Memory, Plan/Organise, and Task-Monitor. There were some similarities and some differences between the two age groups when the scales common to the two versions of the BRIEF were compared. Both groups were relatively strong on Emotional Control and weak on Working Memory, with Inhibit in between. The two age groups differed as regards Plan/Organise and Shift, domains in which the older children showed a more severe

weakness. The greater difficulty in Shift and Plan/Organise in the older group may be because tasks in these domains get harder with age. Comparing the two age groups, preschoolers had higher standardised scores than school-age children with DS in Daily Living Skills and Socialisation. The lower scores seen in the older children reflect not a loss of their abilities, but a slower development of these skills than in the typically developing population. Scores for Communication were equally low in both DS groups, in line with the tendency of individuals with this syndrome to be particularly weak in language development at any age (Silverman, 2007;Grieco et al., 2015). Similarities and differences also emerged in the two groups' adaptive behaviour. They were both relatively strong on Socialisation and weak on Communication and Daily Living Skills, but preschoolers scored higher for Daily Living Skills than school-age children. More variability has been reported regarding Daily Living Skills, and it may be that environmental variables have a role in modulating the development of these skills. The relationship between EFs and adaptive behaviour differed in the two age groups considered here. The two domains seemed quite independent in preschoolers, with significant relationships only between Communication and Working Memory (the latter predicting the former). For school-age children, on the other hand, correlations emerged between almost all EFs and adaptive behaviour domains, emphasising the important role of EFs in everyday functioning at this age.

In ((Onnivello et al., 2022b) we explore and compare verbal and non-verbal intelligence, as assessed with the WPPSI-III, in a sample of 72 individuals with DS. A marked interindividual variability emerged within our sample, revealing three subgroups with different cognitive profiles. The three groups of participants were labelled as follows: C1, the Verbal Profile group (scoring higher on verbal than non-verbal index); C2, the Non-Verbal Profile group (scoring higher on non-verbal index); and C3, the Homogeneous Profile group (with similar verbal and non-verbal indices). The three groups were similar in terms of the numbers of participants in each one. No significant differences emerged between the three groups in terms of chronological age (CA) ($p > .05$, $BF10 = 0.12$), see Table 4.

	Between-subjects Comparison			Within-subjects Comparison		
	Verbal vs Non-Verbal	Verbal vs Homogeneous	Non-Verbal vs Homogeneous	Verbal Profile	Non-Verbal Profile	Homogeneous Profile
Verbal Index	t=10.96 p<.001 d=1.19 BF_{10}=9.53x10^{13}	t =-2.29 p =0.03 d =0.32 BF_{10}=3.17	t =-9.88 p <.001 d =1.40 BF_{10}=3.03x10^{19}	t =5.83 p <.001 d =0.61 BF_{10}=6.69x10^{3}	t =-4.36 p <.001 d =0.60 BF_{10}=1.12x10^{2}	t =-0.94 p =0.36 d =0.10 BF_{10}=0.34
Non-Verbal Index	t =0.41 p =0.70 d =0.05 BF_{10}=0.30	t =-8.13 p =<.001 d =0.96 BF_{10}=2.89x10^{10}	t =-10.44 p <.001 d =0.94 BF_{10}=2.89x10^{7}			

Table 4. Post-hoc analyses, cluster x index. t t-test value; p significance level; d Cohen's d expressing the effect size; BF_{10} Bayes factor expressing the probability of the data given H1 relative to H0

Based on the generally described greater strength in non-verbal than in verbal skills in DS, we might expect individuals with DS to have higher scores in the non-verbal domain than in the verbal one. C2 group, the Non-Verbal Profile had the lowest scores in cognitive test scores compared with the other two groups and showed the typical profile associated with DS. Despite all, this study described different profiles, and a broader and more varied picture within the verbal and non-verbal domain.

4.1.2 Phenotypic signs in subjects with DS

Locatelli and coll. (Locatelli et al., 2022) study allowed the review of the fundamental typical phenotypic features of DS in 233 children with DS. The first objective was to analyse in depth the DS phenotypic characteristics following the so-called Jackson's checklist (Jackson et al., 1976) in order to assess the reliability of the clinical diagnosis. The second objective was to associate the degree of ID with the percentage of Jackson's signs present in DS children.

Considering the frequency of the 24 DS characteristic features available in the Jackson's checklist in our sample population, they are never all present together in a subject, the maximum is 20 signs present in one child. In addition, there is not a single phenotypic sign always present in all children. Oblique eye fissure and joint laxity are the most frequent signs (frequencies > 90%), followed by epicanthic eye-fold, hypotonia and separated hallux (frequencies > 80%); see Figure 11 below.

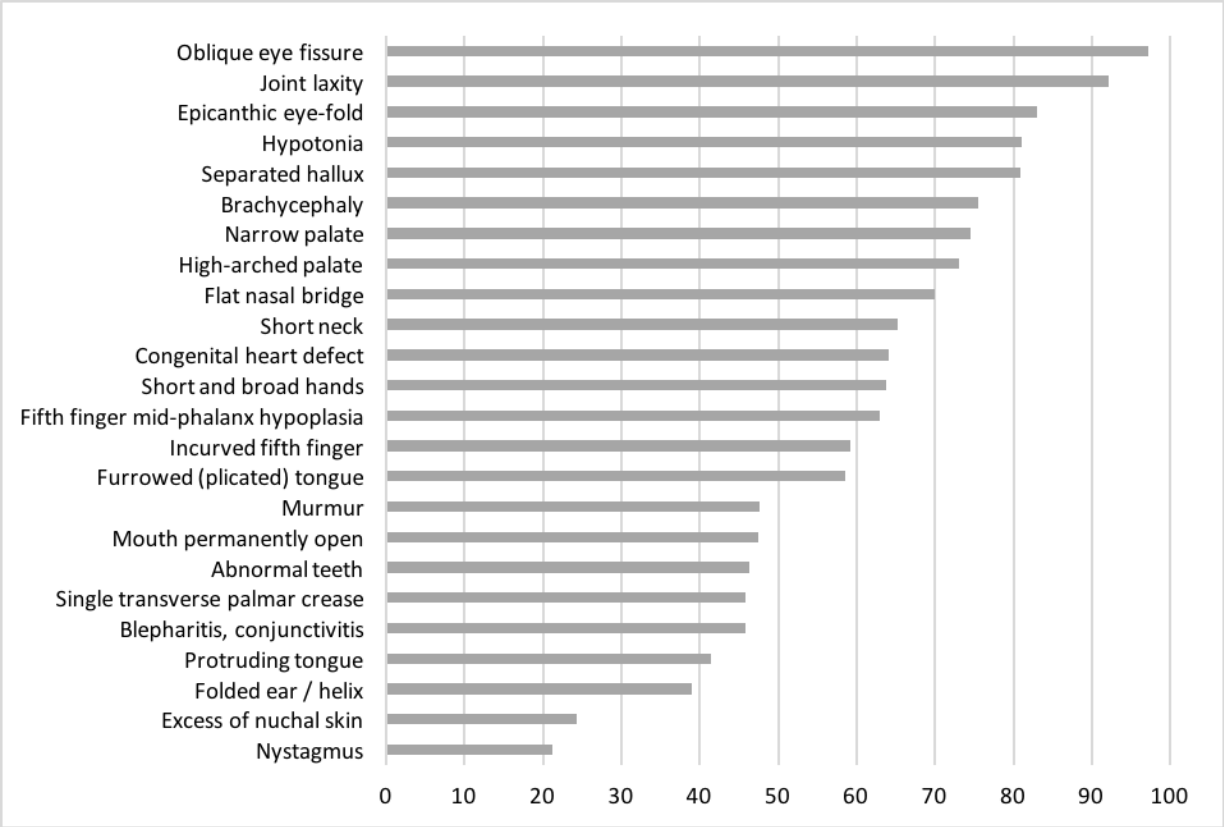

Figure 11. Representation of frequencies of Jackson's signs in our study sample. Brushfield spots was excluded.

Contingency tables and applied Fisher's exact test were used to investigate associations between each possible pair of Jackson's signs. Some of the associations are already known in clinical practice, such as narrow palate with high palate (together called ogival palate) and the presence of heart murmur in congenital heart defects. Interestingly, short neck has the highest number of significant associations (with short and broad hands, brachycephaly, flat nasal bridge, epicanthic eye-fold and joint laxity), followed by brachycephaly (with short neck, short and broad hands and flat nasal bridge). A strong association was found among short neck, brachycephaly and short and broad hands. Their frequency ranges from 63.68% for broad and short hands to 75.47% for brachycephaly. In most cases when one sign is present the other two are also present, while in a small group of subjects none of these signs is present. This observation prompted us to question the possibility of distinguishing two sub-phenotypes within the DS population, which could be called "BHN" (Brachycephaly, short and broad Hands and short Neck) (86 subjects) and "non-BHN" (21 subjects); see Table 5.

Jackson's sign	Jackson's sign	p-value	p-value after FDR
Narrow palate	High-arched palate	<0.00001	<0.00001
Mouth permanently open	Protruding tongue	<0.00001	<0.00001
Congenital heart defect	Murmur	<0.00001	<0.00001
Short and broad hands	**Short neck**	<0.00001	0.00002
Fifth finger mid-phalanx hypoplasia	Incurved fifth finger	<0.00001	0.00002
Brachycephaly	**Short neck**	<0.00001	0.00005
Short and broad hands	Fifth finger mid-phalanx hypoplasia	<0.00001	0.00008
Brachycephaly	**Short and broad hands**	0.00009	0.00301
Flat nasal bridge	**Short neck**	0.00018	0.00559
Epicanthic eye-fold	**Short neck**	0.00061	0.01682
Protruding tongue	Furrowed (plicated) tongue	0.00114	0.02857
Brachycephaly	Flat nasal bridge	0.00132	0.03046
Joint laxity	**Short neck**	0.00154	0.03267

Table 5. Significant associations between Jackson's signs. Brushfield spots feature was excluded. Signs are sorted by increasing p-value after false discovery rate (FDR) correction. Most recurrent features are highlighted in bold.

Contingency analysis was used to define the statistical significance of the associations between IQ scores and each Jackson's sign. Cognitive data were collected studying a total of 114 children/adolescents, 43 children (3 -6 .11 years old) were evaluated with Griffiths-III scales (Green et al., 2016), 71 (7-16 years old) were evaluated through WPPSI-III scales (Wechsler, 2002). The sample population was labelled into two subgroups according to whether their IQ score was higher than/equal to or lower than the mean value calculated in all subjects (40.30), obtaining 56 and 58 subjects respectively. None of the Jackson's signs resulted significantly associated with IQ scores, considering p-value after FDR correction < 0.05. In addition, for each Jackson's sign the mean IQ score was compared through unpaired t-test between subjects with and without that feature, with no significant p-values after FDR correction. The same analysis was repeated, dividing children evaluated with Griffiths-III and with WPPSI-III with no significant results.

4.2 Genomics of Down syndrome: trisomy of full or partial chromosome 21

4.2.1 Partial Trisomy 21 (PT21)

We have reported the description of two patients with PT21: the first subject with a diagnosis of DS and the second one without diagnosis of DS but with a different type of psychomotor development delay. Molecular data showed different trisomic regions, allowing the inclusion of these new PT21 cases in the study of the DS critical region. The data are reported in Pelleri et al. 2022 accepted for publication in *BMC Medical Genomics*.

The first proband is a 2-year-old Italian girl that is the first child of non-consanguineous healthy parents. Her parents were both 32 years old at the time and the diagnosis of DS was not established during pregnancy. The girl was born at 36 weeks of gestation, with natural delivery, because of premature rupture of the membranes. At the time of birth, the newborn's APGAR score was 9 at 1 minute and 9 at 5 minutes and her somatic features were: a weight of 2,550 g, and a recumbent length of 50 cm. The analysis of dysmorphic features showed a clinical pattern compatible with diagnosis of DS (Table 6), also compatible with criteria suggested in the classic work by Jackson and coll. (Jackson et al., 1976). Cytogenetic analysis was required to confirm the diagnosis. Postnatal radiography showed a "double bubble" sign in the upper abdomen suggesting the presence of duodenal atresia or stenosis. No other gastrointestinal associated anomalies were detected, and the nasogastric output was clear and nonbilious. The surgical repair of complete atrioventricular septal defect (AVSD) was performed at the VII month of life and the post-operative period was regular. At 6 months of age an immunological evaluation was recommended due to low IgG value found in a routine blood analysis (IgG concentration=95 mg/dL). The examination confirmed hypogammaglobulinemia, excluding alterations of lymphocyte subpopulations. The same year the child was diagnosed for esophageal reflux, later successfully treated with proton pump inhibitors therapy. Regarding the auxological follow-up of the baby, the measurements: Length (L), Weight (W) and Head Circumference (HC) were performed at 3 months, then every three months during the first year and every six months during the second year of follow-up. Referring to the growth velocity charts of the general population, the growth rate for the baby was below the 10th percentile, both in terms of L, W and HC. During the last year, due to reduction of comorbidities, an improvement in the growth rate reaching the 10-50th percentile both for W and L, was observed. Nevertheless, using growth charts specific for children with DS, the pattern of L, W and HC were inside the normal percentile range, reaching almost the 90th for L and W, and the 50th of HC at 24 months (age at last evaluation).

The second proband is a 9-year-old Italian girl who was born at 39 (2/7) weeks of gestational age by spontaneous vaginal delivery as the second pregnancy of healthy and non-consanguineous parents. Her mother and father were respectively 38 and 29 years old when she was born. Prenatal screening was not performed, and prenatal ultrasound examinations were normal. Regarding anthropometry at birth, her head circumference was 31.5 cm, length was 48.5 and weight was 2810 g. The Apgar score test, performed one minute after birth, was 9/10. The child walked autonomously around 18 months and spoke first words after 12 months, but she never acquired age-appropriate language. She had no convulsion, but the mother noticed she had reduced memory abilities. At 9 years of age (age at last evaluation), she was referred to the Medical Genetics Unit, because of psychomotor development delay and then, intellectual disability. At physical examination, she did not show the DS recognizable phenotype, and peculiar dysmorphic features could not be detected on her face or body (Table 6, <5 signs). Therefore, according with the clinical team, we have classified the girl as non-DS. Attention-Deficit / Hyperactivity Disorder (ADHD) was diagnosed, along with a sleep disorder. The patient was also overweight, had hypertrichosis and showed early pubarca (see Table 6).

Jackson's Checklist	Case 1	Case 2	Frequency in DS subjects (%) (Lee and Jackson, 1972)
Flat Nasal Bridge	+	-	86.7
Oblique eye fissure	+	-	85.1
Epicanthic eye fold	+	-	78.5
Brachycephaly	+	-	75.2
Short neck	-	-	70.2
High-arched palate	+	-	67.7
Narrow palate	+	-	67.7
Gap between first and second toes (right, left)	+	+	64.4
Short and broad hands	-	-	61
Loose skin of the neck	-	-	60.3
Transverse palmar crease (right, left)	+	-	60.3
Joint Hyperflexibility	+	-	59.5
Short fifth finger (right, left)	+	-	51.2
Folded ear (right. left)	-	-	42.9
Incurved fifth finger (right, left)	+	-	42.9
Mouth permanently open	-	-	40.4
Muscular Hypotonia	+	N/A	40.4
Protruding tongue (macroglossia)	-	-	38.0
Brushfield spots (iris color)	N/A	-	34.7
Heart murmur	+	-	33.0
Abnormal teeth	-	-	31.4
Congenital heart defect	+ (AVSD)	-	24.7
Blepharitis, conjunctivitis	+	-	22.3
Furrowed tongue	-	-	22.3
Nystagmus	+	-	17.3

Table 6. Jackson list. Complete list of the 25 Jackson's physical signs reported for Case 1 and Case 2 and their frequencies reported in Jackson et al. (Lee and Jackson, 1972) +: present; -: absent; N/A: data not available

The metaphasic FISH analysis of DNA from Case 1 showed a homogeneous trisomy deriving from an isodicentric chromosome 21, with breakpoints in the 21q22.3 chromosomal region. This analysis also revealed the loss of the terminal part of the long arm of both chromosomes forming the isodicentric one. FISH analysis was performed on the parents, showing two normal Hsa21 in both. Moreover, Array-CGH analysis of the proband showed a duplication from 14,145,727 to 43,860,444 bp (29.715 Mb) and a deletion of about 2.7 Mb from 43,927,315 to 46,670,405 bp (GRCh38).

Concerning Case 2, Array-CGH analysis revealed a 20p13 distal deletion of 2.1 Mb and a 21q22.2q22.3 distal duplication of 7.2 Mb, suggesting the presence of an unbalanced translocation der(20)t(20;21). FISH analysis on metaphases confirmed that the proband carried an unbalanced

translocation, as the subtelomere probe for 20p (D20S1157) was present in the normal chromosome 20 and absent in the derivative chromosome 20 on which the subtelomere probe for 21q (D21S1146) was transposed. FISH analysis on parental metaphases showed that father harbors the balanced translocation.

Bibliographic searches resulted in 92 new papers. Only two studies reported PT21 cases matching the inclusion and exclusion criteria described in the Methods section named Case 3 (Putra et al., 2017) and Case 4 (Chen et al., 2019) in the present work.

Case 3 (Putra et al., 2017) is a female baby with DS. The karyotype with an isodicentric chromosome resulting in a partial trisomy 21 was 46,XX,idic(21)(q22.3). A chromosomal microarray analysis (CMA) confirmed the presence of nearly full trisomy for chromosome 21 and also a monosomy for the 21q22.3 region; in particular the chromosomal alteration has been described as arr[GRCh38]21p11.2q22.3(10810857_45448165)x3,21q22.3(45471378_46664244)x1.

Case 4 (Chen et al., 2019) is a male baby without DS phenotype except congenital heart disease (CHD). Molecular analysis revealed a 0.56 Mb duplication of 21q22.3 described as arr[GRCh38] 21q22.3(46062296_46623792)x3.

Our results are fully consistent with the concept that the HR-DSCR is critical for DS diagnosis being the only duplicated sequence shared by all DS subjects. However, both reviewed and new cases did not allow us to refine the HR-DSCR limits because the breakpoints of their trisomic segments turned out to be outside the HR-DSCR, see Figure 12.

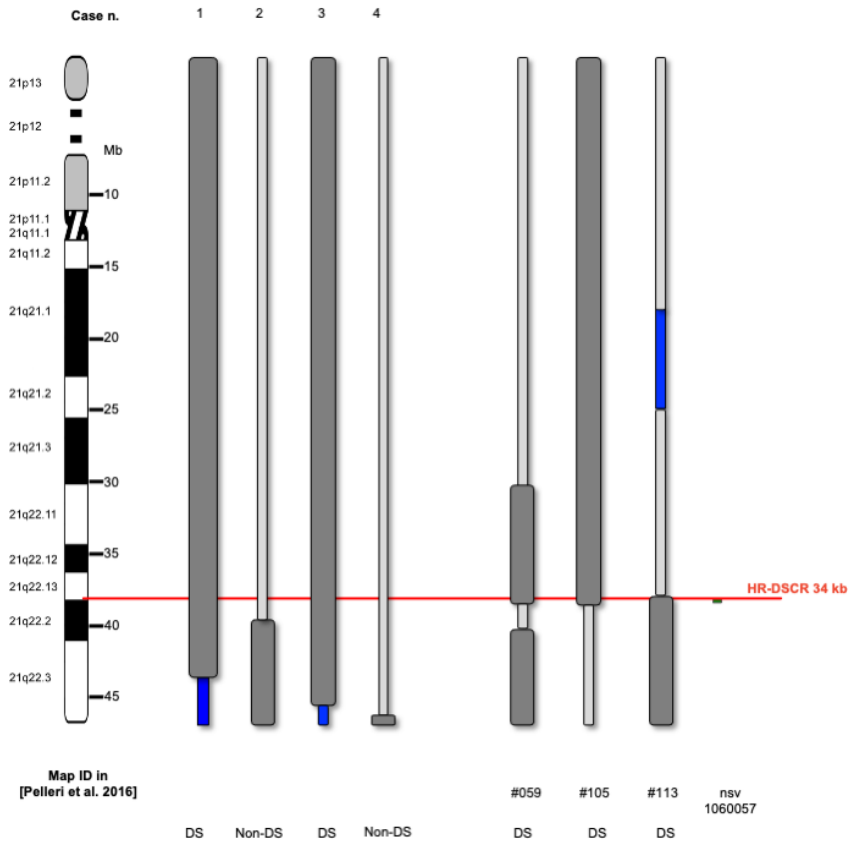

Figure 12. HR-DSCR as highlighted by the partial trisomy 21 integrated map (simplified view). The cases described in the present work are shown (Cases 1, 2, 3, 4); moreover, the cases (#059, #105 and #113, ID used in (Pelleri et al., 2016) and the copy number variant (CNV, nsv1060057, from Database of Genomic Variants, http://dgv.tcag.ca/) strictly defining HR-DSCR limits are shown here. Light grey bar: disomic region; dark grey bar: trisomic region: Blue bar: monosomic region. Case n. 1 (this work); Case n. 2 (this work); Case n. 3 (Putra et al., 2017); Case n. 4 (Chen et al., 2019); #059: Case DUP21SOL (Korbel et al., 2009); #105: (Sato et al., 2008); #113: Case DUP21HAD (Korbel et al., 2009). DS: subject with Down syndrome; non-DS: subject without Down syndrome.

4.2.2 Highly restricted Down syndrome critical region (HR-DSCR)

HR-DSCR is the minimal region of Hsa21 shared by all subjects with PT21 and a confirmed diagnosis of DS. It is described as an intergenic region, but its link with the typical DS symptoms suggests that it could contain active *loci*. In this work, starting from HR-DSCR limits designed by Pelleri and coll. (Pelleri et al., 2016), Ensembl Genome Browser was consulted in order to investigate the presence of transcripts annotated in this region. The data have been published in Antonaros et al. 2021b.

KCNJ6-201 and *DSCR4-201* are validated transcripts and are deposited on the Gene database, even if the role of *DSCR4-201* is not yet well characterized.

All the transcripts were visible on agarose gel after 45 cycles of PCR and only in specific tissues.

We analyzed 86 RNA-Seq experiments and the reads generated by RNA-Seq experiments were aligned with *KCNJ6* and *DSCR4* transcripts.

The entire *KCNJ6-202* transcript was detected in brain, cerebellum, and placenta, while the entire *DSCR4-202* and *DSCR4-203* transcripts were not detected in any tissues. A 177 bp amplicon was detected using a primer pair based on exon 3 and exon 4 of *DSCR4-202* that was not connected with its previous exons. *DSCR4-203* was not detected by either computational and molecular analyses.

No alignments were reported with the entire isoform of *KCNJ6-202*, and *DSCR4-203* transcripts, while the alignments predict the expression of the entire *KCNJ6-201* transcript in cerebral tissues confirming the previous literature (Fagerberg et al., 2014), of the entire *DSCR4-202* transcript in testis and of the entire *DSCR4-201* transcript in placenta and testis, confirming the previous literature data (Saber et al., 2016). A schematic graphical representation of *KCNJ6* and *DSCR4* isoforms is shown in Figure 13.

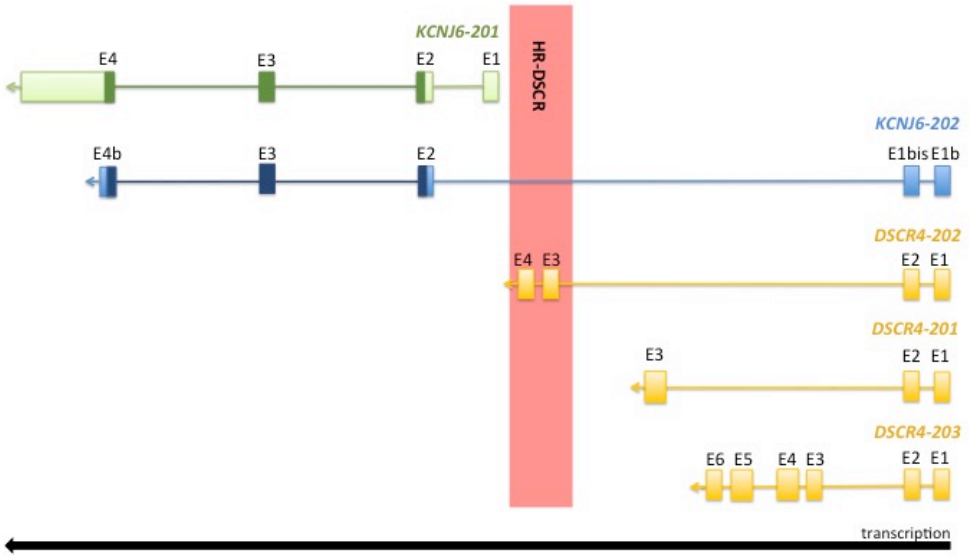

Figure 13. Graphical representation of 21q22.13 locus. Schematic graphical representation of *KCNJ6* and *DSCR4* isoforms.

Reverse Transcription-Polymerase chain reaction (RT-PCR) was used to perform *KCNJ6* and *DSCR4* expression profiles in several tissues. The entire *KCNJ6-201* transcript was detected in adrenal gland, brain, cerebellum, cerebral cortex, heart, placenta, skeletal muscle, skin, thymus, and thyroid (see Figure 14A). Sanger sequencing in brain confirmed PCR results. The entire KCNJ6-202 transcript was detected in brain, cerebellum, and placenta (see Figure 14B). Sanger sequencing in placenta confirmed PCR results. The entire *DSCR4-201* transcript was detected in brain, placenta, testis, and thyroid (Figure 14C). Sanger sequencing in thyroid confirmed PCR results. The

entire *DSCR4-202* transcript was not detected in any tissues, but was detected the expression of 2 exons, located in the HR-DSCR, in placenta and testis confirmed by Sanger sequencing in both tissues (see Figure 14D). The entire or partial *DSCR4-203* transcript was not detected in any tissues.

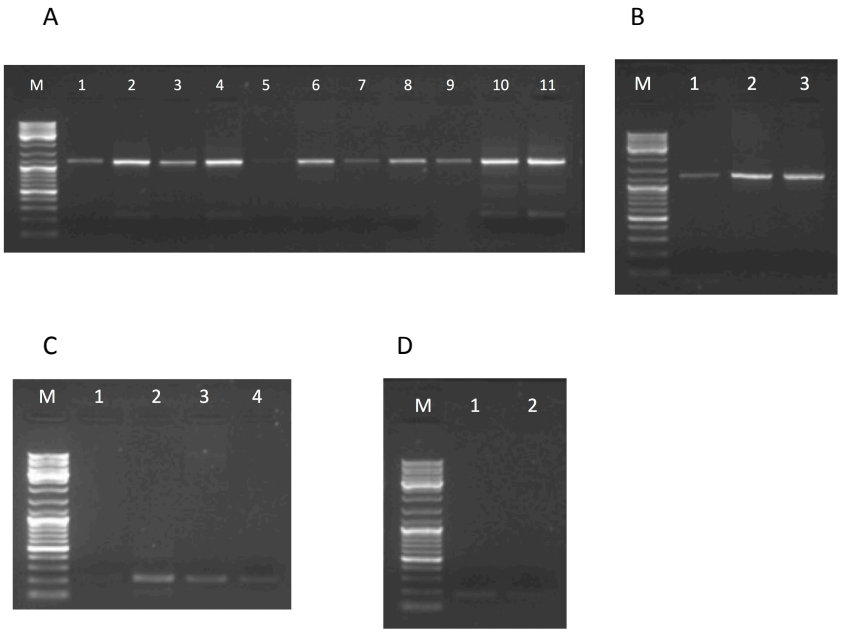

Figure 14. Gel electrophoresis picture of *KCNJ6* and *DSCR4* transcripts. A. Entire *KCNJ6-201* transcript (1167 bp). Adrenal gland (lane 1), brain (lane 2), cerebellum (lane 3), cerebral cortex (lane 4), heart (lane 5), placenta (lane 6), skeletal muscle (lane 7), thymus (lane 8), thyroid (lane 9), T21 fibroblast (lane 10), and normal control fibroblast (lane 11). **B.** Entire *KCNJ6-202* transcript (1244 bp). Brain (lane 1), cerebellum (lane 2), and placenta (lane 3). **C.** Entire *DSCR4-201* transcript (215 bp). Brain (lane 1), placenta (lane 2), testis (lane 3), and thyroid (lane 4). **D.** Partial *DSCR4-202* (177 bp). Placenta (lane 1) and testis (lane 2).

4.3 Transcriptome analysis

We generated RNA-Seq from total RNA isolated from blood cell samples of 4 T21 and 4 normal control individuals. TRAM software was used to obtain 19,378 genes with an available expression value for T21 blood cell transcriptome map, and 19,357 genes with an available expression value for normal control blood cell transcriptome map. These values allowed us to obtain a differential (T21 vs normal control) transcriptome map including the gene expression ratios for 17,867 loci. Detailed results for each map are also available in TRAM software deposited at: https://osf.io/ab3np/?view_only=c8cfbaf81a894f379854722a13efb9ec.

Among the Hsa21 genes we have found 143 genes with a gene expression ratio ≥1.30 and we observed the over-expression of *TSPEAR* and *MX1* genes (ratio=6.76), *MX2* gene (ratio=4.32) encoding for MX dynamin like GTPase 1 and 2, and of *SLC19A1* gene (ratio=3.5) encoding for solute carrier family 19 member 1.

Considering chromosomes, Hsa21 has the highest T21 vs normal control mean expression ratio compared to the other chromosomes (2.01 with a standard deviation of 1.50) see Figure 15. Interestingly, mitochondrial genes have a T21 vs normal control mean expression ratio of 1.56.

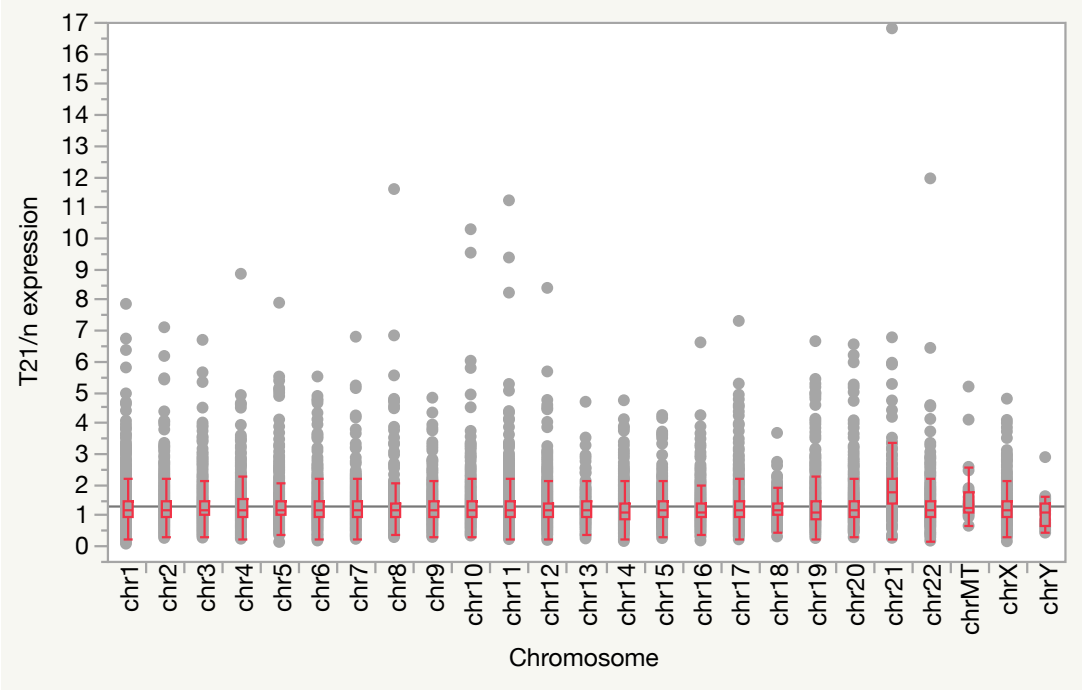

Figure 15. Trisomy 21 (T21) vs normal control (n) expression ratio in blood cell transcriptome map divided by chromosome.

The segment analysis of the differential transcriptome map showed that four segments are statistically significant over-expressed in T21 compared with normal control samples (Table 6). The two segments with the highest expression ratios are on Hsa21, while the other two are on chromosomes 22 and 10 (Table 6).

Chr	Location	Segment start	Segment end	Expression ratio	Genes
Chr21	21q22.2-q22.3	41,250,001	41,750,000	4.16	*MX2 MX1 RIPK4*
Chr21	21q22.3	44,000,001	44,500,000	4.11	*PWP2 TRPM2 TSPEAR*
Chr22	22q11.22	21,750,001	22,250,000	3.65	*IGLV4-69 IGLV8-61 IGLV10-54*
Chr10	10q23.31	89,000,001	89,500,000	2.78	*IFIT2 IFIT3 IFIT1*

Table 6. List of statistically significant over-expressed segments (q<0.05) in trisomy 21 (T21) vs normal control blood cell transcriptome map. Segments are sorted by decreasing T21 vs normal control expression ratio. For simplicity, some segments are not shown because they overlap with those highlighted in one of the listed regions. Chr=chromosome, Location segment cytoband derived from that of the first mapped gene within the segment, Segment start/end chromosomal coordinates for each segment.

No statistically significant under-expressed segments were found. Among the over-expressed genes in all these segments, *MX2, MX1, IFIT2, IFIT3* and *IFIT1* genes encode for proteins involved in the interferon response pathway. *RIPK4* gene encodes for a serine/threonine protein kinase that interacts with protein kinase C-delta and can also activate the nuclear factor kappa B and is required for keratinocyte differentiation. *PWP2* gene is involved in ribosome RNA processing. *TRPM2* gene encodes for a tetrameric cation channel that is permeable to calcium, sodium and potassium and is regulated by free intracellular ADP-ribose. *TSPEAR* gene plays a critical role in tooth and hair follicle morphogenesis through regulation of the Notch signaling pathway and it may play a role in the development or function of the auditory system. *IGLV4-69, IGLV8-61* and *IGLV10-54* genes encode for immunoglobulin lambda variable domains. No statistically significant under-expressed segments were found. All four Hsa21 genes encoding for interferon receptors (*IFNAR1, IFNAR2, IFNGR2, IL10RB*) are over-expressed (expression ratios: 2.33, 2.13, 2.25 and 2.66, respectively) in T21 blood cell samples compared to normal control cells, as is also the case for *IDO1* gene (chromosome 8, expression ratio 1.34) encoding for a known interferon-stimulated protein.

Expression values were selected for genes implicated in the one-carbon metabolic process (Gene Ontology, GO:0006730) and the folic acid-containing compound metabolic process (GO:0006760) due to the hypothesis that those pathways might be involved in the manifestation of the main symptoms in DS (Lejeune, 1979). Among 37 genes for which a T21 vs normal control expression ratio was available (derived by expression values detected in at least two samples in both pools), the global mean expression ratio is 1.22 (with a standard deviation of 0.69), and 22 genes are over-expressed and 15 under-expressed. Among the over-expressed genes, two map on Hsa21: *GART* gene (ratio=1.58), encoding for phosphoribosylglycinamide formyltransferase, phosphoribosylglycinamide synthetase, phosphoribosylaminoimidazole synthetase, and *SLC19A1* gene.

Real-Time RT-PCR experiments were conducted to validate the T21 vs normal control differential transcriptome map obtained through the elaboration of RNA-Seq data by TRAM analysis. Bivariate statistical analysis was performed between the gene expression ratios observed by Real-Time RT-PCR on the 19 selected genes and the differential expression ratios of the same genes obtained by RNA-Seq from 8 subjects (4 subjects with DS and 4 normal controls) ($r=0.91$, $p=0.0001$). Real-Time RT-PCR experiments were also performed on a different and larger cohort of 12 subjects (6 subjects with DS and 6 normal controls), in order to independently confirm the expression level of five genes reported as significantly over-expressed by RNA-Seq. Bivariate statistical analysis was performed between the gene expression ratios observed by Real-Time RT-

PCR on the six selected genes in the cohort of 12 subjects and the expression ratios of the same genes in the original group of 8 subjects whose samples had also been subjected to RNA-Seq ($r=0.88$, $p=0.0186$).

Among the genes with T21/normal expression ratio ≥1.30, we observed that the most significantly enriched biological process associated to the greatest number of genes are: "vesicle organization" (GO:0016050) with 713 genes; "whole membrane" (GO:0098805) with 645 genes; "transferase activity, transferring phosphorus-containing groups" (GO:0016772) with 599 genes; and finally, “Innate Immune System" (GO:1269203) with 517 genes.

Among the genes with T21/normal expression ratio ≤0.76, the most significantly enriched biological process associated to the greatest number of genes are: "cell cycle" (GO:0007049) with 149 genes; "nuclear chromatin" (GO:0000790) with 143 genes; "DNA-binding transcription factor activity, RNA polymerase II-specific" (GO:0000981) with 129 genes; and finally, "Generic Transcription Pathway" (1269650) with 79 genes.

The three transcriptome maps (T21, normal control and T21 vs normal control) obtained by the elaboration of the RNA-Seq results were compared with other blood-derived transcriptome maps obtained through publicly available microarray (Pelleri et al., 2018) and RNA-Seq meta-analyses for WBC (white blood cells) (Powers et al., 2019) see table 7.

Comparison	Tot first study	Tot second study	First study unique genes	Second study unique genes	Common genes	r
T21 blood cells (RNA-Seq) vs T21 WBC (array) (Pelleri et al., 2018)	19,378	24,699	4,336	9,657	15,042	0.7353
n blood cells (RNA-Seq) vs n WBC (array) (Pelleri et al., 2018)	19,357	24,699	4,316	9,658	15,041	0.7319
T21/n blood cells (RNA-Seq) vs T21/n WBC (array) (Pelleri et al., 2018)	17,867	24,699	3,414	10,246	14,453	0.1193
T21 blood cells (RNA-Seq) vs T21 WBC (RNA-Seq) (Powers et al., 2019)	19,378	22,614	3,194	6,430	16,184	0.7137
n blood cells (RNA-Seq) vs n WBC (RNA-Seq) (Powers et al., 2019)	19,357	21,099	3,259	5,001	16,098	0.7097
T21/n blood cells (RNA-Seq) vs T21/n WBC (Powers et al., 2019)	17,867	20,826	2,517	5,476	15,350	0.1718
T21 WBC (array) (Pelleri et al., 2018) vs T21 WBC (Powers et al., 2019)	24,699	22,614	6,082	3,997	18,617	0.8702
n WBC (array) (Pelleri et al., 2018) vs n WBC (Powers et al., 2019)	24,699	21,099	6,835	3,235	17,864	0.8721
T21/n WBC (array) (Pelleri et al., 2018) vs T21/n WBC (Powers et al., 2019)	24,699	20,826	6,939	3,066	17,760	0.3354

Table 7. Comparison among trisomy 21 (T21) or normal control (n) blood cell transcriptome maps obtained by RNA-Seq (present study) and microarray and RNA-Seq (different studies) experiments and analysed by TRAM. For each comparison, the number of genes in common between the two compared studies, and the number of the unique gene for each study are indicated. For each comparison, Spearman correlation coefficients (r) are calculated on common genes ($p<.0001$ by the JMP software for all comparisons). WBC white blood cells.

The best concordance was found between the normal control WBC transcriptome maps obtained through microarray meta-analyses (Pelleri et al., 2018) and RNA-Seq data (Powers et al., 2019) elaborated here by TRAM, as it could be expected due to the similarity of the type of biological samples. A strong correlation was also observed between our RNA-Seq results and the RNA-Seq data from Powers and coll. (Powers et al., 2019) for both T21 and normal control data, and between microarray data from Pelleri and coll. (Pelleri et al., 2018) and RNA-Seq data from Powers and coll. (Powers et al., 2019). The results concerning transcriptome profile in normal and T21 blood cells have been published in Antonaros et al. 2022c.

4.4 Down syndrome and metabolic alterations

4.4.1 Metabolomic profile of subjects with DS through Nuclear Magnetic Resonance (NMR)

PLS-CA analysis of all plasma samples discriminated DS and CTRL groups with an accuracy of 94% in both CPMG and NOESY spectra (Figure 16A, B, respectively). If we only consider fasting subjects, the discrimination accuracy only slightly decreases to 90% with CPMG spectra and 87% with NOESY spectra (Figure 16C, D).

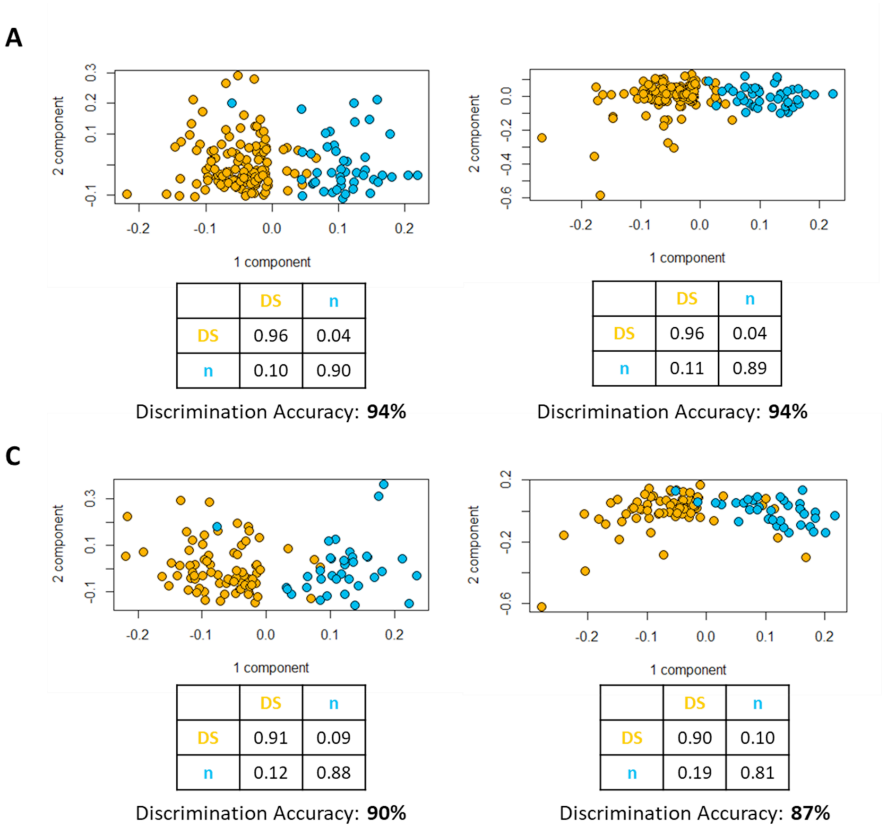

Figure 16. PLS-CA analysis of all the plasma samples: (A) CPMG and (B) NOESY spectra. Score plot, each dot represents a di erent plasma sample. Orange dots: Down syndrome samples (DS, n = 129); blue dots: healthy controls (CTRL, n = 46). PLS-CA analysis of the fasting plasma samples: **(C)** CPMG and **(D)** NOESY spectra. Score plot, each dot represents a different plasma sample. Orange dots: Down syndrome samples (DS, n = 76); blue dots: healthy controls (CTRL, n = 35).

The same analyses were also performed with samples grouped by sex and showed that sex is not a confounding factor; in fact, our results show similar discrimination accuracy between DS and CTRL groups when considering females and males separately in both CPMG and NOESY spectra (Fig. 17A, B, C, D).

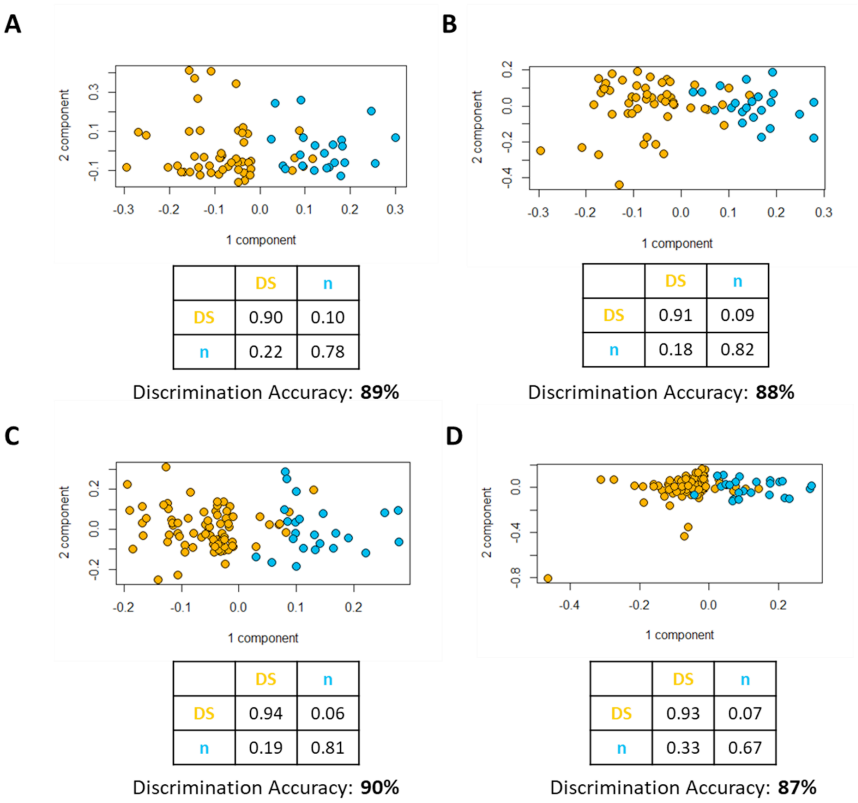

Figure 17. PLS-CA analysis of all the plasma samples from female subjects: (A) CPMG and (B) NOESY spectra. Score plot, each dot represents a di erent plasma sample. Orange dots: Down syndrome samples (DS, n = 51); blue dots: healthy controls (CTRL, n = 22). **PLS-CA analysis of all the plasma samples from male subjects: (C) CPMG and (D) NOESY spectra. S**core plot, each dot represents a di erent plasma sample. Orange dots: Down syndrome samples (DS, n = 78); blue dots: healthy controls (CTRL, n = 24).

The analysis of plasma samples provided the concentrations of 28 different metabolites involved in multiple metabolic pathways. Their levels, together with the levels of 3 unknown signals (unk1, unk2 and unk3), were analyzed through univariate statistical analysis (Tables 7 and 8). Considering the samples from all subjects, the analysis showed in DS group a significantly increased concentrations of acetate, pyruvate, acetone, creatine, formate, acetoacetate, unk3 and succinate (DS/CTRL ratio > 1); and a significantly reduced levels of unk1, tyrosine, histidine and threonine (DS/CTRL ratio < 1) (Table 7). Considering only fasting samples, acetone, threonine and unk1 resulted not significantly different in the two groups, while methionine resulted as significantly increases in DS plasma (Table 8). The univariate analysis confirmed the significant alterations of the levels of metabolites involved in processes related to mitochondrial metabolism in DS highlighted by Caracausi et al. (Caracausi et al., 2018).

Metabolites	DS (median)	CTRL (median)	DS/CTRL median	p-value	p-value after FDR Correction
Leucine	0.00344507	0.003570211	0.96	0.1372	0.2658
Isoleucine	0.00040417	0.000429518	0.94	0.0794	0.1797
Valine	0.00352026	0.003575671	0.98	0.2910	0.4748
Alanine	0.00475446	0.004815092	0.99	0.4072	0.5460
Acetate	0.00089010	0.000736686	1.21	**0.0086**	**0.0443**
Pyruvate	0.00222810	0.002017161	1.10	**0.0110**	**0.0485**
Acetone	0.00057313	0.000491021	1.17	**0.0461**	0.1190
Glutamine	0.00628499	0.006405399	0.98	0.8455	0.8455
Citrate	0.00041200	0.000393842	1.05	0.3132	0.4855
Glycine	0.00210159	0.002229647	0.94	0.4507	0.5589
Creatine	0.00115954	0.001007514	1.15	**0.0002**	**0.0018**
Creatinine	0.00041121	0.000458047	0.90	0.0812	0.1797
Lactate	0.00396610	0.003596582	1.10	0.1983	0.3616
Glucose	0.02785484	0.027973926	1.00	0.6730	0.7194
Mannose	7.778E-05	8.34062E-05	0.93	0.6267	0.7011
Tyrosine	0.00059000	0.000668668	0.88	**0.0184**	0.0651
Histidine	0.00031190	0.000349493	0.89	**0.0189**	0.0651
Phenylalanine	0.00035077	0.000352009	1.00	0.4818	0.5745
Formate	0.00020871	0.000183081	1.14	**0.0085**	**0.0443**
Fumarate	0.00001230	1.15222E-05	1.07	0.4227	0.5460
Threonine	0.00019038	0.000220489	0.86	**0.0315**	0.0880
Lysine	0.00047591	0.000466559	1.02	0.8111	0.8382
Acetatoacetate	0.00027010	0.000167440	1.61*	**0.0241**	0.0746
Methionine	0.00079102	0.000732161	1.08	0.0924	0.1909
unk1	0.00006890	8.40005E-05	0.82	**0.0039**	**0.0305**
unk2	5.3121E-05	4.60515E-05	1.15	0.2154	0.3709
unk3	0.00099389	0.000691254	1.44*	**0.0000001**	**0.0000009**
3-hydroxybutyrate	0.00041516	0.000380792	1.09	0.4091	0.5460
Succinate	0.00006360	4.63183E-05	1.37*	**0.000001**	**0.000009**
2-hydroxybutyrate	0.00010237	7.38223E-05	1.39*	0.6333	0.7013
Proline	0.00025393	0.000246843	1.03	0.4188	0.5460

Table 7. Univariate statistical analysis of all plasma samples (Down syndrome (DS), n = 129; healthy control (CTRL), n = 46). The table contains the list of metabolites analyzed with NMR. We reported both p-value of the univariate Wilcoxon test and p-value a er FDR correction for each metabolite. Metabolites that show signi cant concentration di erences in the two groups (p-value < 0.05) and/or show values in the interval next to 3:2 are reported in bold. *Values in the interval next to 3:2 (range 1.3–1.7).

Metabolites	DS (median)	CTRL (median)	DS/CTRL median	p-value	p-value after FDR Correction
Leucine	0.00361293	0.003694505	0.98	0.3591	0.4840
Isoleucine	0.00042202	0.000475091	0.89	0.1063	0.2059
Valine	0.00374662	0.003824309	0.98	0.5700	0.6796
Alanine	0.00483927	0.004903123	0.99	0.5277	0.6544
Acetate	0.00090934	0.000736206	1.24	**0.0015**	**0.0137**
Pyruvate	0.00226253	0.002109906	1.07	**0.0085**	0.0528
Acetone	0.00057523	0.000517008	1.11	0.1857	0.3199
Glutamine	0.00642759	0.006454857	1.00	0.8415	0.8696
Citrate	0.00042516	0.000385006	1.10	0.0996	0.2058
Glycine	0.00215948	0.002230915	0.97	0.6409	0.7358
Creatine	0.00114727	0.001000137	1.15	**0.0018**	**0.0137**
Creatinine	0.00045933	0.000489828	0.94	0.7342	0.7848
Lactate	0.00413212	0.003602912	1.15	0.0495	0.1395
Glucose	0.02830345	0.027789163	1.02	0.3054	0.4303
Mannose	0.00008250	8.55137E-05	0.96	0.6963	0.7709
Tyrosine	0.00060915	0.000681629	0.89	**0.0166**	0.0828
Histidine	0.00034121	0.000361783	0.94	**0.0307**	0.1030
Phenylalanine	0.00035893	0.000336898	1.07	0.4111	0.5311
Formate	0.00020937	0.00018	1.16	**0.0187**	0.0828
Fumarate	0.00001415	1.25068E-05	1.13	0.2377	0.3879
Threonine	0.00020752	0.000231226	0.90	0.0932	0.2058
Lysine	0.00049623	0.000488073	1.02	0.9873	0.9873
Acetatoacetate	0.00026706	0.000167242	1.60*	**0.0265**	0.1029
Methionine	0.00082180	0.000730695	1.12	**0.0332**	0.1030
unk1	0.00008045	8.6702E-05	0.93	0.0920	0.2058
unk2	0.00005625	4.58131E-05	1.23	0.0957	0.2058
unk3	0.00104660	0.000699813	1.50*	**0.0000016**	**0.000025**
3-hydroxybutyrate	0.00042926	0.000398342	1.08	0.2994	0.4303
Succinate	7.3119E-05	4.65665E-05	1.57*	**0.0000001**	**0.0000035**
2-hydroxybutyrate	0.00011189	7.75603E-05	1.44*	0.1753	0.3196
Proline	0.00025412	0.000230208	1.10	0.2878	0.4303

Table 8. Univariate statistical analysis of fasting samples (Down syndrome (DS), n = 76; healthy control (CTRL), n = 35). The table contains the list of metabolites analyzed with NMR from samples taken from fasting patient. We reported both p-value of the univariate Wilcoxon test and p-value a er FDR correction for each metabolite. Metabolites that show signi cant concentration di erences in the two groups (p-value < 0.05) and/ or show values in the interval next to 3:2 are reported in bold. *Values in the interval next to 3:2 (range 1.3–1.7).

In order to obtain more information about the alteration of the metabolic pathways in DS we compared the correlations (corrected by age) among the levels of metabolites in DS subjects and CTRL groups, separately. Importantly, we observed that some correlations are strong/moderate ($r > 0.4$ or $r < 0.4$) and significant ($p < 0.05$) in CTRL samples but lose their significance or weaken their correlation in DS samples. These results are referred to metabolites involved in the Krebs cycle (pyruvate, citrate and succinate), formate and lactate and amino acids like alanine, threonine and tyrosine. On the contrary, some statistically significant correlations are found only in DS samples, like associations between phenylalanine and branched amino acids. Accordingly, the

inverse correlation between lactate and succinate characteristic of CTRL samples becomes direct in DS samples.

Even if metabolic imbalance clearly discriminates between DS and CTRL groups, metabolomic profiles cannot be associated with the degree of ID, as shown by both the low discrimination accuracies obtained when comparing the metabolomic profiles of DS patients with different IQ disability and the lack of correlation between the levels of the investigated metabolites and the scores obtained by cognitive tests. All these data have been published in Antonaros et al. 2020.

4.4.2 One-carbon cycle characterization through blood routine analyses in subjects with DS

Many studies had already reported an impaired metabolic profile in subjects with DS (Pogribna et al., 2001;Meguid et al., 2010), so we decided to analyse Hcy, vitamin B12, folate, UA and creatinine levels due to their involvement in the one-carbon cycle. A total of 147 children/young adults with a confirmed diagnosis of trisomy 21 and age>2 years were enrolled for this study and the information regarding age, sex and fasting state were collected. For 77 subjects, metabolite levels were correlated with cognitive tests, Griffiths-III test was administered to 28 subjects (3.08-6.16 years) and WPPSI-III test was administered to 49 subjects (7.08-16.08 years). The results are reported in Antonaros et al. 2021a.

First, our results confirmed a significant correlation between Hcy plasma levels and the *MTHFR* C677T genotype. Hcy concentration level and *MTHFR* C677T polymorphism were studied in all 147 subjects enrolled. PCR-RFLP analysis divided the 147 subjects into three genotype groups: 40 CC (27.2%), 69 CT (46.9%) and 38 TT (25.9%). These groups resulted in being homogeneous for sex after contingency test ($p=0.339$) and for age after Kruskal-Wallis test ($p=0.718$), so we searched for a correlation between Hcy concentrations and *MTHFR* genotype. One-way analysis of variance (ANOVA) was performed to compare Hcy levels among the three groups of *MTHFR* C677T genotype showing a significant difference in Hcy mean concentration (μm/L) among the three groups (CC=8.125; CT=9.158; TT=10.482) ($p=0.045$). Post-hoc analysis with Tukey's test showed a significant difference in Hcy mean concentration between TT and CC genotypes ($p=0.035$).

A linear correlation, established between the level of metabolites (Hcy, vitamin B12, UA and creatinine) and age at the time of blood sampling, shows the increase of Hcy, UA and creatinine levels with the increase of age. The unpaired t-test was performed to underline a correlation between sex and metabolite levels, and between fasting state and metabolite levels. All metabolites

analysed resulted independent from sex and Hcy; folate and creatinine were not affected by fasting state.

Partial correlation controlled by age at blood draw between the level of each metabolite and the levels of all the other metabolites showed significantly moderate positive correlations: between Hcy and UA, (r=0.456, p-value after FDR correction <0.001), between Hcy and creatinine (r=0.417, p-value after FDR correction <0.001) and between UA and creatinine (r=0.541; p-value after FDR correction <0.001). These analyses included only subjects in fasting state (n= 83).

Being Hcy, folate and creatinine independent from fasting state, their concentration levels were tested for correlation with all subjects with Griffiths-III and WPPSI-III test scores. For vitamin B12 and UA, which resulted dependent on fasting state, we tested these correlations only for fasting subjects. Hcy concentrations resulted statistically significantly associated with total age equivalent (AE), verbal AE and IQ of WPPSI-III test with a weak negative correlation (Table 9). Vitamin B12 levels were associated with IQ scores of WPSSI-III test with a weak positive statistically significant correlation (Table 9).

		Griffiths-III Test			WPPSI-III Test			
		A AE	**B AE**	**IQ**	**Total AE**	**Verbal AE**	**Non-verbal AE**	**IQ**
Hcy n=28 (G) n=49 (W)	**r**	0.092	0.257	0.174	-0.346	-0.329	-0.204	-0.376
	p-value	0.660	0.216	0.375	0.016*	0.022*	0.164	0.008*
Folate n=26 (G) n=49 (W)	**r**	0.347	0.099	0.370	0.104	0.158	-0.049	0.112
	p-value	0.089	0.638	0.063	0.482	0.285	0.741	0.442
Uric Acid n=12 (G) n=27 (W)	**r**	0.410*	0.575*	0.363	-0.023	-0.161	0.267	-0.189
	p-value	0.239	0.082	0.247	0.912	0.433	0.187	0.346
Creatinine n=28 (G) n=49 (W)	**r**	0.023	0.194	0.028	0.061	0.007	0.132	-0.135
	p-value	0.913	0.353	0.888	0.679	0.963	0.369	0.355
Vit. B12 n=11 (G) n=27 (W)	**r**	0.054	0.313	0.117	0.282	0.276	0.169	0.386
	p-value	0.881	0.349	0.733	0.163	0.172	0.409	0.046*

Table 9. ***Correlation between metabolite levels and Griffiths-III or WPPSI-III test scores.*** Partial correlations (r) correct by age was done between Griffiths-III or WPPSI-III subtest scores and metabolite levels; bivariate correlations (r) were done between IQ scores and metabolite levels. *= p-value ≤0.05 or moderate correlation 0.4<r<0.7. Correlation between vitamin B12 (Vit. B12)/UA levels and Griffiths-III or WPPSI-III test scores was analysed only in fasting subjects. AE=age equivalent; A=evaluation of "foundations of learning"; B=evaluation of "language and communication"; IQ=intelligence quotient. (G): number of subjects with Griffiths-III test scores; (W): number of subjects with WPPSI-III test scores.

Taking as a model the study of Guéant and coll. (Gueant et al., 2005) for Hcy, folate, vitamin B12, UA and creatinine, we used the concentration values of 25th, 50th or 75th percentiles as references for dividing the subjects into two groups, one with a metabolite concentration value lower than the reference (Low or L group) and the other with a concentration value higher than or equal to the reference (High or H group). In the younger group (3.08-6.16 years), we found no statistically significant correlation. In the older group the statistical analysis showed a moderate negative correlation between the H group of the 25th percentile value of Hcy (Hcy ≥7.35 µmol/L; 37 subjects) and the total AE scores (r=-0.455; p=0.005), the non-verbal AE scores (r=-0.428; p=0.009) and the IQ scores (r=-0.47; p=0.003) (Figure 18). The non-verbal AE is the only area that still had a moderate negative correlation for Hcy ≥8.9 µmol/L, the H group of the 50th percentile threshold, (r=-0.457; p=0.022; 26 subjects) and for Hcy ≥10.45 µmol/L, the H group of the 75th percentile, (r=-0.618; p=0.043; 12 subjects).

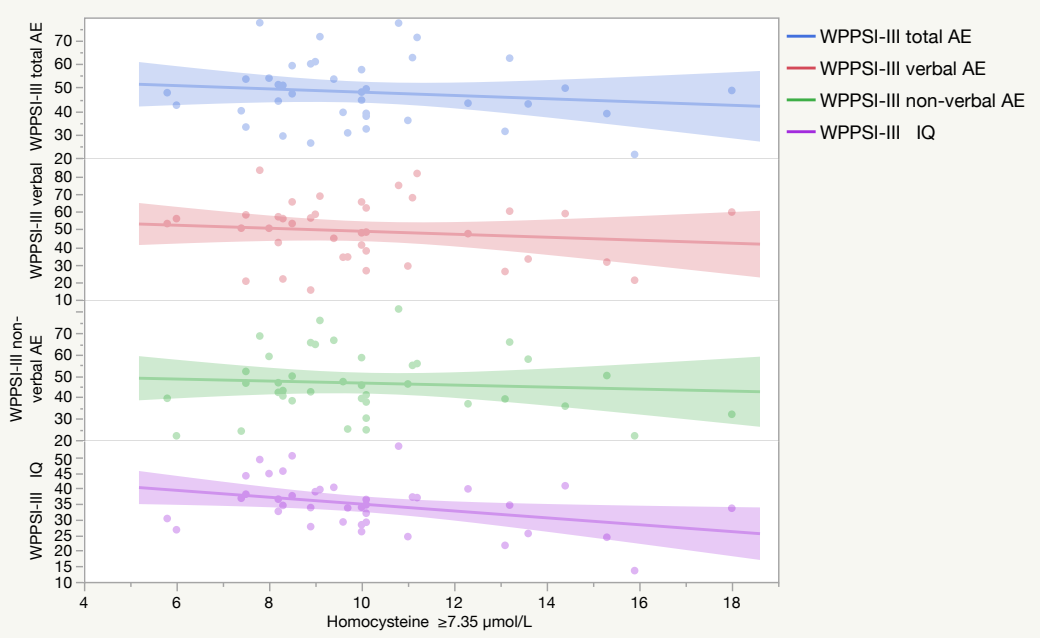

Figure 18. Scatter plot of the main correlation between homocysteine levels and WPPSI-III test scores. Correlation between homocysteine ≥ 7.35 µmol/L (H = High group of 25th percentile threshold) and WPPSI- III non-verbal AE scores, verbal AE scores, total AE scores and IQ scores of 37 subjects. Each dot represents a sample subject. Each line represents a correlation analysed.

Among statistically significant correlations found for vitamin B12 percentile groups, vitamin B12 <442 pg/mL (L group of the 75th percentile threshold; 20 subjects) showed a moderate positive correlation with verbal AE scores (r=0.527; p=0.02; 20 subjects), non-verbal AE scores (r=0.606; p=0.006; 20 subjects), total AE scores (r=0.643 p=0.003) and IQ scores (r=0.572 p=0.008) (Figure 19).

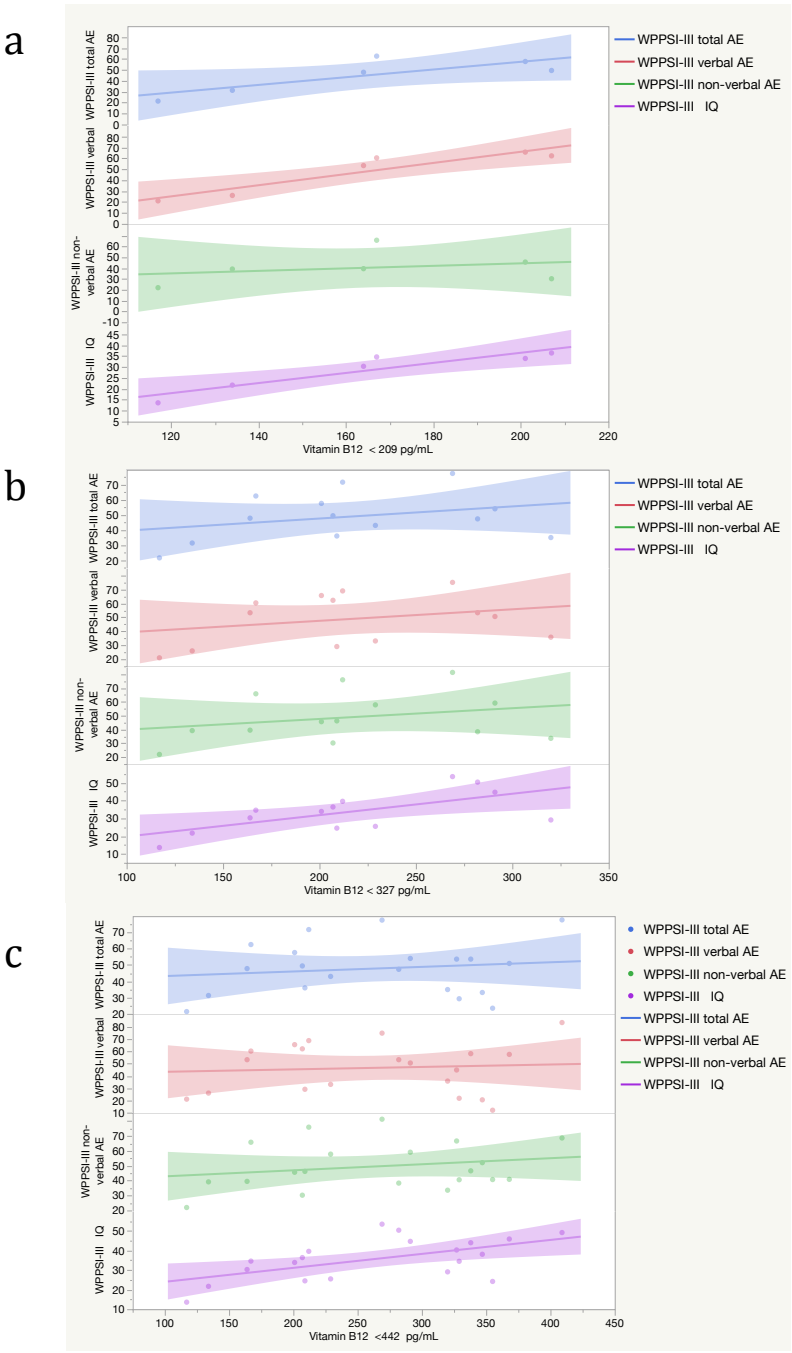

Figure 19. Scatter plot representing correlations between vitamin B12 and cognitive scores in the WPPSI-III group. (a) Correlations between vitamin B12 < 209 pg/mL (L group of 25th percentile threshold; 6 subjects) and WPPSI-III subtests' scores. (b) Correlations between vitamin B12 < 327 pg/mL (L group of 50th percentile threshold; 13 subjects) and WPPSI-III subtests' scores. (c) Correlations between vitamin B12 < 442 pg/mL (L group of 75th percentile threshold; 20 subjects) and WPPSI-III subtests' scores. Each dot represents a sample subject. Each line represents a correlation analysed.

4.4.3 One-carbon cycle characterization through ELISA assay

To understand more about one-carbon alteration in Down syndrome, in another work (Vione, 2022) we decided to dosage 5 metabolites involved in this cycle. Our results highlight plasma level alteration of some intermediates of one-carbon metabolism in a group of subjects with DS compared to a group of euploid subjects as control. We selected 164 subjects with DS and 54 euploid subjects. It was not possible to obtain the metabolite level in all the selected subjects for several reasons: the amount of plasma was not sufficient, the absorbance (O.D., optical density) mean values of plasma samples were out of the range, or there was a technical problem during the assay. The unpaired t-test did not identify differences between males and females concerning the concentration of all the molecules investigated. A statistically significant moderate correlation was found between age and Hcy concentration levels in the DS group ($r=0.593$ and p-value < 0.001). The unpaired t-tests comparing values in fasting or non-fasting state highlighted a statistically significant difference in vitamin B12 levels in the DS group.

Unpaired student t-test showed a statistically significant difference of THF (p-value=0.0041), 5-methyl-THF (p-value=0.015) and SAH (p-value=0.0001) plasma levels between DS and control groups. Concerning 5-formyl-THF and SAM, the difference is not statistically significant (respectively p-value=0.3881 and 0.1853). Figure 20 shows the variation of all metabolite's concentrations in subjects with DS and normal control subjects.

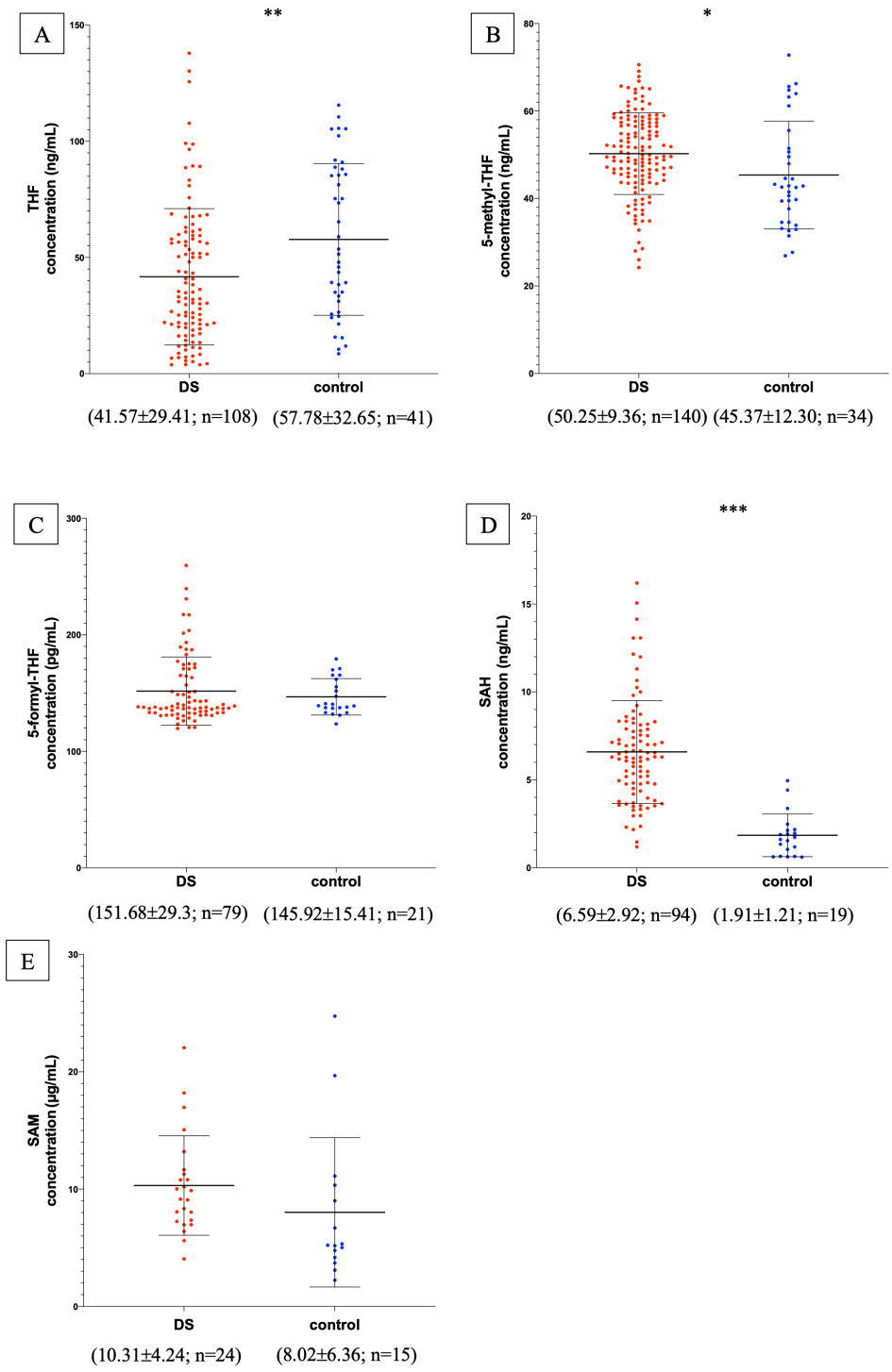

Figure 20. Metabolite concentrations in subjects with DS and normal control subjects. The graphs report metabolite plasma levels of each subject in the study. On the x-axis there is the subdivision of subjects in DS (red dots) and control groups (blue dots). On the y-axis the concentration of the metabolite in µg/mL, ng/mL or pg/mL is reported. The asterisks above the graph indicate the level of statistical significance (*=p<0.05; **=p<0.005; ***=p<0.0005). The middle black lines indicate the mean concentration values for each group and the external black lines indicate standard deviation (SD) values. The mean concentration, SD values and the number of subjects (n) are reported below each graph for DS and control groups. Figure 20(A) shows THF concentrations; Figure 20(B) shows 5-methyl-THF concentrations; Figure 20(C) shows 5-formyl-THF concentrations; Figure 20(D) shows SAH concentrations; Figure 20(E) shows SAM concentrations. The graphs were created with GraphPad Prism software v.6.0 (San Diego, CA).

Our results show that THF plasma concentration is lower than normal in subjects with DS and the median concentration ratio between DS and control groups is 0.66, that is a 2:3 ratio (see Table 10), strongly suggesting a correlation with the imbalanced original event or the presence of a third Hsa21. Moreover, THF concentration level shows a statistically significant weak correlation with age in the control group (r=0.395 and p-value=0.011). Interestingly, the correlation between THF and age is lost in the DS group (r=0.089 and p-value=0.362).

Concerning 5-methyl-THF, even if unpaired student t-test showed a statistically significant difference between the two groups**,** its plasma concentration is equal in subjects with DS compared to normal control subjects and the median concentration ratio between DS and control groups is 0.99, that is a 1:1 ratio (see Table 10).

SAH plasma concentration results much higher than normal in subjects with DS and the median concentration ratio between DS and control groups is 3.63 (see Table 10).

Even if there is not a statistically significant difference of SAM plasma levels between the DS and control groups due to the distribution of the values, SAM concentration is higher than normal in subjects with DS and the median concentration ratio between DS and control groups is 1.82 (see Table 10).

	THF	**5-methyl-THF**	**5-formyl-THF**	**SAH**	**SAM**
Subjects	DS n=108 Control n=41	DS n=140 Control n=34	DS n=24 Control n=15	DS n=79 Control n=21	DS n=94 Control n=19
Mean ratio DS/Control	0.72	1.11	1.04	3.45	1.28
Median ratio DS/Control	0.66	1.16	0.99	3.63	1.82
p-value	0.0041*	0.015*	0.8103	0.0001*	0.1853
t-value	2.9137	2.5537	801[a]	6.8373	1.3499

Table 10. Difference of metabolite concentration between DS and control groups. Ratio of mean and median values between DS and control groups are given. Statistical test was t-student except for 5-formyl-THF for which Mann-Whitney test was used. Significant p-values (<0.05) are marked with a "*".

SAM/SAH ratio was lower in individuals with DS, indeed the SAM/SAH mass median ratio is 1511 in subjects with DS and 3008 in control subjects, suggesting that SAM/SAH median ratio in subjects with DS is half (exactly 0.50) compared to control subjects. SAM/SAH ratio is a well-known indicator of cellular methylation capacity and when it is decreased can correlate with reduced methylation potential (Clarke, 2001;Petrossian and Clarke, 2011).

The linear correlation analysis identified a statistically significant moderate negative correlation (r=-0.628 and p-value=0.029) between SAM and vitamin B12 levels in the non-fasting DS group. A statistically significant strong positive correlation (r=0.81 and p-value=0.003) between SAM and 5-formyl-THF levels was found in DS group. The correlation was not maintained in the control group.

4.5 Trisomic induced pluripotent stem cells (iPSCs)

4.5.1 iPSC maintenance, neural crest induction and Nanoamycin treatment

In the present study two iPSC lines from healthy donors (CTL10; JLBI) and three iPSC lines from individuals with full trisomy 21 (DS1.1, DS2B, DS3.1) have been subjected to STRs genotyping confirm the previous literature (Uhlin et al., 2017;Schuster et al., 2020;Vasylovska et al., 2020) and expression of pluripotency markers by flowcytometry confirm the iPSCs status (see figure 21).

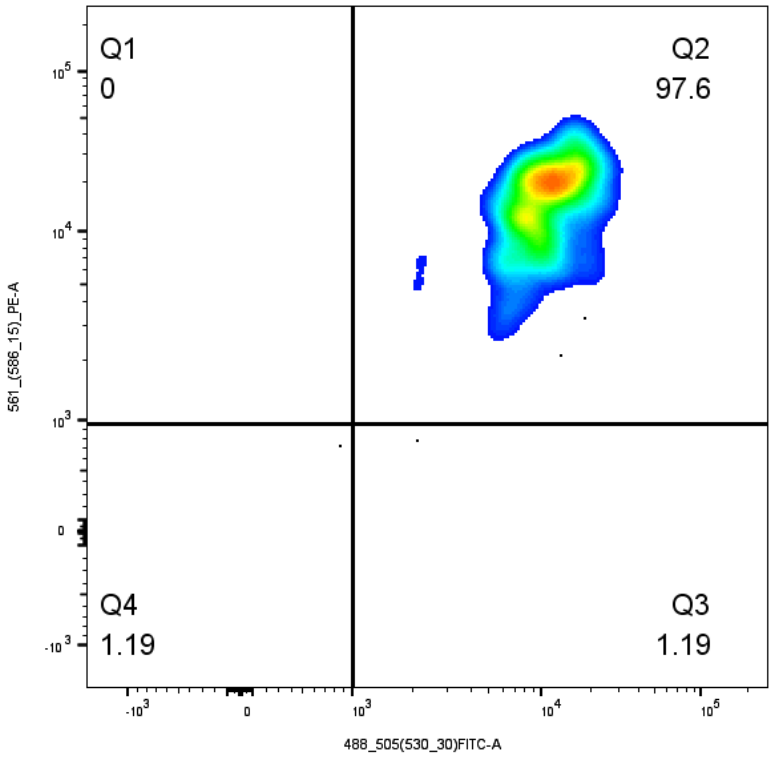

Figure 21. Expression of pluripotency markers by flowcytometry. Concerning flowcytometry, iPSC cultures were labelled for pluripotency using LSR Fortessa Flowcytometer.

In order to study human NCC we adapted a previously described protocol for directed differentiation of iPSC using top-down inhibition of BMP signaling (Hackland et al., 2017). This

approach allowed us to generate NCC, which showed at optical microscope typical “cobblestone” morphology of cells (see figure 22).

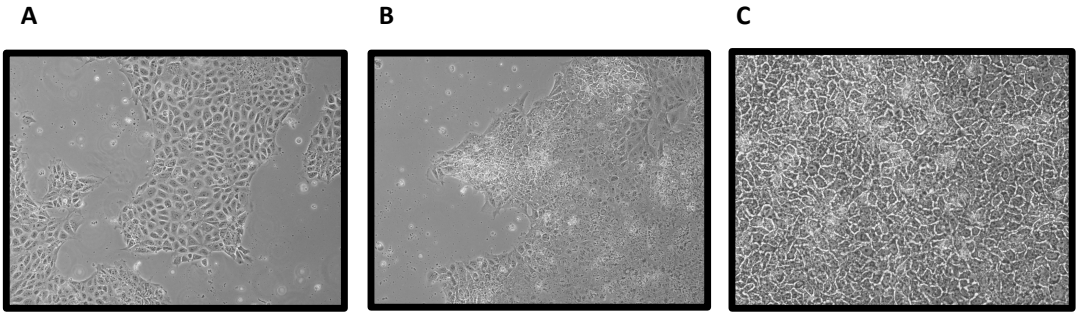

Figure 22. NNC view at optical microscope. A. JLBI at day 5 of NCC induction; **B.** JLBI treatted with 0,75 μM of Nanaomycin at day 5 of NCC induction **C**. DS1.1 at day 5 of NCC induction.

4.5.2 Insertion of target segments in the linearized vector

We obtained the two target frangments: EcoRI-DNMT3B-GFP (figure 23A) and DNMT3B-GFP-BamHi (figure 23B).

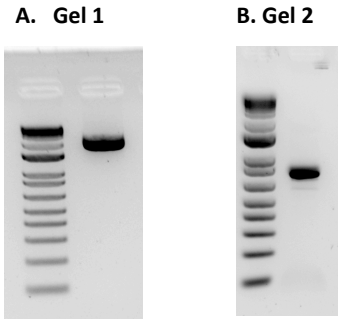

Figure 23. Agarose gel at 2% was used to check correct amplification of EcoRI-DNMT3B-GFP and DNMT3B-GFP-BamHi fragments. A. Gel 1. Lane 1: marker (1 Kb Plus DNA Ladder, Invitrogen, Grand Island, NY, USA); lane 2: purified EcoRI-DNMT3B-GFP (2500 bp). **B.** Gel 2. lane 1: marker (1 Kb Plus DNA Ladder, Invitrogen, Grand Island, NY, USA); lane 2: purified DNMT3B-GFP-BamHi (700 bp)

Linearized pLVX-TetOne-Puro vector and target fragments were subjected to ligation reaction. To determine the correct sequence of the construct we restricted it with *Bam*HI and of *Eco*RI in order to obtaine two fragments of 9,194 nt and 3,254 nt. Figure 24 shows the vector including *DNMT3B* and *GFP* sequences and the *Bam*HI and *Eco*RI restriction sites.

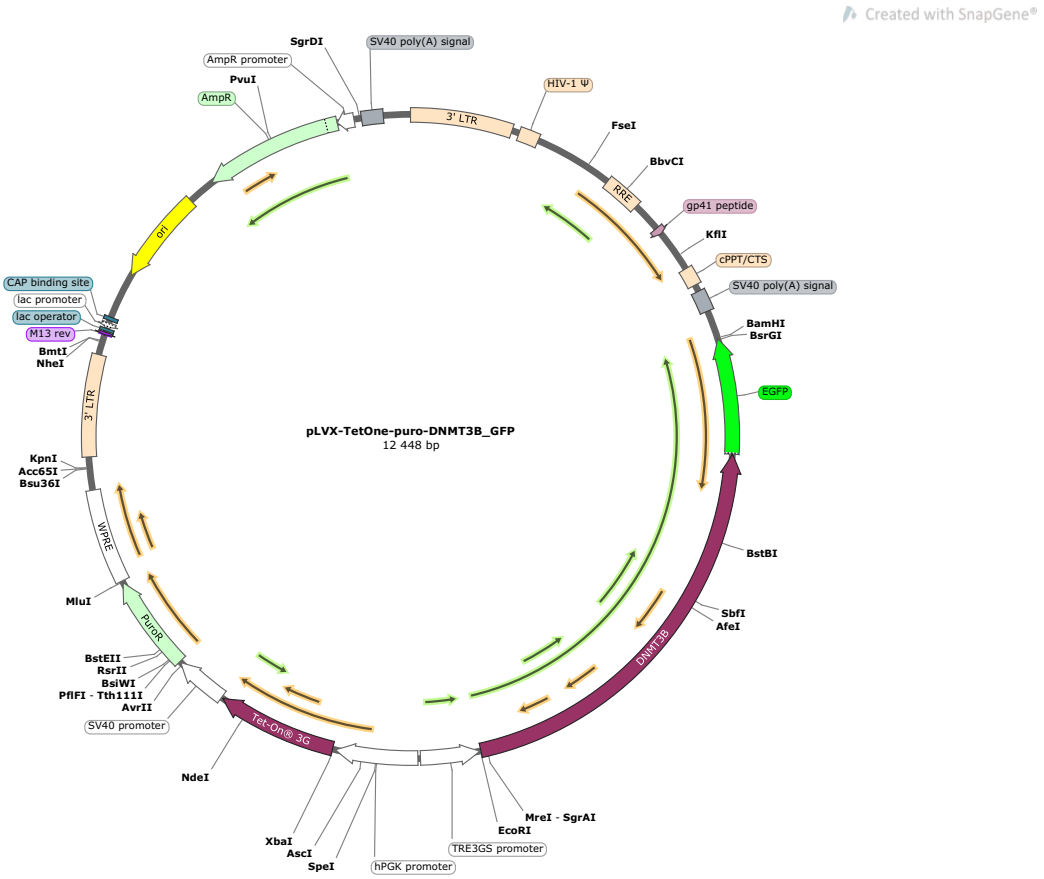

Figure 24. pLVX-TetOne-Puro+ DNMT3B+GFP vector. Figure was created by SnapGene.

Figure 25 shows 2% agarose gel where was added TetOne+DNMT3B+GFP vector restricted with *Eco*RI and *Bam*HI. We observe the correct construct in lane 5.

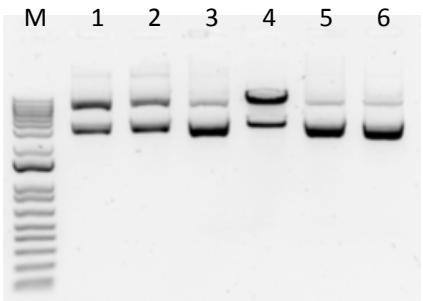

Figure 25. TetOne+DNMT3B+GFP cutted vector. Gel 1. Lane 1: marker (1 Kb Plus DNA Ladder, Invitrogen, Grand Island, NY, USA); lane 4: correct TetOne+DNMT3B+GFP vector restricted with *Eco*RI and *Bam*HI (9,194; 3,254).

The whole construct "pLVX-TetOne-Puro+DNMT3B+GFP vector" sequence was confirmed by Sanger sequencing (see figure 26).

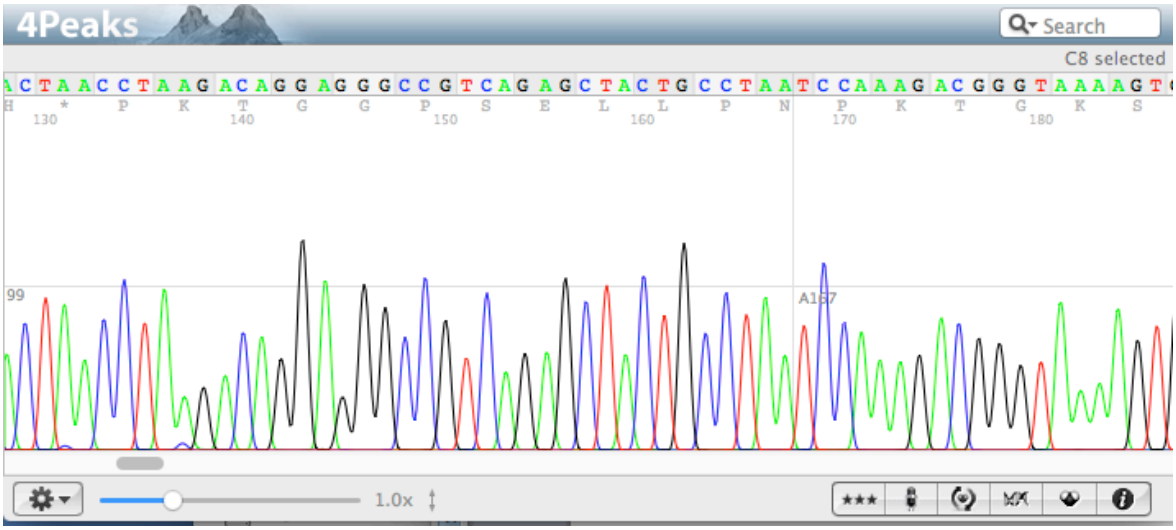

Figure 26. Representative figure of Sanger sequencing. Part of the pLVX-TetOne-Puro+DNMT3B+GFP sequence obtained with DNMT3B-GFPfw primer.

5. DISCUSSION

A complex and variable phenotype characterizes subjects with DS; still, at the same time, they present a specific neurocognitive and neurobehavioral profile and the association with several clinical features, of which the most constant are ID and craniofacial dysmorphisms.

In the first part of this work, we explore the acquisition of developmental milestones, executive functions (EFs), adaptive behaviour and the cognitive profile of children with DS, exceptionally verbal and non-verbal intelligence. These studies (Locatelli et al., 2021;Onnivello et al., 2022a;Onnivello et al., 2022b) allowed us to understand the developmental profiles of children with DS and to explore how the acquisition of some skills affects future development. In particular, the knowledge of early predictors of later development is very helpful to plan early phenotype-informed interventions that have the potential to influence positive trajectories in community living and participation across an individual's lifespan. These results showed a great interindividual cognitive variability of children with DS and the importance of evaluating DS cognitive impairment in order to positively influence the future development of these children.

Great variability was reported also in phenotypic signs; indeed, DS signs are never all displayed by the same subject, and there is not a phenotypic sign always present in all affected children. In Locatelli 2021, we reviewed the Jackson checklist (Locatelli et al., 2021). In this work we showed that even if some signs (oblique eye fissure, joint laxity, epicanthic eye-fold, hypotonia and separated hallux) are present most frequently, the wide SD is characterized by a great interindividual variability. The most interesting result is the lack of significant associations between IQ level and the various Jackson's signs and between IQ scores and number of Jackson's sign present. These results highlight the impossibility to identify a physical characteristic predictive of greater ID. In conclusion, our review of Jackson's signs in many children with DS provides great statistical significance to the analyses and documents their current validity for clinical use.

These previous studies emphasize the crucial importance of the general population and professional caregivers to encourage children with DS in educational goals, in achieving cognitive skills in line with his or her potential, regardless of physical characteristics.

These clinical evaluations were accompanied by genetic, molecular and metabolic evaluations to better understand the origin of the phenotypic variability of this syndrome and possible correlations with altered gene expression or metabolic pathways.

Concerning genomic analysis, we know that Down syndrome is cause by three copies of Hsa21. While it is widely accepted that excess genetic material from Hsa21 is responsible for the typical picture of DS in particular ID, to date there is no pathogenetic model linking specific structural and functional aspects of Hsa21 to DS picture. The study of PT21 is a fundamental model

to study the phenotype-genotype correlation in DS. The systematic reanalysis of PT21 cases proved to be a valid method for identifying the "minimal" Hsa21 region associated with the diagnosis of DS, thus likely associated with DS "core" features, in particular ID. In 2016 Pelleri and coll. (Pelleri et al., 2016) identified the “highly restricted Down syndrome critical region” (HR-DSCR) a region of Hsa21 present in three copies in all individuals with PT21 and a diagnosis of DS. This region, located on distal 21q22.13, is 34 kbp long and does not include characterized genes. In the present work (Pelleri et al. 2022 accepted *BMC Medical Genomics*), we described detailed clinical reports and cytogenetic characterizations of two new cases of PT21 with different phenotypes. In Case 1, a 2-year-old girl, the duplication involves the whole long arm of Hsa21, except for the last 2.7 Mb, which are deleted because of an isodicentric 21: the HR-DSCR is within the duplicated regions and the child is diagnosed with DS. In Case 2, a 9-year-old female, the duplication involves 7.1 Mb of distal 21q22, with a deletion of 2.1 Mb of proximal 20p, because of an unbalanced translocation: the HR-DSCR is not duplicated, and the child presents with psychomotor development delay but the clinical condition not classifiable as DS. This study confirm that diagnosis of DS is associated to the presence in three copies of the HR-DSCR (Case 1), while two copies of the region have not been sufficient to lead to diagnosis of DS in Case 2. Then, we accurately searched for any new PT21 reports published in the last year in order to update the integrated comparative map and possibly confirm the HR-DSCR model. Our bibliographic searches identified two clinical cases of interest (Cases 3 and 4). Case 3 is a female newborn with DS that, despite the presence of unusual defects like esophageal atresia and tethered cord syndrome, has a clear DS phenotype (Putra et al., 2017). Indeed, the karyotype showed the trisomy of approximately the whole long arm of the Hsa21 excluding a segment of almost 1,2 Mb at the 21q22.3 terminal, which turned out to be monosomic. Case 4 is a male baby without DS and a familial 21q22.3 microduplication (Chen et al., 2019). Both cases confirm the association between HR-DSCR and DS diagnosis. These findings underline the need for a better understanding of the structure of the HR-DSCR, which has been poorly investigated.

Recently, we have challenged the concept that HR-DSCR is an intergenic region, as it appears from the human genome browsers. By both *in silico* and *in vitro* analyses, *KCNJ6-202* and *DSCR4-202* isoforms have been identified (Antonaros et al., 2021b). *KCNJ6-202* shares the coding sequence with the known transcript *KCNJ6-201*, encoding a potassium channel which is involved in many physiological processes, including heart rate in cardiac cells and circuit activity in neuronal cells. *DSCR4-202* transcript has the first two exons in common with *DSCR4-201*, the only experimentally verified gene uniquely present in Hominidae. *KCNJ6* locus (OMIM # 600877) seems to be expressed in brain areas known to be specifically altered in DS, such as pituitary gland,

cerebellum, hippocampus and cortex (Cooper et al., 2012). Recently, wild-type *DSCR4* was overexpressed in human non-cancerous cells and differential gene expression analysis was performed to measure the consequences on the cell transcriptome. The results suggested that *DSCR4* could have a role in the regulation of interconnected biological pathways related to cell migration, coagulation and immune system consistent with well-known pathways affected in subjects with DS (Saber et al., 2021) and confirming the complexity of its gene function. All the transcripts were visible on agarose gel after 45 cycles of PCR and only in specific tissues. These characteristics are typical of lncRNA, which follow a specific timing and tissue expression pattern, and have a key role in cell differentiation, organogenesis, and tissue homeostasis (Schmitz et al., 2016). LncRNAs can interact with DNA and RNA molecules, transcription factors, and they participate in various biological processes such as DNA methylation, histone modification, chromatin remodeling, up-regulation or down-regulation of target genes (Li et al., 2016;Kaikkonen and Adelman, 2018). All *DSCR4* isoforms are annotated as lncRNA in Ensembl database and HR-DSCR could contain regulatory RNA elements in its genomic *locus*. Instead, *KCNJ6-202* function is associated to *KCNJ6-201* because it is thought that they code for the same protein. In order to understand the function of the HR-DSCR it is necessary to define the function of the transcripts included in it. Further studies are necessary to characterize the organization of the HR-DSCR *locus* and of the *KCNJ6-202* and *DSCR4-202* transcripts that intersect it and to clarify their properties and function in the tissues analyzed.

The presence of full or partial trisomy 21 is associated to DS clinical features as described above. However, altered gene expression patterns and metabolic pathways need to be clarified. First, we focused on possible consequences of trisomy 21 on gene expression patterns. The expression levels of Hsa21 genes and the global gene expression of the whole genome have been profiling on DS cells to assess their expression and their involvement in the pathogenesis of DS. In Antonaros 2021 and coll. (Antonaros et al., 2021c) we analyzed T21 vs normal control blood cell transcriptome by RNA-Seq. These data were integrated and elaborated by the TRAM (Transcriptome Mapper) software generating a quantitative transcriptome map for each condition and a differential transcriptome map between them. Gene expression profiles were validated through real-time reverse transcription polymerase chain reaction (RT-PCR) assay and then compared with previously published data.

In particular, we present a differential quantitative blood cell transcriptome map between T21 and normal control blood cells for 17,867 loci and a post-analysis through transcriptome mapping aimed at identifying the segmental (regional) variation of the expression level across the whole genome (segment-based analysis of expression). At the segment level the expression analysis

showed that the two most over-expressed segments are on Hsa21, highlighting the presence of the third copy of Hsa21. We also observe the over-expression of the segment on chromosome 10 containing *IFIT2*, *IFIT3* and *IFIT1* genes involved in the interferon signaling (Pelleri et al., 2018). The interferon signaling pathway alteration was further supported by the over-expression at single gene level of *MX1*, *MX2* (mapping on chr21) and *IFIT1* (mapping on chr10) which are known to participate in the cellular antiviral response (John et al., 2018;Ciminski et al., 2019;Ma et al., 2019). In particular, *MX2* over-expression is involved in the suppression of cell proliferation, migration and invasion in glioblastoma cells (Wang et al., 2019), while *MX2* gene has an important role in the morphology and function of the mitochondrial membrane (Cao et al., 2020). Both aspects, suppression of cell proliferation and mitochondrial membrane structure, are consistent with two main DS features: reduced incidence of solid tumors and alteration of mitochondrial functions. Another gene reported as over-expressed in our work is *RSAD2* gene whose protein product is another interferon-inducible antiviral protein and belongs to the S-adenosyl-L-methionine (SAM) superfamily of enzymes (Dumbrepatil et al., 2020). It plays a role in the fatty acid b-oxidation. The over-expression observed at chromosomal level of the Hsa21, and mitochondrial genome (2.01 and 1.50, respectively) compared to the other chromosomes in T21 supports the hypothesis of the alteration of mitochondrial functions in Down syndrome (Caracausi et al., 2018;Pecze et al., 2020). We found the over-expression of *SLC19A1* gene encoding for a transporter of folate, thus involved in the regulation of intracellular concentrations of folate, and the over-expression of genes like *GART* (21q22.1, gene expression ratio=1.58), *SLC46A1* (17q11.2, gene expression ratio=1.67), and *SLC19A1* (21q22.3, gene expression ratio=3.50), provides interesting hints about the hypothesis regarding the alteration of the one-carbon pathway in the manifestation of ID in DS (Lejeune et al., 1986;Vitale et al., 2019). In conclusion, this study confirms that the presence in three copies of Hsa21 produce a genome wide deregulation which involves both Hsa21 genes and Hsa21 interactors. The gene expression alteration seems to be link with the marked deregulation of various metabolic cycles, i.e., folate cycle, energy production and with a general state inflammation reported in DS.

Second, not only gene expression profiles, but also metabolic patterns can be altered by the presence of trisomy 21. Thus, we investigated some metabolic pathways.

In Antonaros 2020 (Antonaros et al., 2020), we confirmed the presence of significantly different plasma metabolomic profiles of DS and CTRL groups with a higher discrimination accuracy than in our previous analysis (Caracausi et al., 2018), reaching 94% both with CPMG and NOESY spectra. The analysis showed significantly increased concentrations (p-value after FDR correction < 0.05) of the following metabolites: acetate; pyruvate; succinate; formate and creatine.

All of them are involved in energy production. Acetate is fundamental in supporting acetyl-coenzyme A metabolism and thus Krebs cycle progression and lipogenesis (Liu et al., 2018). Pyruvate and succinate are produced before and during the Krebs cycle (Martinez-Reyes and Chandel, 2020). Formate is known to be necessary for the formylation of mitochondrial tRNAs21 and for the formylation of tetrahydrofolate during the folic acid cycle and the purine synthesis pathway. Finally, creatine is used by muscles to produce ATP (Barclay, 2017). Previous works demonstrated that measurable enzymes whose genes are located on Hsa21 adhere to the 3:2 overexpression model expected in trisomy (Feaster et al., 1977;Ducker and Rabinowitz, 2017;Pelleri et al., 2018). Although the dependence of the levels of the metabolites on the enzyme concentration is complex and not easily interpretable, we point out that a ratio DS/CRTL near to 3:2 (1.5) or 2:3 (0.67) is observed for a certain set of molecules. In this framework, interesting data are the significant alterations of succinate in DS vs CTRL. Succinate levels increase in DS samples with a DS/CTRL ratio close to 3:2. The alterations of succinate metabolism may play a role in the development of ID, but to date there is no strong evidence. However, it is already known that some enzymes which metabolize succinate are involved in developmental delay and brain injuries (Wang et al., 2019). Furthermore, alterations of activities for the Krebs cycle enzymes were also observed in some brain disorders such as Alzheimer's disease (Bubber et al., 2005) and Huntington's disease (Naseri et al., 2016). In both diseases, the increase of succinate dehydrogenase and malate dehydrogenase and the decrease of the pyruvate dehydrogenase complex, isocitrate dehydrogenase, and the alpha-ketoglutarate dehydrogenase complex were observed, suggesting that a mitochondrial alteration occurs. Importantly, we observed that some correlations are strong/moderate ($r>0.4$ or $r<-0.4$) and significant ($p<0.05$) in CTRL samples but lose their significance or weaken their correlation in DS samples and *vice-versa*. In DS samples we found statistically significant correlations between phenylalanine and branched amino acids. Moreover, the inverse correlation between lactate and succinate characteristic of CTRL samples becomes direct in DS samples. These findings support the hypothesis of an altered metabolism in Down syndrome, strengthening the idea of the involvement of the Krebs cycle and of a few amino acids like leucine, phenylalanine, tyrosine and alanine. Leucine and phenylalanine are both involved in brain metabolism: the role of leucine as a nitrogen donor in the glutamine/glycine pathway may influence the function of some neurotransmitters (Sperringer et al., 2017), while modifications in the phenylalanine pathway can alter dopamine levels (Nelson, 2017).

Even if metabolic imbalance clearly discriminates between DS and CTRL groups, it appears that specific metabolomic profiles cannot be associated with the degree of ID. It would be interesting to test if strengthening the statistical power of the models by increasing the number of

patients in each range of ID could reveal such a correlation, as it would be of immense value in identifying critical points of metabolism as treatment targets. An alternative or complementary explanation for this result might be that the effect of metabolome on patient's skills might be mediated by environmental factors (such as family environment, school, early intervention, etc.), so further study is required here. In addition, it is possible that metabolites critically altered in DS are not included among those we have investigated (i.e., fall below the NMR detection limit). This hypothesis should be further investigated by studying a larger number of metabolites using complementary analytical platforms. By increasing the number of measured metabolites, extended metabolic network models could be developed and might provide deeper insight in the biochemical origin of cognitive impairment.

In our recent work (Antonaros et al., 2021a) interesting data emerged from the analysis of correlations between cognitive scores and metabolite levels. We dosage Hcy, vitamin B12, folate, UA and creatinine levels in subjects with DS due to their involvement in the One-carbon cycle. Thanks to routine whole blood analyses, we managed to analyse these metabolites and their association with cognitive scores. Results showed that an increasing level of Hcy above a specific threshold is associated with a decrease of cognitive test performance while a decreased concentration of vitamin B12 below a specific threshold is correlated with a worse cognitive test score, both correlations appeared in the older group (7-16 years) evaluated by WPPSI-III tests. Analyses showed that the verbal area had a weak strength of significant correlation with the Hcy levels ($r=-0.332$, $p=0.048$, Hcy$\geq$7.35 µmol/L) and this is coherent with influences from different environmental variables (ex. family environment, school education, speech therapy, external stimuli, etc.). The non-verbal area is the only one that conserved a stable and increased moderate and statistically significant correlation in groups with Hcy$\geq$7.35 µmol/L, coherently with the idea that this area is less influenced by environmental factors (Lanfranchi et al., 2004) and that the increase of Hcy concentration over 7.35 µmol/L might be already suggestive of a negative influence in this cognitive area in the DS population (similarly to what Guéant and coll. found (Gueant et al., 2005). The negative association of Hcy levels with cognitive scores confirmed literature data in which the increase of Hcy plasma levels is reported as an early marker of cognitive impairment in the elderly population (Lehmann et al., 1999) and as increased in psychiatric phenotype (Almuqbil et al., 2019). The vitamin B12 trend might indicate that a decrease of vitamin B12 levels under 442 pg/mL is correlated with a worse cognitive score and this threshold could be considered in the DS population which might have greater vitamin requirements. Vitamin B12 plays an important role in the synthesis of myelin, in the regeneration of nerves and in the antioxidant action of reduced glutathione (Pavlov et al., 2019). For these reasons, a low level of vitamin B12 is associated with

impaired neurotransmitter production and myelin lesion such as sclerosis of the spinal cord, polyneuritis, neuropathy, myelopathy, optic nerve atrophy and impaired cognitive functions (Calderon-Ospina and Nava-Mesa, 2020). The relevance and originality of the present findings is the detection of a specific metabolite threshold related with a better or worse cognitive score, independent from the metabolite physiological range.

Finally, in subjects with DS, one-carbon metabolism was considered to be imbalanced by several authors (Lejeune, 1979;Rosenblatt et al., 1982;Peeters et al., 1995;Song et al., 2015;Funk et al., 2020) and interesting data in the same direction have been obtained by the analyses previously described (Antonaros et al. 2021a; Antonaros et al. 2021c): in particular, altered expression of genes involved in the folate cycle and specific alterations in homocysteine metabolism, two related pathways part of one-carbon metabolism. For these reasons we decided to investigate plasma level alteration of 5 intermediates of one-carbon metabolism in a group of subjects with DS compared to a group of euploid subjects as control (Vione, 2022). We reported a statistically significant difference of THF (p-value=0.0041), 5-methyl-THF (p-value=0.015) and SAH (p-value=0.0001) plasma levels between DS and control groups. Concerning 5-formyl-THF and SAM, the difference is not statistically significant (respectively p-value=0.3881 and 0.1853).

THF is the metabolic active form of folates in cells and it serves as one-carbon carrier in most folate-mediated reactions (Zheng and Cantley, 2019). THF is the folate form most interconnected in the folate pathway and it is the product of ten enzymatic reactions as shown in figure 5. In our results THF plasma concentration is lower than normal in subjects with DS and the median concentration ratio between DS and control groups is 0.66, that is a 2:3 ratio, strongly suggesting a correlation with the imbalanced original event or the presence of a third Hsa21. Moreover, THF concentration level shows a statistically significant weak correlation with age in the control group (r=0.395 and p-value=0.011) confirming previous literature (Pfeiffer et al., 2015). Interestingly, the correlation between THF and age is lost in the DS group (r=0.089 and p-value=0.362) suggesting that the plasma level alteration of THF in subjects with DS may be a stable consequence of trisomy 21 masking variation with age.

5-methyl-THF is the most abundant folate form in blood circulation and the only form able to cross the blood-brain barrier (Ducker and Rabinowitz, 2017). Our results suggest that 5-methyl-THF plasma concentration is slightly higher than normal in subjects with DS and the median concentration ratio between DS and control groups is 1.16, that is a 1:1 ratio.

5-formyl-THF is a reserve of one-carbon units in cells, and it does not play a direct biosynthetic role (Ducker and Rabinowitz, 2017). Our results suggest that 5-formyl-THF plasma

concentration is equal in subjects with DS compared to normal control subjects and the median concentration ratio between DS and control groups is 0.99, that is a 1:1 ratio.

SAH is part of homocysteine-methionine cycle in which the universal methyl donor named S-adenosyl-methionine (SAM) is transformed in SAH by methyltransferases (Mentch and Locasale, 2016). Our results suggest that SAH plasma concentration is much higher than normal in subjects with DS and the median concentration ratio between DS and control groups is 3.63. Even if there is not a statistically significant difference of SAM plasma levels between the DS and control groups due to the distribution of the values, SAM concentration is higher than normal in subjects with DS and the median concentration ratio between DS and control groups is 1.82 (see table 10). In a previous work (Obeid et al., 2012), both SAH and SAM were found to be significantly higher in young individuals with DS compared to control subjects of comparable age, and the median SAM/SAH ratio was lower in individuals with DS. We find here that that SAM/SAH median ratio in subjects with DS is half (exactly 0.50) compared to control subjects. SAM/SAH ratio is a well-known indicator of cellular methylation capacity and when it is decreased can correlate with reduced methylation potential (Clarke, 2001;Petrossian and Clarke, 2011). An alteration of the methylation capacity is reported in DS and was connected to aging acceleration supporting the notion that DS is a progeroid trait (Franceschi et al., 2019). Our results confirm that there is a dysregulation of the one-carbon pathway in subjects with DS that could be related to cognitive impairment.

Concerning iPSCs, methods related to maintenance and NCC induction have been established. Further analyses will be performed to check the effects of Nanaomycin A treatment in euploid cells over the course of the first week of NCC induction. Being Nanaomycin A specific inhibitor of DNMT3B protein (Kuck et al., 2010), lysates from euploid cells (CTLR10 and JLBI) exposed to Nanaomycin A will be analysed to check if Nanaomycin A inhibits DNMT3B. scRNAseq and qPCR on treated euploid NCCs will show if DNMT3B down-regulation influences gene expression. To check if the phenotype of treated euploid cells simulate the DS one flowcytometry and staining on coverslips collected at day 7-14-21 of NCC induction will be performed.

Lentivirus containing the "pLVX-TetOne-Puro+DNMT3B+GFP" expression vector was successfully designed. Further analyses are necessary to infect iPSC trisomic cells with Lentivirus vector. scRNAseq and qPCR on the edited trisomic NCCs will show if gene expression will return to a comparable level with controls and observe the possible recovery of the phenotype. The recovery of the phenotype will be checked with flowcytometry and staining on cover-slips collected

at day 7-14-21 of NCC induction. Cell lysates from transfected cells will be stored to check if the down-regulation of *DNMT3B* gene correspond to a down-regulation of DNMT3B protein.

We will perform the same scRNAseq, qPCR and staining analyses, on unmanipulated trisomic and untreated euploid lines, at the same time point (see figure 8). Methylation analyses will be performed on DNA collected from all the cell lines (trisomic transfected with *DNMT3B* vector, euploid treated with Nanaomycin A, untreated/unmanipulated euploid and trisomic).

In conclusion, we have presented here results advancing our knowledge of genotype-phenotype correlations in trisomy 21 at different levels of investigation, opening the way for an integration of this findings in a model possibly leading to a rational treatment of the ID associated to DS. Significant alterations in gene expression and metabolic profiles have been identified, as well as significant correlations with clinical and cognitive aspects. Specific genes and the HR-DSCR may play a role in these alterations: cell models need to be developed to investigate this role. Neural derivatives from trisomic iPSCs are a promising model to better understand genotype-phenotype correlations in DS.

6. REFERENCES

Allison, D.B., Gomez, J.E., Heshka, S., Babbitt, R.L., Geliebter, A., Kreibich, K., et al. (1995). Decreased resting metabolic rate among persons with Down Syndrome. Int J Obes Relat Metab Disord 19, 858-861.

Almuqbil, M.A., Waisbren, S.E., Levy, H.L., and Picker, J.D. (2019). Revising the Psychiatric Phenotype of Homocystinuria. Genet Med 21, 1827-1831.

Amr, N.H. (2018). Thyroid Disorders in Subjects with Down Syndrome: An Update. Acta Biomed 89, 132-139.

Antonarakis, S.E. (2017). Down syndrome and the complexity of genome dosage imbalance. Nature reviews. Genetics 18, 147-163.

Antonarakis, S.E., Avramopoulos, D., Blouin, J.L., Talbot, C.C., Jr., and Schinzel, A.A. (1993). Mitotic errors in somatic cells cause trisomy 21 in about 4.5% of cases and are not associated with advanced maternal age. Nat Genet 3, 146-150.

Antonarakis, S.E., Skotko, B.G., Rafii, M.S., Strydom, A., Pape, S.E., Bianchi, D.W., et al. (2020). Down syndrome. Nat Rev Dis Primers 6, 9.

Antonaros, F., Ghini, V., Pulina, F., Ramacieri, G., Cicchini, E., Mannini, E., et al. (2020). Plasma metabolome and cognitive skills in Down syndrome. Sci Rep 10, 10491.

Antonaros, F., Lanfranchi, S., Locatelli, C., Martelli, A., Olivucci, G., Cicchini, E., et al. (2021a). One-carbon pathway and cognitive skills in children with Down syndrome. Sci Rep 11, 4225.

Antonaros, F., Olivucci, G., Cicchini, E., Ramacieri, G., Pelleri, M.C., Vitale, L., et al. (2019). MTHFR C677T polymorphism analysis: A simple, effective restriction enzyme-based method improving previous protocols. Mol Genet Genomic Med 7, e628.

Antonaros, F., Pitocco, M., Abete, D., Vione, B., Piovesan, A., Vitale, L., et al. (2021b). Structural Characterization of the Highly Restricted Down Syndrome Critical Region on 21q22.13: New KCNJ6 and DSCR4 Transcript Isoforms. Front Genet 12, 770359.

Antonaros, F., Zenatelli, R., Guerri, G., Bertelli, M., Locatelli, C., Vione, B., et al. (2021c). The transcriptome profile of human trisomy 21 blood cells. Human genomics 15, 25.

Araujo, B.H.S., Kaid, C., De Souza, J.S., Gomes Da Silva, S., Goulart, E., Caires, L.C.J., et al. (2018). Down Syndrome iPSC-Derived Astrocytes Impair Neuronal Synaptogenesis and the mTOR Pathway In Vitro. Mol Neurobiol 55, 5962-5975.

Araya, P., Waugh, K.A., Sullivan, K.D., Núñez, N.G., Roselli, E., Smith, K.P., et al. (2019). Trisomy 21 dysregulates T cell lineages toward an autoimmunity-prone state associated with interferon hyperactivity. Proc Natl Acad Sci U S A 116, 24231-24241.

Ascenção, K., Dilek, N., Augsburger, F., Panagaki, T., Zuhra, K., and Szabo, C. (2021). Pharmacological induction of mesenchymal-epithelial transition via inhibition of H2S biosynthesis and consequent suppression of ACLY activity in colon cancer cells. Pharmacol Res 165, 105393.

Bacalini, M.G., Gentilini, D., Boattini, A., Giampieri, E., Pirazzini, C., Giuliani, C., et al. (2015). Identification of a DNA methylation signature in blood cells from persons with Down Syndrome. Aging (Albany NY) 7, 82-96.

Baker, G.T., 3rd, and Sprott, R.L. (1988). Biomarkers of aging. Exp Gerontol 23, 223-239.

Banka, S., Blom, H.J., Walter, J., Aziz, M., Urquhart, J., Clouthier, C.M., et al. (2011). Identification and characterization of an inborn error of metabolism caused by dihydrofolate reductase deficiency. Am J Hum Genet 88, 216-225.

Barclay, C.J. (2017). Energy demand and supply in human skeletal muscle. J Muscle Res Cell Motil 38, 143-155.

Barrett, T., and Edgar, R. (2006). Gene expression omnibus: microarray data storage, submission, retrieval, and analysis. Methods Enzymol 411, 352-369.

Benjamini, Y., and Hochberg, Y. (2000). On the Adaptive Control of the False Discovery Rate in Multiple Testing With Independent Statistics. Journal of Educational and Behavioral Statistics 25, 60-83.
Bhattacharyya, R., Sanyal, D., and Bhattacharyya, S. (2018). Diagnostic algorithm of Down syndrome by minor physical anomaly. Indian J Psychiatry 60, 398-403.
Boada, R., Hutaff-Lee, C., Schrader, A., Weitzenkamp, D., Benke, T.A., Goldson, E.J., et al. (2012). Antagonism of NMDA receptors as a potential treatment for Down syndrome: a pilot randomized controlled trial. Transl Psychiatry 2, e141.
Borelli, V., Vanhooren, V., Lonardi, E., Reiding, K.R., Capri, M., Libert, C., et al. (2015). Plasma N-Glycome Signature of Down Syndrome. J Proteome Res 14, 4232-4245.
Bottiglieri, T. (2013). Folate, vitamin B_{12}, and S-adenosylmethionine. Psychiatr Clin North Am 36, 1-13.
Bottiglieri, T., and Reynolds, A. (2010). "Folate and Neurological Disease: Basic Mechanisms," in Folate in Health and Disease, ed. L.B. Bailey (New York: CRC Press Taylor & Francis Group), 355-380.
Brás, A., Rodrigues, A.S., Gomes, B., and Rueff, J. (2018). Down syndrome and microRNAs. Biomed Rep 8, 11-16.
Briggs, J.A., Sun, J., Shepherd, J., Ovchinnikov, D.A., Chung, T.L., Nayler, S.P., et al. (2013). Integration-free induced pluripotent stem cells model genetic and neural developmental features of down syndrome etiology. Stem Cells 31, 467-478.
Brosnan, M.E., Macmillan, L., Stevens, J.R., and Brosnan, J.T. (2015). Division of labour: how does folate metabolism partition between one-carbon metabolism and amino acid oxidation? Biochem J 472, 135-146.
Bubber, P., Haroutunian, V., Fisch, G., Blass, J.P., and Gibson, G.E. (2005). Mitochondrial abnormalities in Alzheimer brain: mechanistic implications. Ann Neurol 57, 695-703.
Bull, M.J. (2020). Down Syndrome. N Engl J Med 382, 2344-2352.
Butler, R.N., Sprott, R., Warner, H., Bland, J., Feuers, R., Forster, M., et al. (2004). Biomarkers of aging: from primitive organisms to humans. J Gerontol A Biol Sci Med Sci 59, B560-567.
Calderon-Ospina, C.A., and Nava-Mesa, M.O. (2020). B Vitamins in the nervous system: Current knowledge of the biochemical modes of action and synergies of thiamine, pyridoxine, and cobalamin. CNS Neurosci Ther 26, 5-13.
Cao, H., Krueger, E.W., Chen, J., Drizyte-Miller, K., Schulz, M.E., and Mcniven, M.A. (2020). The anti-viral dynamin family member MxB participates in mitochondrial integrity. Nat Commun 11, 1048.
Caracausi, M., Ghini, V., Locatelli, C., Mericio, M., Piovesan, A., Antonaros, F., et al. (2018). Plasma and urinary metabolomic profiles of Down syndrome correlate with alteration of mitochondrial metabolism. Sci Rep 8, 2977.
Cario, H., Smith, D.E., Blom, H., Blau, N., Bode, H., Holzmann, K., et al. (2011). Dihydrofolate reductase deficiency due to a homozygous DHFR mutation causes megaloblastic anemia and cerebral folate deficiency leading to severe neurologic disease. Am J Hum Genet 88, 226-231.
Chen, C.P., Chen, C.Y., Chern, S.R., Wu, P.S., Chen, S.W., Chuang, T.Y., et al. (2019). Detection of a familial 21q22.3 microduplication in a fetus associated with congenital heart defects. Taiwan J Obstet Gynecol 58, 869-871.
Chen, X.Q., Xing, Z., Chen, Q.D., Salvi, R.J., Zhang, X., Tycko, B., et al. (2021). Mechanistic Analysis of Age-Related Clinical Manifestations in Down Syndrome. Front Aging Neurosci 13, 700280.
Chiang, J.C., Jiang, J., Newburger, P.E., and Lawrence, J.B. (2018). Trisomy silencing by XIST normalizes Down syndrome cell pathogenesis demonstrated for hematopoietic defects in vitro. Nat Commun 9, 5180.

Chomczynski, P., and Sacchi, N. (1987). Single-step method of RNA isolation by acid guanidinium thiocyanate-phenol-chloroform extraction. Anal Biochem 162, 156-159.
Ciminski, K., Pulvermüller, J., Adam, J., and Schwemmle, M. (2019). Human MxA is a potent interspecies barrier for the novel bat-derived influenza A-like virus H18N11. Emerg Microbes Infect 8, 556-563.
Clarke, S.a.B., K. (2001). "S-adenosylmethionine-dependent methyltransferases," in Homocysteine in Health and Disease, eds R. Carmel, and D. W. Jackobsen. Cambridge University Press.
Clemson, C.M., Mcneil, J.A., Willard, H.F., and Lawrence, J.B. (1996). XIST RNA paints the inactive X chromosome at interphase: evidence for a novel RNA involved in nuclear/chromosome structure. J Cell Biol 132, 259-275.
Cogliati, S., Enriquez, J.A., and Scorrano, L. (2016). Mitochondrial Cristae: Where Beauty Meets Functionality. Trends Biochem Sci 41, 261-273.
Cole, J.H., Annus, T., Wilson, L.R., Remtulla, R., Hong, Y.T., Fryer, T.D., et al. (2017). Brain-predicted age in Down syndrome is associated with beta amyloid deposition and cognitive decline. Neurobiol Aging 56, 41-49.
Colombo, J.A., Reisin, H.D., Jones, M., and Bentham, C. (2005). Development of interlaminar astroglial processes in the cerebral cortex of control and Down's syndrome human cases. Exp Neurol 193, 207-217.
Conti, A., Fabbrini, F., D'agostino, P., Negri, R., Greco, D., Genesio, R., et al. (2007). Altered expression of mitochondrial and extracellular matrix genes in the heart of human fetuses with chromosome 21 trisomy. BMC Genomics 8, 268.
Cooper, A., Grigoryan, G., Guy-David, L., Tsoory, M.M., Chen, A., and Reuveny, E. (2012). Trisomy of the G protein-coupled K+ channel gene, Kcnj6, affects reward mechanisms, cognitive functions, and synaptic plasticity in mice. Proc Natl Acad Sci U S A 109, 2642-2647.
Cunningham, F., Achuthan, P., Akanni, W., Allen, J., Amode, M.R., Armean, I.M., et al. (2019). Ensembl 2019. Nucleic Acids Res 47, D745-d751.
Dall'olio, F., Vanhooren, V., Chen, C.C., Slagboom, P.E., Wuhrer, M., and Franceschi, C. (2013). N-glycomic biomarkers of biological aging and longevity: a link with inflammaging. Ageing Res Rev 12, 685-698.
Daniel, A. (1979). Normal phenotype and partial trisomy for the G positive region of chromosome 21. J Med Genet 16, 227-229.
Davisson, M.T., Schmidt, C., and Akeson, E.C. (1990). Segmental trisomy of murine chromosome 16: a new model system for studying Down syndrome. Prog Clin Biol Res 360, 263-280.
De Toma, I., Sierra, C., and Dierssen, M. (2021). Meta-analysis of transcriptomic data reveals clusters of consistently deregulated gene and disease ontologies in Down syndrome. PLoS Comput Biol 17, e1009317.
Delabar, J.M., Theophile, D., Rahmani, Z., Chettouh, Z., Blouin, J.L., Prieur, M., et al. (1993). Molecular mapping of twenty-four features of Down syndrome on chromosome 21. Eur J Hum Genet 1, 114-124.
Ducker, G.S., and Rabinowitz, J.D. (2017). One-Carbon Metabolism in Health and Disease. Cell Metab 25, 27-42.
Dumbrepatil, A.B., Zegalia, K.A., Sajja, K., Kennedy, R.T., and Marsh, E.N.G. (2020). Targeting viperin to the mitochondrion inhibits the thiolase activity of the trifunctional enzyme complex. J Biol Chem 295, 2839-2849.
Dykens, E.M., Hodapp, R.M., and Evans, D.W.
Eckmann-Scholz, C., Bens, S., Kolarova, J., Schneppenheim, S., Caliebe, A., Heidemann, S., et al. (2012). DNA-methylation profiling of fetal tissues reveals marked epigenetic differences between chorionic and amniotic samples. PLoS One 7, e39014.

Edgin, J.O., Mason, G.M., Spano, G., Fernandez, A., and Nadel, L. (2012). Human and mouse model cognitive phenotypes in Down syndrome: implications for assessment. Prog Brain Res 197, 123-151.

Evenhuis, H.M., Theunissen, M., Denkers, I., Verschuure, H., and Kemme, H. (2001). Prevalence of visual and hearing impairment in a Dutch institutionalized population with intellectual disability. J Intellect Disabil Res 45, 457-464.

Fagerberg, L., Hallstrom, B.M., Oksvold, P., Kampf, C., Djureinovic, D., Odeberg, J., et al. (2014). Analysis of the human tissue-specific expression by genome-wide integration of transcriptomics and antibody-based proteomics. Mol Cell Proteomics 13, 397-406.

Falk, A., Koch, P., Kesavan, J., Takashima, Y., Ladewig, J., Alexander, M., et al. (2012). Capture of neuroepithelial-like stem cells from pluripotent stem cells provides a versatile system for in vitro production of human neurons. PLoS One 7, e29597.

Falk, M.J., Zhang, Z., Rosenjack, J.R., Nissim, I., Daikhin, E., Nissim, I., et al. (2008). Metabolic pathway profiling of mitochondrial respiratory chain mutants in C. elegans. Mol Genet Metab 93, 388-397.

Feaster, W.W., Kwok, L.W., and Epstein, C.J. (1977). Dosage effects for superoxide dismutase-1 in nucleated cells aneuploid for chromosome 21. Am J Hum Genet 29, 563-570.

Fidler, D.J. (2008). "Down syndrome," in Diseases and Disorders in Infancy and Early Childhood, ed. J. Benson (San Diego, CA, USA: Elsevier), 138-145.

Fidler, D.J., Schworer, E., Prince, M.A., Will, E.A., Needham, A.W., and Daunhauer, L.A. (2019). Exploratory behavior and developmental skill acquisition in infants with Down syndrome. Infant Behav Dev 54, 140-150.

Field, A.E., Robertson, N.A., Wang, T., Havas, A., Ideker, T., and Adams, P.D. (2018). DNA Methylation Clocks in Aging: Categories, Causes, and Consequences. Mol Cell 71, 882-895.

Franceschi, C., Garagnani, P., Gensous, N., Bacalini, M.G., Conte, M., and Salvioli, S. (2019). Accelerated bio-cognitive aging in Down syndrome: State of the art and possible deceleration strategies. Aging Cell 18, e12903.

Friedman, N.P., Miyake, A., Corley, R.P., Young, S.E., Defries, J.C., and Hewitt, J.K. (2006). Not all executive functions are related to intelligence. Psychol Sci 17, 172-179.

Funk, R.S., Talib, N.J., Zimmerman, K.O., Van Haandel, L., and Becker, M.L. (2020). Altered Folate Homeostasis in Children with Down Syndrome: A Potential Basis for Enhanced Methotrexate Toxicity. J Pediatr 221, 235-239.

Gao, A.W., Smith, R.L., Van Weeghel, M., Kamble, R., Janssens, G.E., and Houtkooper, R.H. (2018). Identification of key pathways and metabolic fingerprints of longevity in C. elegans. Exp Gerontol 113, 128-140.

Garcia-Cazorla, A., Quadros, E.V., Nascimento, A., Garcia-Silva, M.T., Briones, P., Montoya, J., et al. (2008). Mitochondrial diseases associated with cerebral folate deficiency. Neurology 70, 1360-1362.

García-Hoyos, M., Riancho, J.A., and Valero, C. (2017). Bone health in Down syndrome. Med Clin (Barc) 149, 78-82.

Gardiner, K., Herault, Y., Lott, I.T., Antonarakis, S.E., Reeves, R.H., and Dierssen, M. (2010). Down syndrome: from understanding the neurobiology to therapy. J Neurosci 30, 14943-14945.

Garlet, T.R., Parisotto, E.B., De Medeiros Gda, S., Pereira, L.C., Moreira, E.A., Dalmarco, E.M., et al. (2013). Systemic oxidative stress in children and teenagers with Down syndrome. Life Sci 93, 558-563.

Gensous, N., Bacalini, M.G., Franceschi, C., and Garagnani, P. (2020). Down syndrome, accelerated aging and immunosenescence. Semin Immunopathol 42, 635-645.

Gioia, G.A., Espy, K. A. & Isquith, P. K. (2003). Behaviour Rating Inventory of Executive Function-Preschool Version. Psychological Assessment Resources, Lutz, FL. .

Gioia, G.A., Isquith, P. K., Guy, S. C. & Kenworthy, L. (2000). Behaviour Rating Inventory of Executive Function. Psychological Assessment Resources, Odessa, FL.
Grapp, M., Wrede, A., Schweizer, M., Hüwel, S., Galla, H.J., Snaidero, N., et al. (2013). Choroid plexus transcytosis and exosome shuttling deliver folate into brain parenchyma. Nat Commun 4, 2123.
Green, E., Stroud, L., Bloomfield, S., Cronje, J., Foxcroft, C., Hurter, K., et al. (2016). Griffiths scales of child development, third edition (Griffiths III)
Grieco, J., Pulsifer, M., Seligsohn, K., Skotko, B., and Schwartz, A. (2015). Down syndrome: Cognitive and behavioral functioning across the lifespan. Am J Med Genet C Semin Med Genet 169, 135-149.
Gueant, J.L., Anello, G., Bosco, P., Gueant-Rodriguez, R.M., Romano, A., Barone, C., et al. (2005). Homocysteine and related genetic polymorphisms in Down's syndrome IQ. J Neurol Neurosurg Psychiatry 76, 706-709.
Guedj, F., Pennings, J.L., Massingham, L.J., Wick, H.C., Siegel, A.E., Tantravahi, U., et al. (2016). An Integrated Human/Murine Transcriptome and Pathway Approach To Identify Prenatal Treatments For Down Syndrome. Sci Rep 6, 32353.
Hackland, J.O.S., Frith, T.J.R., Thompson, O., Marin Navarro, A., Garcia-Castro, M.I., Unger, C., et al. (2017). Top-Down Inhibition of BMP Signaling Enables Robust Induction of hPSCs Into Neural Crest in Fully Defined, Xeno-free Conditions. Stem Cell Reports 9, 1043-1052.
Halevy, T., Biancotti, J.C., Yanuka, O., Golan-Lev, T., and Benvenisty, N. (2016). Molecular Characterization of Down Syndrome Embryonic Stem Cells Reveals a Role for RUNX1 in Neural Differentiation. Stem Cell Reports 7, 777-786.
Hall, B. (1966). Mongolism in newborn infants. An examination of the criteria for recognition and some speculations on the pathogenic activity of the chromosomal abnormality. Clin Pediatr (Phila) 5, 4-12.
Hamerton, J.L. (1971). Banding patterns of metaphase chromosomes in Down's syndrome. Lancet 2, 709.
Hanney, M., Prasher, V., Williams, N., Jones, E.L., Aarsland, D., Corbett, A., et al. (2012). Memantine for dementia in adults older than 40 years with Down's syndrome (MEADOWS): a randomised, double-blind, placebo-controlled trial. Lancet 379, 528-536.
Hattori, M., Fujiyama, A., Taylor, T.D., Watanabe, H., Yada, T., Park, H.S., et al. (2000). The DNA sequence of human chromosome 21. Nature 405, 311-319.
Helguera, P., Seiglie, J., Rodriguez, J., Hanna, M., Helguera, G., and Busciglio, J. (2013). Adaptive downregulation of mitochondrial function in down syndrome. Cell Metab 17, 132-140.
Hirata, S., Hirai, H., Nogami, E., Morimura, N., and Udono, T. (2017). Chimpanzee Down syndrome: a case study of trisomy 22 in a captive chimpanzee. Primates 58, 267-273.
Horvath, S., Garagnani, P., Bacalini, M.G., Pirazzini, C., Salvioli, S., Gentilini, D., et al. (2015). Accelerated epigenetic aging in Down syndrome. Aging Cell 14, 491-495.
Horvath, S., and Raj, K. (2018). DNA methylation-based biomarkers and the epigenetic clock theory of ageing. Nature reviews. Genetics 19, 371-384.
Ifergan, I., Shafran, A., Jansen, G., Hooijberg, J.H., Scheffer, G.L., and Assaraf, Y.G. (2004). Folate deprivation results in the loss of breast cancer resistance protein (BCRP/ABCG2) expression. A role for BCRP in cellular folate homeostasis. J Biol Chem 279, 25527-25534.
Iyer, A.M., Van Scheppingen, J., Milenkovic, I., Anink, J.J., Adle-Biassette, H., Kovacs, G.G., et al. (2014). mTOR Hyperactivation in down syndrome hippocampus appears early during development. J Neuropathol Exp Neurol 73, 671-683.
Izzo, A., Mollo, N., Nitti, M., Paladino, S., Calì, G., Genesio, R., et al. (2018). Mitochondrial dysfunction in down syndrome: molecular mechanisms and therapeutic targets. Mol Med 24, 2.

Izzo, A., Nitti, M., Mollo, N., Paladino, S., Procaccini, C., Faicchia, D., et al. (2017). Metformin restores the mitochondrial network and reverses mitochondrial dysfunction in Down syndrome cells. Hum Mol Genet 26, 1056-1069.
Jackson, J.F., North, E.R., 3rd, and Thomas, J.G. (1976). Clinical diagnosis of Down's syndrome. Clin Genet 9, 483-487.
Jiang, J., Jing, Y., Cost, G.J., Chiang, J.C., Kolpa, H.J., Cotton, A.M., et al. (2013). Translating dosage compensation to trisomy 21. Nature 500, 296-300.
Jin, S., Lee, Y.K., Lim, Y.C., Zheng, Z., Lin, X.M., Ng, D.P., et al. (2013). Global DNA hypermethylation in down syndrome placenta. PLoS genetics 9, e1003515.
John, S.P., Sun, J., Carlson, R.J., Cao, B., Bradfield, C.J., Song, J., et al. (2018). IFIT1 Exerts Opposing Regulatory Effects on the Inflammatory and Interferon Gene Programs in LPS-Activated Human Macrophages. Cell reports 25, 95-106.e106.
Johnson, T.E. (2006). Recent results: biomarkers of aging. Exp Gerontol 41, 1243-1246.
Jonas, S., and Izaurralde, E. (2015). Towards a molecular understanding of microRNA-mediated gene silencing. Nature reviews. Genetics 16, 421-433.
Justice, E.D., Barnum, S.J., and Kidd, T. (2017). The WAGR syndrome gene PRRG4 is a functional homologue of the commissureless axon guidance gene. PLoS genetics 13, e1006865.
Kaikkonen, M.U., and Adelman, K. (2018). Emerging Roles of Non-Coding RNA Transcription. Trends Biochem Sci 43, 654-667.
Karmiloff-Smith, A., Al-Janabi, T., D'souza, H., Groet, J., Massand, E., Mok, K., et al. (2016). The importance of understanding individual differences in Down syndrome. F1000Research 5.
Kerkel, K., Schupf, N., Hatta, K., Pang, D., Salas, M., Kratz, A., et al. (2010). Altered DNA methylation in leukocytes with trisomy 21. PLoS genetics 6, e1001212.
Kim, H.I., Kim, S.W., Kim, J., Jeon, H.R., and Jung, D.W. (2017). Motor and Cognitive Developmental Profiles in Children With Down Syndrome. Ann Rehabil Med 41, 97-103.
Kleschevnikov, A.M., Belichenko, P.V., Salehi, A., and Wu, C. (2012). Discoveries in Down syndrome: moving basic science to clinical care. Prog Brain Res 197, 199-221.
Knox, A.J., Graham, C., Bleskan, J., Brodsky, G., and Patterson, D. (2009). Mutations in the Chinese hamster ovary cell GART gene of de novo purine synthesis. Gene 429, 23-30.
Korbel, J.O., Tirosh-Wagner, T., Urban, A.E., Chen, X.N., Kasowski, M., Dai, L., et al. (2009). The genetic architecture of Down syndrome phenotypes revealed by high-resolution analysis of human segmental trisomies. Proc Natl Acad Sci U S A 106, 12031-12036.
Kuck, D., Caulfield, T., Lyko, F., and Medina-Franco, J.L. (2010). Nanaomycin A selectively inhibits DNMT3B and reactivates silenced tumor suppressor genes in human cancer cells. Mol Cancer Ther 9, 3015-3023.
Kusters, M.A., Verstegen, R.H., Gemen, E.F., and De Vries, E. (2009). Intrinsic defect of the immune system in children with Down syndrome: a review. Clin Exp Immunol 156, 189-193.
Lanfranchi, S., Cornoldi, C., and Vianello, R. (2004). Verbal and visuospatial working memory deficits in children with Down syndrome. Am J Ment Retard 109, 456-466.
Laurent, A.P., Kotecha, R.S., and Malinge, S. (2020). Gain of chromosome 21 in hematological malignancies: lessons from studying leukemia in children with Down syndrome. Leukemia 34, 1984-1999.
Lee, L.G., and Jackson, J.F. (1972). Diagnosis of Down's syndrome: clinical vs. laboratory. Clin Pediatr (Phila) 11, 353-356.
Lee, N.R., Fidler, D.J., Blakeley-Smith, A., Daunhauer, L., Robinson, C., and Hepburn, S.L. (2011). Caregiver report of executive functioning in a population-based sample of young children with Down syndrome. Am J Intellect Dev Disabil 116, 290-304.
Lehmann, M., Gottfries, C.G., and Regland, B. (1999). Identification of cognitive impairment in the elderly: homocysteine is an early marker. Dement Geriatr Cogn Disord 10, 12-20.

Lejeune, J. (1966). Chromosomal studies in psychiatry. Recent Adv Biol Psychiatry 9, 13-20.
Lejeune, J. (1977). On the mechanism of mental deficiency in chromosomal diseases. Hereditas 86, 9-14.
Lejeune, J. (1979). [Biochemical investigations and trisomy 21 (author's transl)]. Ann Genet 22, 67-75.
Lejeune, J., Gauthier, M., and Turpin, R. (1959a). [Human chromosomes in tissue cultures]. Comptes rendus hebdomadaires des seances de l'Academie des sciences 248, 602-603.
Lejeune, J., Rethore, M.O., De Blois, M.C., Maunoury-Burolla, C., Mir, M., Nicolle, L., et al. (1986). [Metabolism of monocarbons and trisomy 21: sensitivity to methotrexate]. Ann Genet 29, 16-19.
Lejeune, J., Turpin, R., and Gautier, M. (1959b). [Chromosomic diagnosis of mongolism]. Arch Fr Pediatr 16, 962-963.
Lenzi, L., Facchin, F., Piva, F., Giulietti, M., Pelleri, M.C., Frabetti, F., et al. (2011). TRAM (Transcriptome Mapper): database-driven creation and analysis of transcriptome maps from multiple sources. BMC Genomics 12, 121.
Letourneau, A., Santoni, F.A., Bonilla, X., Sailani, M.R., Gonzalez, D., Kind, J., et al. (2014). Domains of genome-wide gene expression dysregulation in Down's syndrome. Nature 508, 345-350.
Li, L.B., Chang, K.H., Wang, P.R., Hirata, R.K., Papayannopoulou, T., and Russell, D.W. (2012). Trisomy correction in Down syndrome induced pluripotent stem cells. Cell Stem Cell 11, 615-619.
Li, R., Zhu, H., and Luo, Y. (2016). Understanding the Functions of Long Non-Coding RNAs through Their Higher-Order Structures. Int J Mol Sci 17.
Liu, C., Belichenko, P.V., Zhang, L., Fu, D., Kleschevnikov, A.M., Baldini, A., et al. (2011). Mouse models for Down syndrome-associated developmental cognitive disabilities. Dev Neurosci 33, 404-413.
Liu, X., Cooper, D.E., Cluntun, A.A., Warmoes, M.O., Zhao, S., Reid, M.A., et al. (2018). Acetate Production from Glucose and Coupling to Mitochondrial Metabolism in Mammals. Cell 175, 502-513.e513.
Locatelli, C., Onnivello, S., Antonaros, F., Feliciello, A., Filoni, S., Rossi, S., et al. (2021). Is the Age of Developmental Milestones a Predictor for Future Development in Down Syndrome? Brain Sci 11, 655.
Locatelli, C., Onnivello, S., Gori, C., Ramacieri, G., Pulina, F., Marcolin, C., et al. (2022). A reassessment of Jackson's checklist and identification of two Down syndrome sub-phenotypes. Sci Rep 12, 3104.
Lockstone, H.E., Harris, L.W., Swatton, J.E., Wayland, M.T., Holland, A.J., and Bahn, S. (2007). Gene expression profiling in the adult Down syndrome brain. Genomics 90, 647-660.
Lott, I.T. (2012). Neurological phenotypes for Down syndrome across the life span. Prog Brain Res 197, 101-121.
Loveall, S.J., Conners, F.A., Tungate, A.S., Hahn, L.J., and Osso, T.D. (2017). A cross-sectional analysis of executive function in Down syndrome from 2 to 35 years. J Intellect Disabil Res 61, 877-887.
Lu, S.C. (2013). Glutathione synthesis. Biochim Biophys Acta 1830, 3143-3153.
Lukowski, A.F., Milojevich, H.M., and Eales, L. (2019). Cognitive Functioning in Children with Down Syndrome: Current Knowledge and Future Directions. Adv Child Dev Behav 56, 257-289.
Lyle, R., Bena, F., Gagos, S., Gehrig, C., Lopez, G., Schinzel, A., et al. (2009). Genotype-phenotype correlations in Down syndrome identified by array CGH in 30 cases of partial trisomy and partial monosomy chromosome 21. Eur J Hum Genet 17, 454-466.

Lyle, R., Gehrig, C., Neergaard-Henrichsen, C., Deutsch, S., and Antonarakis, S.E. (2004). Gene expression from the aneuploid chromosome in a trisomy mouse model of down syndrome. Genome Res 14, 1268-1274.
Ma, H., Yang, W., Zhang, L., Liu, S., Zhao, M., Zhou, G., et al. (2019). Interferon-alpha promotes immunosuppression through IFNAR1/STAT1 signalling in head and neck squamous cell carcinoma. Br J Cancer 120, 317-330.
Maclean, G.A., Menne, T.F., Guo, G., Sanchez, D.J., Park, I.H., Daley, G.Q., et al. (2012). Altered hematopoiesis in trisomy 21 as revealed through in vitro differentiation of isogenic human pluripotent cells. Proc Natl Acad Sci U S A 109, 17567-17572.
Magnani, M., Stocchi, V., Novelli, G., Dachà, M., and Fornaini, G. (1987). Red blood cell glucose metabolism in Down's syndrome. Clin Physiol Biochem 5, 9-14.
Mao, R., Zielke, C.L., Zielke, H.R., and Pevsner, J. (2003). Global up-regulation of chromosome 21 gene expression in the developing Down syndrome brain. Genomics 81, 457-467.
Marchal, J.P., Maurice-Stam, H., Houtzager, B.A., Rutgers Van Rozenburg-Marres, S.L., Oostrom, K.J., Grootenhuis, M.A., et al. (2016). Growing up with Down syndrome: Development from 6 months to 10.7 years. Res Dev Disabil 59, 437-450.
Martin, G.M. (1978). Genetic syndromes in man with potential relevance to the pathobiology of aging. Birth Defects Orig Artic Ser 14, 5-39.
Martinez-Reyes, I., and Chandel, N.S. (2020). Mitochondrial TCA cycle metabolites control physiology and disease. Nat Commun 11, 102.
Mattson, M.P., and Shea, T.B. (2003). Folate and homocysteine metabolism in neural plasticity and neurodegenerative disorders. Trends Neurosci 26, 137-146.
Mazzarino, R.C., Baresova, V., Zikánová, M., Duval, N., Wilkinson, T.G., 2nd, Patterson, D., et al. (2021). Transcriptome and metabolome analysis of crGART, a novel cell model of de novo purine synthesis deficiency: Alterations in CD36 expression and activity. PLoS One 16, e0247227.
Mcclure, H.M., Belden, K.H., Pieper, W.A., and Jacobson, C.B. (1969). Autosomal trisomy in a chimpanzee: resemblance to Down's syndrome. Science 165, 1010-1012.
Mccormick, M.K., Schinzel, A., Petersen, M.B., Stetten, G., Driscoll, D.J., Cantu, E.S., et al. (1989). Molecular genetic approach to the characterization of the "Down syndrome region" of chromosome 21. Genomics 5, 325-331.
Meguid, N.A., Dardir, A.A., El-Sayed, E.M., Ahmed, H.H., Hashish, A.F., and Ezzat, A. (2010). Homocysteine and oxidative stress in Egyptian children with Down syndrome. Clin Biochem 43, 963-967.
Mentch, S.J., and Locasale, J.W. (2016). One-carbon metabolism and epigenetics: understanding the specificity. Ann N Y Acad Sci 1363, 91-98.
Miyake, A., Friedman, N.P., Emerson, M.J., Witzki, A.H., Howerter, A., and Wager, T.D. (2000). The unity and diversity of executive functions and their contributions to complex "Frontal Lobe" tasks: a latent variable analysis. Cogn Psychol 41, 49-100.
Mollo, N., Cicatiello, R., Aurilia, M., Scognamiglio, R., Genesio, R., Charalambous, M., et al. (2020). Targeting Mitochondrial Network Architecture in Down Syndrome and Aging. Int J Mol Sci 21.
Naseri, N.N., Bonica, J., Xu, H., Park, L.C., Arjomand, J., Chen, Z., et al. (2016). Novel Metabolic Abnormalities in the Tricarboxylic Acid Cycle in Peripheral Cells From Huntington's Disease Patients. PLoS One 11, e0160384.
Natunen, S., Satomaa, T., Pitkänen, V., Salo, H., Mikkola, M., Natunen, J., et al. (2011). The binding specificity of the marker antibodies Tra-1-60 and Tra-1-81 reveals a novel pluripotency-associated type 1 lactosamine epitope. Glycobiology 21, 1125-1130.
Ncbi Resource Coordinators (2018). Database resources of the National Center for Biotechnology Information. Nucleic Acids Res 46, D8-d13.

Nelson, D.L., Cox, M. M. (2017). "Biosynthesis of aminoacids, nucleotides and related molecules," in Principles of Biochemistry, ed. W.H. Freeman (New York: macmillan education).
Nelson, D.L., and Gibbs, R.A. (2004). Genetics. The critical region in trisomy 21. Science 306, 619-621.
Niebuhr, E. (1974). Down's syndrome. The possibility of a pathogenetic segment on chromosome no. 21. Humangenetik 21, 99-101.
Nuffield Council on Bioethics (2002). "Genetics and human behaviour: the ethical context--summary and recommendations," in Genetics and Human Behaviour: The Ethical Context. (London).
Obeid, R., Hartmuth, K., Herrmann, W., Gortner, L., Rohrer, T.R., Geisel, J., et al. (2012). Blood biomarkers of methylation in Down syndrome and metabolic simulations using a mathematical model. Mol Nutr Food Res 56, 1582-1589.
Olmos-Serrano, J.L., Kang, H.J., Tyler, W.A., Silbereis, J.C., Cheng, F., Zhu, Y., et al. (2016). Down Syndrome Developmental Brain Transcriptome Reveals Defective Oligodendrocyte Differentiation and Myelination. Neuron 89, 1208-1222.
Onnivello, S., Colaianni, S., Pulina, F., Locatelli, C., Marcolin, C., Ramacieri, G., et al. (2022a). Executive functions and adaptive behaviour in individuals with Down syndrome. J Intellect Disabil Res 66, 32-49.
Onnivello, S., Pulina, F., Locatelli, C., Marcolin, C., Ramacieri, G., Antonaros, F., et al. (2022b). Cognitive profiles in children and adolescents with Down syndrome. Sci Rep 12, 1936.
Panagaki, T., Pecze, L., Randi, E.B., Nieminen, A.I., and Szabo, C. (2022). Role of the cystathionine β-synthase / H(2)S pathway in the development of cellular metabolic dysfunction and pseudohypoxia in down syndrome. Redox Biol 55, 102416.
Panagaki, T., Randi, E.B., Augsburger, F., and Szabo, C. (2019). Overproduction of H(2)S, generated by CBS, inhibits mitochondrial Complex IV and suppresses oxidative phosphorylation in Down syndrome. Proc Natl Acad Sci U S A 116, 18769-18771.
Papavassiliou, P., York, T.P., Gursoy, N., Hill, G., Nicely, L.V., Sundaram, U., et al. (2009). The phenotype of persons having mosaicism for trisomy 21/Down syndrome reflects the percentage of trisomic cells present in different tissues. Am J Med Genet A 149a, 573-583.
Pareek, V., Pedley, A.M., and Benkovic, S.J. (2021). Human de novo purine biosynthesis. Crit Rev Biochem Mol Biol 56, 1-16.
Park, I.H., Arora, N., Huo, H., Maherali, N., Ahfeldt, T., Shimamura, A., et al. (2008). Disease-specific induced pluripotent stem cells. Cell 134, 877-886.
Patterson, D. (2009). Molecular genetic analysis of Down syndrome. Hum Genet 126, 195-214.
Pavlov, C.S., Damulin, I.V., Shulpekova, Y.O., and Andreev, E.A. (2019). Neurological disorders in vitamin B12 deficiency. Ter Arkh 91, 122-129.
Pecze, L., Randi, E.B., and Szabo, C. (2020). Meta-analysis of metabolites involved in bioenergetic pathways reveals a pseudohypoxic state in Down syndrome. Mol Med 26.
Pecze, L., and Szabo, C. (2021). Meta-analysis of gene expression patterns in Down syndrome highlights significant alterations in mitochondrial and bioenergetic pathways. Mitochondrion 57, 163-172.
Peeters, M.A., Rethore, M.O., and Lejeune, J. (1995). In vivo folic acid supplementation partially corrects in vitro methotrexate toxicity in patients with Down syndrome. Br J Haematol 89, 678-680.
Pellegrini, L., Bonfio, C., Chadwick, J., Begum, F., Skehel, M., and Lancaster, M.A. (2020). Human CNS barrier-forming organoids with cerebrospinal fluid production. Science 369.
Pelleri, M.C., Cattani, C., Vitale, L., Antonaros, F., Strippoli, P., Locatelli, C., et al. (2018). Integrated Quantitative Transcriptome Maps of Human Trisomy 21 Tissues and Cells. Front Genet 9, 125.

Pelleri, M.C., Cicchini, E., Locatelli, C., Vitale, L., Caracausi, M., Piovesan, A., et al. (2016). Systematic reanalysis of partial trisomy 21 cases with or without Down syndrome suggests a small region on 21q22.13 as critical to the phenotype. Hum Mol Genet 25, 2525-2538.

Pelleri, M.C., Cicchini, E., Petersen, M.B., Tranebjaerg, L., Mattina, T., Magini, P., et al. (2019). Partial trisomy 21 map: Ten cases further supporting the highly restricted Down syndrome critical region (HR-DSCR) on human chromosome 21. Mol Genet Genomic Med 7, e797.

Pelleri, M.C., Gennari, E., Locatelli, C., Piovesan, A., Caracausi, M., Antonaros, F., et al. (2017). Genotype-phenotype correlation for congenital heart disease in Down syndrome through analysis of partial trisomy 21 cases. Genomics 109, 391-400.

Pelleri, M.C., Piovesan, A., Caracausi, M., Berardi, A.C., Vitale, L., and Strippoli, P. (2014). Integrated differential transcriptome maps of Acute Megakaryoblastic Leukemia (AMKL) in children with or without Down Syndrome (DS). BMC Med Genomics 7, 63.

Pennington, B.F., and Ozonoff, S. (1996). Executive functions and developmental psychopathology. J Child Psychol Psychiatry 37, 51-87.

Pereira, A.C., Schettert, I.T., Morandini Filho, A.A., Guerra-Shinohara, E.M., and Krieger, J.E. (2004). Methylenetetrahydrofolate reductase (MTHFR) c677t gene variant modulates the homocysteine folate correlation in a mild folate-deficient population. Clin Chim Acta 340, 99-105.

Perluigi, M., Tramutola, A., Pagnotta, S., Barone, E., and Butterfield, D.A. (2020). The BACH1/Nrf2 Axis in Brain in Down Syndrome and Transition to Alzheimer Disease-Like Neuropathology and Dementia. Antioxidants (Basel) 9.

Petrossian, T.C., and Clarke, S.G. (2011). Uncovering the human methyltransferasome. Mol Cell Proteomics 10, M110.000976.

Pfeiffer, C.M., Sternberg, M.R., Fazili, Z., Lacher, D.A., Zhang, M., Johnson, C.L., et al. (2015). Folate status and concentrations of serum folate forms in the US population: National Health and Nutrition Examination Survey 2011-2. Br J Nutr 113, 1965-1977.

Piccoli, C., Izzo, A., Scrima, R., Bonfiglio, F., Manco, R., Negri, R., et al. (2013). Chronic pro-oxidative state and mitochondrial dysfunctions are more pronounced in fibroblasts from Down syndrome foeti with congenital heart defects. Hum Mol Genet 22, 1218-1232.

Pogribna, M., Melnyk, S., Pogribny, I., Chango, A., Yi, P., and James, S.J. (2001). Homocysteine metabolism in children with Down syndrome: in vitro modulation. Am J Hum Genet 69, 88-95.

Pope, S., Artuch, R., Heales, S., and Rahman, S. (2019). Cerebral folate deficiency: Analytical tests and differential diagnosis. J Inherit Metab Dis 42, 655-672.

Postolache, L., and Parsa, C.F. (2018). Brushfield spots and Wölfflin nodules unveiled in dark irides using near-infrared light. Sci Rep 8, 18040.

Powers, R.K., Culp-Hill, R., Ludwig, M.P., Smith, K.P., Waugh, K.A., Minter, R., et al. (2019). Trisomy 21 activates the kynurenine pathway via increased dosage of interferon receptors. Nat Commun 10, 4766.

Prandini, P., Deutsch, S., Lyle, R., Gagnebin, M., Delucinge Vivier, C., Delorenzi, M., et al. (2007). Natural gene-expression variation in Down syndrome modulates the outcome of gene-dosage imbalance. Am J Hum Genet 81, 252-263.

Putra, M., Surti, U., Hu, J., Steele, D., Clemens, M., Saller, D.N., et al. (2017). Beyond Down syndrome phenotype: Paternally derived isodicentric chromosome 21 with partial monosomy 21q22.3. Am J Med Genet A 173, 3153-3157.

Rahmani, Z., Blouin, J.L., Creau-Goldberg, N., Watkins, P.C., Mattei, J.F., Poissonnier, M., et al. (1989). Critical role of the D21S55 region on chromosome 21 in the pathogenesis of Down syndrome. Proc Natl Acad Sci U S A 86, 5958-5962.

Ramaekers, V.T., Rothenberg, S.P., Sequeira, J.M., Opladen, T., Blau, N., Quadros, E.V., et al. (2005). Autoantibodies to folate receptors in the cerebral folate deficiency syndrome. N Engl J Med 352, 1985-1991.

Rodan, L.H., Qi, W., Ducker, G.S., Demirbas, D., Laine, R., Yang, E., et al. (2018). 5,10-methenyltetrahydrofolate synthetase deficiency causes a neurometabolic disorder associated with microcephaly, epilepsy, and cerebral hypomyelination. Mol Genet Metab 125, 118-126.

Roizen, N.J., and Patterson, D. (2003). Down's syndrome. Lancet 361, 1281-1289.

Rosenblatt, D.S., Whitehead, V.M., Matiaszuk, N.V., Pottier, A., Vuchich, M.J., and Beaulieu, D. (1982). Differential effects of folinic acid and glycine, adenosine, and thymidine as rescue agents in methotrexate-treated human cells in relation to the accumulation of methotrexate polyglutamates. Mol Pharmacol 21, 718-722.

Rueda, N., Florez, J., and Martinez-Cue, C. (2012). Mouse models of Down syndrome as a tool to unravel the causes of mental disabilities. Neural Plast 2012, 584071.

Rueda Revilla, N., and Martínez-Cué, C. (2020). Antioxidants in Down Syndrome: From Preclinical Studies to Clinical Trials. Antioxidants (Basel) 9.

Saber, M.M., Adeyemi Babarinde, I., Hettiarachchi, N., and Saitou, N. (2016). Emergence and Evolution of Hominidae-Specific Coding and Noncoding Genomic Sequences. Genome Biol Evol 8, 2076-2092.

Saber, M.M., Karimiavargani, M., Uzawa, T., Hettiarachchi, N., Hamada, M., Ito, Y., et al. (2021). Possible roles for the hominoid-specific DSCR4 gene in human cells. Genes Genet Syst 96, 1-11.

Salvi, A., Vezzoli, M., Busatto, S., Paolini, L., Faranda, T., Abeni, E., et al. (2019). Analysis of a nanoparticleenriched fraction of plasma reveals miRNA candidates for Down syndrome pathogenesis. Int J Mol Med 43, 2303-2318.

Sato, D., Kawara, H., Shimokawa, O., Harada, N., Tonoki, H., Takahashi, N., et al. (2008). A girl with Down syndrome and partial trisomy for 21pter-q22.13: a clue to narrow the Down syndrome critical region. Am J Med Genet A 146a, 124-127.

Schalock, R.L., Luckasson, R., and Tassé, M.J. (2010). An Overview of Intellectual Disability: Definition, Diagnosis, Classification, and Systems of Supports (12th ed.). Am J Intellect Dev Disabil 126, 439-442.

Schmitz, S.U., Grote, P., and Herrmann, B.G. (2016). Mechanisms of long noncoding RNA function in development and disease. Cell Mol Life Sci 73, 2491-2509.

Schober, P., Boer, C., and Schwarte, L.A. (2018). Correlation Coefficients: Appropriate Use and Interpretation. Anesth Analg 126, 1763-1768.

Schuster, J., Hoeber, J., Sobol, M., Fatima, A., Annerén, G., and Dahl, N. (2020). Generation of two human iPSC lines (UUIGPi013-A and UUIPGi014-A) from cases with Down syndrome and full trisomy for chromosome 21 (T21). Stem cell research 49, 102081.

Shapiro, B.L. (1999). The Down syndrome critical region. J Neural Transm Suppl 57, 41-60.

Silverman, W. (2007). Down syndrome: cognitive phenotype. Ment Retard Dev Disabil Res Rev 13, 228-236.

Smirnova, E., Griparic, L., Shurland, D.L., and Van Der Bliek, A.M. (2001). Dynamin-related protein Drp1 is required for mitochondrial division in mammalian cells. Mol Biol Cell 12, 2245-2256.

Sobol, M., Klar, J., Laan, L., Shahsavani, M., Schuster, J., Annerén, G., et al. (2019). Transcriptome and Proteome Profiling of Neural Induced Pluripotent Stem Cells from Individuals with Down Syndrome Disclose Dynamic Dysregulations of Key Pathways and Cellular Functions. Mol Neurobiol 56, 7113-7127.

Sobol, M., Raykova, D., Cavelier, L., Khalfallah, A., Schuster, J., and Dahl, N. (2015). Methods of Reprogramming to Induced Pluripotent Stem Cell Associated with Chromosomal Integrity and Delineation of a Chromosome 5q Candidate Region for Growth Advantage. Stem Cells Dev 24, 2032-2040.

Song, C., He, J., Chen, J., Liu, Y., Xiong, F., Wang, Y., et al. (2015). Effect of the onecarbon unit cycle on overall DNA methylation in children with Down's syndrome. Mol Med Rep 12, 8209-8214.
Sparrow, S.S., Cicchetti, D. V. & Balla, D. A. (2005). Vineland Adaptive Behaviour Scales: (VABS). NCS Pearson.
Sperringer, J.E., Addington, A., and Hutson, S.M. (2017). Branched-Chain Amino Acids and Brain Metabolism. Neurochem Res 42, 1697-1709.
Strippoli, P., Pelleri, M.C., Piovesan, A., Caracausi, M., Antonaros, F., and Vitale, L. (2019a). Genetics and genomics of Down syndrome. Int Rev Res Dev Disabil 56, 1-39.
Strippoli, P., Pelleri, M.C., Piovesan, A., Caracausi, M., Antonaros, F., and Vitale, L. (2019b). "Genetics and genomics of Down syndrome," in State of the Art of Research on Down Syndrome: Academic Press), 1-39.
Stuss, D.T.B., D. F. (1986). The frontal lobes. New York: Raven Press.
Sullivan, K.D., Lewis, H.C., Hill, A.A., Pandey, A., Jackson, L.P., Cabral, J.M., et al. (2016). Trisomy 21 consistently activates the interferon response. eLife 5.
Szabo, C. (2020). The re-emerging pathophysiological role of the cystathionine-beta-synthase - hydrogen sulfide system in Down syndrome. Febs j.
Tanner, L.B., Goglia, A.G., Wei, M.H., Sehgal, T., Parsons, L.R., Park, J.O., et al. (2018). Four Key Steps Control Glycolytic Flux in Mammalian Cells. Cell systems 7, 49-62.e48.
Tsao, R., and Kindelberger, C. (2009). Variability of cognitive development in children with Down syndrome: relevance of good reasons for using the cluster procedure. Res Dev Disabil 30, 426-432.
Tudella, E., Pereira, K., Basso, R.P., and Savelsbergh, G.J. (2011). Description of the motor development of 3-12 month old infants with Down syndrome: the influence of the postural body position. Res Dev Disabil 32, 1514-1520.
Uhlin, E., Rönnholm, H., Day, K., Kele, M., Tammimies, K., Bölte, S., et al. (2017). Derivation of human iPS cell lines from monozygotic twins in defined and xeno free conditions. Stem cell research 18, 22-25.
Vaiserman, A., and Krasnienkov, D. (2020). Telomere Length as a Marker of Biological Age: State-of-the-Art, Open Issues, and Future Perspectives. Front Genet 11, 630186.
Valenti, D., Manente, G.A., Moro, L., Marra, E., and Vacca, R.A. (2011). Deficit of complex I activity in human skin fibroblasts with chromosome 21 trisomy and overproduction of reactive oxygen species by mitochondria: involvement of the cAMP/PKA signalling pathway. Biochem J 435, 679-688.
Valenti, D., Rossi, L., Marzulli, D., Bellomo, F., De Rasmo, D., Signorile, A., et al. (2017). Inhibition of Drp1-mediated mitochondrial fission improves mitochondrial dynamics and bioenergetics stimulating neurogenesis in hippocampal progenitor cells from a Down syndrome mouse model. Biochim Biophys Acta Mol Basis Dis 1863, 3117-3127.
Valenti, D., Tullo, A., Caratozzolo, M.F., Merafina, R.S., Scartezzini, P., Marra, E., et al. (2010). Impairment of F1F0-ATPase, adenine nucleotide translocator and adenylate kinase causes mitochondrial energy deficit in human skin fibroblasts with chromosome 21 trisomy. Biochem J 431, 299-310.
Vanhooren, V., Desmyter, L., Liu, X.E., Cardelli, M., Franceschi, C., Federico, A., et al. (2007). N-glycomic changes in serum proteins during human aging. Rejuvenation Res 10, 521-531a.
Vanhooren, V., Liu, X.E., Franceschi, C., Gao, C.F., Libert, C., Contreras, R., et al. (2009). N-glycan profiles as tools in diagnosis of hepatocellular carcinoma and prediction of healthy human ageing. Mech Ageing Dev 130, 92-97.
Vasylovska, S., Schuster, J., Brboric, A., Carlsson, P.O., Dahl, N., and Lau, J. (2020). Generation of human induced pluripotent stem cell (iPSC) lines (UUMCBi001-A, UUMCBi002-A) from two healthy donors. Stem cell research 50, 102114.

Vaziri, H., Schächter, F., Uchida, I., Wei, L., Zhu, X., Effros, R., et al. (1993). Loss of telomeric DNA during aging of normal and trisomy 21 human lymphocytes. Am J Hum Genet 52, 661-667.

Vezmar, S., Schüsseler, P., Becker, A., Bode, U., and Jaehde, U. (2009). Methotrexate-associated alterations of the folate and methyl-transfer pathway in the CSF of ALL patients with and without symptoms of neurotoxicity. Pediatr Blood Cancer 52, 26-32.

Vilardell, M., Rasche, A., Thormann, A., Maschke-Dutz, E., Perez-Jurado, L.A., Lehrach, H., et al. (2011). Meta-analysis of heterogeneous Down Syndrome data reveals consistent genome-wide dosage effects related to neurological processes. BMC Genomics 12, 229.

Vione, B., Ramacieri G., Zavaroni G., Piano A., La Rocca G., Caracausi M., Vitale L., Piovesan A., Gori C., Pirazzoli G.L., Strippoli P., Cocchi G., Corvaglia L., Locatelli C, Pelleri M.C., Antonaros F. (2022). One-carbon pathway metabolites are altered in the plasma of subjects with Down syndrome: relation to chromosomal dosage. Submitted.

Vitale, L., Piovesan, A., Antonaros, F., Strippoli, P., Pelleri, M.C., and Caracausi, M. (2017). A molecular view of the normal human thyroid structure and function reconstructed from its reference transcriptome map. BMC Genomics 18, 739.

Vitale, L., Serpieri, V., Lauriola, M., Piovesan, A., Antonaros, F., Cicchini, E., et al. (2019). Human trisomy 21 fibroblasts rescue methotrexate toxic effect after treatment with 5-methyl-tetrahydrofolate and 5-formyl-tetrahydrofolate. J Cell Physiol.

Wang, P., Cai, F., Cao, L., Wang, Y., Zou, Q., Zhao, P., et al. (2019). Clinical diagnosis and mutation analysis of four Chinese families with succinic semialdehyde dehydrogenase deficiency. BMC Med Genet 20, 88.

Warren, A.C., Chakravarti, A., Wong, C., Slaugenhaupt, S.A., Halloran, S.L., Watkins, P.C., et al. (1987). Evidence for reduced recombination on the nondisjoined chromosomes 21 in Down syndrome. Science 237, 652-654.

Watkins, D., and Rosenblatt, D.S. (2012). Update and new concepts in vitamin responsive disorders of folate transport and metabolism. J Inherit Metab Dis 35, 665-670.

Wechsler, D. (2002). Wechsler Preschool and Primary Scale of Intelligence-Third edition. WPPSI-III.

Weick, J.P., Held, D.L., Bonadurer, G.F., 3rd, Doers, M.E., Liu, Y., Maguire, C., et al. (2013). Deficits in human trisomy 21 iPSCs and neurons. Proc Natl Acad Sci U S A 110, 9962-9967.

Welsh, M.C., Pennington, B. F. & Groisser, D. B. (1991). A normative-developmental study of executive function: a window on prefrontal function in children. Dev Neuropsychol, 131-149.

Whooten, R., Schmitt, J., and Schwartz, A. (2018). Endocrine manifestations of Down syndrome. Curr Opin Endocrinol Diabetes Obes 25, 61-66.

Winders, P., Wolter-Warmerdam, K., and Hickey, F. (2019). A schedule of gross motor development for children with Down syndrome. J Intellect Disabil Res 63, 346-356.

Xanthopoulos, M.S., Walega, R., Xiao, R., Prasad, D., Pipan, M.M., Zemel, B.S., et al. (2017). Caregiver-Reported Quality of Life in Youth with Down Syndrome. J Pediatr 189, 98-104.e101.

Xu, K., Li, S., Muskens, I.S., Elliott, N., Myint, S.S., Pandey, P., et al. (2022). Accelerated epigenetic aging in newborns with Down syndrome. Aging Cell 21, e13652.

Yoon, P.W., Freeman, S.B., Sherman, S.L., Taft, L.F., Gu, Y., Pettay, D., et al. (1996). Advanced maternal age and the risk of Down syndrome characterized by the meiotic stage of chromosomal error: a population-based study. Am J Hum Genet 58, 628-633.

Yu, T., Li, Z., Jia, Z., Clapcote, S.J., Liu, C., Li, S., et al. (2010). A mouse model of Down syndrome trisomic for all human chromosome 21 syntenic regions. Hum Mol Genet 19, 2780-2791.

Zamponi, N., Zamponi, E., Cannas, S.A., Billoni, O.V., Helguera, P.R., and Chialvo, D.R. (2018). Mitochondrial network complexity emerges from fission/fusion dynamics. Sci Rep 8, 363.
Zelazo, P.D., Carter A., Reznick, J. S. & Frye, D. (1997). Early development of executive function: a problem solving framework. . Review of General Psychology. 1, 198-226.
Zheng, Y., and Cantley, L.C. (2019). Toward a better understanding of folate metabolism in health and disease. J Exp Med 216, 253-266.
Zöllner, N. (1982). Purine and pyrimidine metabolism. Proc Nutr Soc 41, 329-342.